Design and Optimisation of a Microfluidic System for Single Cell Encapsulation

A thesis submitted to the University of Manchester for the degree of Doctor of Philosophy in the Faculty of Engineering and Physical Sciences

2016

Soumya Mohammad Abbas Jabur

School of Chemical Engineering and Analytical Sciences

Table of Contents

List of Figures

List of Tables

Abstract

This thesis describes a novel approach for cell encapsulation in alginate gel microbeads. The main aim of the thesis was to optimise a microfluidic setup and chip to encapsulate cells in monodisperse alginate gel microbeads. A number of cytotoxicity tests were therefore carried out to determine the effect of formulations used for the production, degradation and gelation of calcium alginate gel beads. Results from these tests revealed that the formulations used had little or no significant effect on cell growth, and therefore, alginate was deemed to be a suitable cell encapsulating material for further investigations.

Alginate gel microbeads were produced using hydrodynamic focusing techniques. For this purpose two different microfluidic setups were constructed. Fluids (oil, acidified oil and samples) were driven through the microfluidic setup by gravity. However, a number of drawbacks using this setup arose, such as polydispersity and reproducibility. Syringe pumps were introduced into the design of the second microfluidic setup as a means of driving fluids through the setup.

In addition three different microfluidic chips were fabricated with the aim of producing the ideal alginate gel microbead. The first microfluidic chip (PMMA MC1) was fabricated from PMMA and involved producing alginate gel microbeads that were internally gelified. This chip suffered from a number of drawbacks such as continuous blockages within the microfluidic channels, which led to the development of the second microfluidic chip. This chip was also fabricated from PMMA (PMMA MC2) but in contrast to PMMA MC1, gelification occurred externally, i.e. gelation took place off chip, and in this case the alginate microdroplets were dropped into a well containing 1 mL of acidified oil. This encapsulating procedure caused immediate cell death, which indicated that the internal gelation of alginate gel microbeads was favoured. These results also indicated that the design of the microfluidic chip needed developing in order to produce the ideal microbeads that can be used for cell encapsulation. This led to the fabrication of a novel microfluidic chip (PC MC3) which was fabricated from polycarbonate (PC) and involved internal gelation of the calcium alginate gel microbeads.

The combination of using the optimised microfluidic setup and PC MC3, in addition to alternations in some of the solutions used to make the alginate microbeads, resulted in the production of the desired ideal gel microbeads containing cells. Snap shots of the encapsulated cells obtained using fluorescence microscopy after 24 hours of encapsulation, revealed that the cells showed some characteristics of living cells, yet at the same time they also showed some characteristics of dead cells. These findings demonstrate the potential use of the optimised microfluidic setup and PC MC3 chip for many biological and medical applications.

Declaration

No portion of the work referred to in the thesis has been submitted in support of an application for another degree or qualification of this or any other university or other institute of learning.

Copyright Statement

Dedication

I dedicate this Thesis to my wonderful and loving parents Mr. Mohammad Abbas Jabur and Mrs. Hillah Jabur, to my amazing siblings Mr. Omar Jabur, Mr. Ahmad Jabur and Miss Bettool Jabur, to my prince charmers Yousuf Nabeersool and Firas Nabeerasool, and to my loving and supporting husband Dr. Mohammed Akmez Nabeerasool.

Acknowledgements

I would like to thank God for everything and everyone in my life.

I would like to express my appreciation to my supervisors (Prof. Nick Goddard, Dr. Josip Lovric', Prof. Peter Fielden and Dr. Anne Marie-Buckle). My PhD was initially supervised by Prof. Peter Fielden from the School of Engineering and Analytical Sciences, Faculty of Engineering and Physical Sciences and Dr. Anne Marie Buckle from the Faculty of Life Sciences.

Special thanks go to Prof. Peter Fielden, for accepting me as a PhD research student in his group and for all his support and encouragement throughout the first half of my PhD research programme. Prof. Fielden left his post at the University of Manchester half way through my research and was appointed as Head of Department at Lancaster University. I would also like to extend my thankfulness to the late Dr. Anne-Marie Buckle for agreeing to take me on as a PhD student in collaboration with Prof. Fielden. Sadly, a month after starting my research, Dr. Anne-Marie Buckle was diagnosed with breast cancer and passed away a year later.

Words cannot describe how grateful I was when Dr. Josip Lovric' agreed to become my co-supervisor with Prof. Fielden. Dr. Lovric' took on my supervision almost a year after Dr. Buckle sadly passed away, and has been a great role model, extremely supportive and gave me votes of confidence to strive further, not just though my PhD studies but also during my B.Sc. and M.Sc. degrees, which I obtained from the University of Manchester. I would also like to thank Dr. Lovric' for reading my Thesis and giving me valuable feedback. My gratitude extends to Prof. Nick Goddard for taking on the supervisory role of my PhD project, on the departure of Prof. Fielden, despite having other students and

academic duties of his own. Prof. Goddard has been nothing but supportive throughout my PhD programme and attended project meetings even before he officially became my supervisor. I would also like to thank Dr. Bernard Treves Brown not only for his help and support with technical related issues throughout the years, but also for supervising my PhD project at a crucial stage on the retirement of Prof. Goddard. I would also like to thank Dr. Brown for reading my Thesis and for the valuable feedback, meetings and opportunities to discuss and debate my work.

A special to thanks goes to my colleagues present and past, in particular I would like to thank Dr. Stephan Mohr for his help with constructing the optimised microfluidic setup used in this PhD project, and for his on-going support and discussions. In addition, I would also like to express my appreciation to Mr. Robert Beresford for his help with handling samples until deemed safe during my pregnancy period, and for his continuous support.

I would also like to thank Dr. Pawel Paszek, Dr. David Spiller for their help with the fluorescence imaging and for providing me with Jurkat cells to carry out the experiments in Chapter three and four.

I would like to thank appreciation to Dr. Martin Read for his on-going support in the cell culture laboratory and for his continuous support and encouragement. I would also like to extend my gratitude to Dr. Vicky Workman for her on-going support and for proofreading the result chapters in my Thesis.

During the course of my PhD research, I have experienced some happy and joyful moments as well as well emotional ones. I got married to my loving and caring husband Dr. Mohammed Akmez Nabeerasool, who has been nothing but supportive and a shoulder to lean on. I have also been blessed with my two beautiful boys Yousuf M. A. G.

Nabeerasool and Firas M. A. G Nabeerasool. Despite, the sleepless nights, my sons have brought nothing but love, joy and laughter into our lives.

Sadly, my big cousin Hassan Omar passed away before seeing me submit this Thesis after his battle with cancer in December 2014. My cousin was nothing but supportive, cheerful and was loved by everyone, it was a great loss to the family. We were also saddened on another occasion this April 2015, when my Uncle in law Mohammad Nasser Nubee passed away from a sudden heart attack. Uncle Naseer was nothing but supportive and was waiting to see the day I submit my PhD thesis, he always welcome me and my family with open arms.

I would like to express my gratitude to my parents Mr. Mohammad Abbas Jabur and Mrs. Hillah Jabur for all their love, support and encouragement. My parents supported and encouraged my decision to embrace a PhD, and have continued to help and support my little family and I. My thanks also extend to my siblings Mr. Omar Jabur, Mr. Ahmad Jabur and Miss Bettool Jabur and my sister in laws Safiya Nurein and Hajar Bin-Laksar. My love and thanks also goes to my nieces and nephews for all the joy and laughter they bring into our lives. In order of age: Diana, Maram, Ahmad, Maryam, Aisha, Sarah and Laith. My gratitude is also extended to the rest of my family (aunties, uncles and cousins) for all their support and encouragement. A big thankyou also goes to my father in law and mother in law Mr. Goolab Nabeerasool and Mrs, Amenah Nabeerasool, my brother in laws Mr. Fahez Nabeerasool and Mr. Fhadeel Nabeerasool, and my sister in laws Miss Samira Kourdouli and Mrs. Nooree Nabeerasool.

List of Abbreviations

CAD	Computer Assisted design.
DNA	Deoxyribose nucleic acid.
i.d.	Internal diameter.
PBS	Phosphate Buffered Saline.
PDMS	Polydimethilsiloxane.
PMMA	Polymethylmethacrylate.
PC	Polycarbonate.
UV	Ultra violet.
2D	Two dimension
3D	Three dimension
PAA	Poly(acrylic acid)
HEMA	Poly(2-hydroxyethyl methacrylate)
PNIPAM	Poly(N-isopropylacrylamide)
LCST	Lower critical solution temperature
FDA	Food and Drug Admission
PEO	Poly(ethylene oxide)
PLA	Poly(lactic acid)
PVA	Poly(vinyl alcohol)
HEPES	4-(2-Hydroxyethyl)piperazine-1-ethanesulfonic acid
Ca^{2+}	Calcium
Mg^{2+}	Magnesium
$CaCl_2$	Calcium chloride
Ml	Milliliter
µl	Microliter
CO_2	Carobone dioxide
%	Percentage
Cm	Centimetre
G	Grams
v/w	Volume to weight
RPMI-1640	Roswell Park Memorial Institute- 1640 cell culture medium
PMMA MC1	Polymethylmethacrylate microchip 1
PMMA MC2	Polymethylmethacrylate microchip 2
PC MC3	Polycarbonte microchip 3
PTFE	Polytetrafluoroethylene
Min	Minutes
Hr	Hours
(PNIPAM)	Poly(N-isopropylacrylamide (PNIPAM)
SAV	Surface area to volume
PC	Polycarbonate
RGD	Arginine-glycine aspartic acid

FBS	Fetal Bovine Serum
DMSO	Dimethyl Sulfoxide
Rpm	Rotations per minute
PI	Propidium iodide
Gly	Glycine
Xaa and Yaaa	Any other amino acid residue
DM	Degree of methacrylation
KPa	Kilo Pascal
KDa	Kilo Dalton
WP	Water phase
OP	Oil phase
GFP	Green fluorescence protein
BaCl2	Barium chloride
HepG2	Hepatocellular carcinoma cell line
BSA	Bovine Serum Albumin
PLL	Poly-L-Lysine

1 Chapter ONE Introduction

1.1 General overview and grand challenges:

Encapsulating cells in biocompatible microbeads has become more popular in the field of tissue engineering due to many advantages that they have to offer, for example providing a platform to study cell behaviour and support for cell-cell interactions (2). The work carried out in this thesis demonstrates the use of an optimised microfluidic setup, which was attached to a simple yet novel microfluidic chip in order to encapsulate single cells/ small group of cells in alginate gel microbeads. Microfluidic technology offers numerus benefits in cell encapsulating studies, such as reduced amounts of samples, formulations, analysis time and high throughput. This thesis reports the optimisation of a microfluidic setup including a microfluidic chip (PC MC3), which can be used to encapsulate low numbers of cells in alginate gel microbeads with diameters of 150- 200 μm. This microfluidic chip is reusable, provides high throughput and can be used by cell biologists. Chapter two demonstrates the suitability of alginate as an encapsulating material for viable Jurkat cells, while chapters three and four detail the development of a microfluidic setup used to encapsulate Jurkat cells in polydisperse alginate gel microbeads. A microfluidic setup that is capable of enclosing a small group of viable cells in polydisperse microbeads has great potentials in many cell biology and clinical applications. Furthermore, the encapsulated cells can be stained with fluorescent dyes to monitor cell viability.

At present a number of challenges related to cell encapsulation needs to be addressed. Firstly, the ability to control and reduce the size of the microbeads is vital. Currently, most microgels are produced using a nozzle or a needle resulting in the production of relatively large hydrogels (500-1000 μm) (3). The ability to reduce the size of the microbeads is advantageous as it will reduce the diffusion distance and provide a high surface to volume

ratio, which is vital for nutrients to reach to the cells and for wastes to be disposed. Secondly, the polydispersity of microbeads has an effect on the rate of oxygen and nutrient diffusion, leading to difficulties in predicting cell survival upon encapsulation (4). Finally, the production of deformed microbeads is common and can have a significant impact on fibrotic overgrowth once implantations have been carried out (5). To overcome these challenges, emulsions have been used to produce relatively small microbeads with diameters <500 μm providing an alternative approach to encapsulate cells in polydisperse and spherical microbeads (6).

The gelation process of alginate microdroplets has been conducted by external and internal crosslinks with a calcium ion source such as calcium chloride ($CaCl_2$) and calcium carbonate ($CaCO_3$) (7). The external gelation of alginate micro-droplets containing cells is carried out by delivering the alginate/ cell solution to a calcium ion reservoir (8). Whereas the internal gelation of alginate microdroplets occurs when the alginate droplets themselves contain a calcium salt such as ($CaCO_3$) and are passed through an acid such as acetic acid promoting the release of calcium ions.

One of the most crucial challenges that emerge when encapsulating cells in microbeads is the ability to preserve cell viability when the micro-droplets are formed and polymerised, in addition to when the oil phase is discarded. Immediately after cell encapsulation occurs, a number of studies reported the initial percentage of cell viability to be over 80%. However, the cell viability dropped over prolonged periods, due to the oil phase inhibiting nutrient replenishment (9,10). Triggering the release of calcium from an insoluble calcium salt should be carried out with care, as lowering the pH could be detrimental to the cells over prolonged periods of time (11). Furthermore, the immiscible phase is usually removed by centrifuging the microdroplets, which are suspended in a culture medium and an oil phase. Furthermore, the choice of oil used has a significant effect on the percentage of cell

viability since remaining residues could be detrimental to cells (6). The process of centrifuging microbeads containing live cells could lead to a reduction in the rate of cell survival due to damages exerted to the microbeads and increased mechanical forces on the cells (12).

A brief overview of thesis structure is detailed in the following section.

1.2 Thesis Structure

This thesis has been divided into five chapters. Chapter One includes a brief introduction to the thesis, the aims and objectives and a literature survey on a number of different topics concerning cell encapsulation. In particular the literature survey conducted in this Chapter focuses on comparing materials used for producing microbeads, materials for fabricating microfluidic chips, methods for fabricating microfluidic chips, in addition to providing an insight into some fundamental microfluidic concepts.

Chapter Two describes the materials, methodologies and experimental procedures, which were used to make up the solutions that were needed to form alginate gel beads containing cells. Furthermore, results from cytotoxicity tests are shown in this Chapter. These tests were carried out in order to study the effect of the materials and formulations used on cell growth. Findings showed that alginate is indeed a suitable material that can be used for cell encapsulation. Alginate was therefore used to encapsulate cells in subsequent investigations throughout this Thesis.

Chapter three describes the materials, methodologies and experimental procedures that were used to produce alginate gel microbeads containing cells. A microfluidic setup driven by gravity also includes a detailed description of a microfluidic setup and its components. This microfluidic setup was constructed specifically to produce alginate gel microbeads. Furthermore, the microfluidic chip (PMMA MC1) described in this Chapter was fabricated from PMMA and allowed for the production of solidified alginate gel microbeads to occur internally (on chip) by the addition of an acidified oil inlet.

Chapter four gives a detailed description of the materials, methodologies and experimental procedures used to produce alginate gel microbeads using an optimised microfluidic setup. The microfluidic setup was optimised using syringe pumps to drive the fluids through the

system. Furthermore an additional two microfluidic chips (PMMA MC2 and PC MC3) were fabricated from polymethyl methacrylate (PMMA) and Polycarbonate (PC) respectively. This allowed for a direct comparison between both fabricating materials to take place. In addition, PMMA MC3 was designed with an acidified oil inlet; hence gelation occurred off chip (externally). These features allowed for direct comparisons between solidifying the alginate gel microbeads using both external and internal gelation methods. Results obtained showed that the optimised microfluidic setup produced polydisperse alginate microbeads containing cells that survived for 24 hours.

Chapter five concludes the work carried out in this Thesis and provides recommendations for future work.

1.3 Introduction

In recent years, an increased interest in developing three dimensional culture systems has emerged in the fields of cell biology and in particular cancer biology (13). This growing interest is due to increasing concerns that traditional 2D culture systems do not mimic the extracellular matrices of biological molecules that are found in tissues of living organisms. Therefore many cellular activities, such as cell-cell interactions and cell singling pathways cannot take place (13,14). Consequently, results obtained from 2D culture systems may be misleading. This means that there is a need to develop 3D culture systems, in order to encapsulate human and animal cells to conduct further extensive research studies. Furthermore, the development of a reliable 3D culture system at the microscale has great potentials for many biological and medical applications (15-20).

The materials and formulations used for the production of gel beads should be harmless to the encapsulated cell and should not produce any toxic by-products (21). Therefore, a diverse range of natural (22-47) and synthetic (48-69) polymers have been used to encapsulate cells in microbeads. A brief summary of the chemical structures, advantages and disadvantages of some of the natural materials used to encapsulate cells are described in this chapter. Investigations carried out in this Thesis involved using alginate as an encapsulating material because of the many advantages that this natural material has to offer such as: biocompatibility, its ease of crosslinking with an active form of an ion such as calcium, and because it was successfully used in our research group to fabricate microfluidic chips.

A selection of different materials have been used to fabricate microfluidic chips such as silicon (70,71), glass (72), polymethyl methacrylate (PMMA) (73,74) and Polycarbonate (PC) (74). PMMA and PC were used to fabricate the microfluidic chips described in this Thesis for a number of reasons as described in chapter 3 and 4. Besides this, there a

number of different technologies that can be used to fabricate the microfluidic chips. However, the choice of technology largely depends on the materials used to fabricate the chips. A summary of some of the most common technologies (75-77) used to fabricate the microfluidic chips are described in this chapter. This chapter also gives a brief overview of some of the most important physical concepts of droplet microfluidics are also reported in this Chapter. In addition this chapter provides a critical review on the different methods previously reported by other research groups on the production of microbeads, with emphasis on a number of different approaches employed for producing calcium gel alginate microbeads for cell encapsulation purposes.

1.4 Aims and Objectives

The main aim of this research work was to construct a microfluidic setup that was attached to a novel microfluidic chip, in order to encapsulate viable cells in spherical monodispersed calcium alginate gel microbeads while also aiming at a minimum survival rate of 24 hours, giving enough time for potential physiological process to occur as well as any necessary experiments to be carried out on the cells. Specific objectives of work carried out in this thesis aimed to:

- Determine the effect of formulations used for the production and degradation of the alginate gel beads on cell viability.
- Monitor the viability of encapsulated cells in calcium alginate gel beads.
- Construct a novel microfluidic setup, including a simple novel and reusable microfluidic chip to encapsulate single cells in calcium alginate gel microbeads.
- Determine the cell viability of encapsulated cells using the optimal microfluidic setup.

1.5 Literature Review

This section provides a detailed literature survey on a number of different aspects that need to be taken into consideration when producing beads to encapsulate live cells, and especially at the micro-scale. More specifically the literature focuses on providing a summary of some of the most common materials that have been used for cell encapsulation and fabricating microfluidic chips. In addition brief descriptions of the different technologies used to fabricate the microfluidic chips and a summary of the physics behind microfluidics are also provided in this literature survey.

1.5.1 Microfluidic technology

Microfluidics is the science and technology that involves processing and manipulating minute amounts of fluids, by means of microchannel networks. Microfluidics has gained popularity due to the many advantages that this technology has to offer, including: small amounts of samples and reagents are sufficient enough for analysing samples, the ability to separate and detect samples with high resolution and sensitivity, cost effectiveness and short analysis time (78).

At present, microfluidic systems in its simplest form compromise a chain of common components, including: means of introducing fluids such as samples and reagents to the system, moving fluids in the chip and mixing and combining fluids (72).

1.5.1.1 Microfluidic chips

Microfluidic chips have been fabricated using a broad range of materials including silicon (70), glass, polymers, ceramic and metals. Silicon was the first material used to fabricate microsensors in the early 1970s. However as technology progressed, non-silicon based materials were developed, which led to the establishment of a new field termed microelectromechanical systems (MEMS) (70). Furthermore, the use of inkjet printer heads showed that significantly small amounts of fluids in microchannels can be

manipulated (70). Terry and colleagues reported the construction of a miniature gas analysis system based on the concept of gas chromatography. This system involved fabricating the main components in silicon, which decreased the size of the system by 3 orders in comparison to conventional instruments (70,71). Subsequent studies showed that it was possible to handle sample of minute volumes, which led to the introduction of the miniaturised total chemical analysis systems (μTAS) concept in 1990 (70,78). Shortly after the introduction of this concept, many companies started to adopt such systems for applications in life science, which led to the usage of polymers instead of silicon. The rapid development in this field led to the introduction of new terminologies amongst researchers for example: microfluidics and lab on a chip (LOC) (70). The use of silicon to fabricate microfluidic chips is adventurous for many chemical reactions, such as those that require high temperature and strong solvents. Despite these advantages, alternative materials to silicon have been used to fabricate microfluidic chips for several reasons, including the high cost, optical opacity and is not is suitable for biological application. In addition, micromachining is laborious, costly and needs specialised skills and instruments (79).

Glass is another material that has been used to fabricate microfluidic chips due the many advantages it has to offer, including its optical properties and well known structure. However, the use of both glass and silicon to fabricate microfluidic chips is quite often unnecessary, unsuitable, hard to machine, breaks easily and is costly. Most importantly, these materials do not have all the properties that are needed for living cell to function properly, for example the cells attach to glass and permeability to gases is limited (80). Therefore, as microfluidics continues to be in cooperated in biological and medical applications, the need to explore other materials was needed. This led to the use of other materials for fabrication purposes, such as polydimethylsiloxane (PDMS) (73), polymethyl methacrylate (PMMA) (73) and polycarbonate (PC). Subsequently, these polymers have

been extensively used as an alternative to silicon and glass, since these materials offer many advantages, some of which include:

- Gas permeable (81).
- Relatively inexpensive.
- The ability to produce microfluidic chips on a large scale using injection molding and CNC milling techniques, which are relatively inexpensive and fast techniques.
- The optical and mechanical properties of these natural polymers as well as their resistance to chemicals such as acids makes them suitable for use in almost any application (82,83).

1.5.2 Advantages and disadvantages of microfluidics

Microfluidics offers many advantages, some of which are listed below:

- **Portability:** The size of microfluidic setups and in particular the microfluidic chip is small enough to be transferred from one place to another. This is an essential element in many fields for example, in the healthcare profession, forensic sciences and the detections of chemical and biochemical wastes (84,85).
- **Reduced consumption:** Minute amounts of samples and reagents are needed in microfluidic studies, which in turn reduce the overall cost and waste (84,85). This a major advantage in biological and medical related research since reagents such as antibiotic are expensive and samples are often limited.
- **Parallelism:** Microfluidics allows for reactions to take place in a parallel manner. This is a major advantage in many fields such as biochemistry, genomics and the pharmaceutical industries (84).

- **Safety:** Microfluidics offers a safer environment to carryout biological and chemical studies. This advantage is due to the reduced size of samples and formulations needed.
- **Reduced size:** The sizes of channels in the microfluidic chips that are fabricated to produce microbeads in this Thesis have dimension as small as 100 μm and can be made even smaller if needed, which is an optimal feature to manipulate single cells.

The development of microfluidics is still ongoing, however, there still remain some challenges that have been encountered in the work carried out in this Thesis and reported by others in the literature, some of which are listed below:

- **Physical and chemical properties:** Some physical and chemical properties may prevail at smaller scales.
- **Reusability and sterility of the microfluidic chips:** Most microfluidic chips are not reusable and if they are it is difficult to keep them sterilised (86).
- **Initial costing:** Initially the fabrication of the microfluidic setup can be expensive (86).
- **Mixing the fluids together can be challenging**

1.5.3 The physics of microfluidics

This section summarises a number of physical phenomena observed at the microscale.

1.5.3.1 Reynold number

Reynolds number is an important concept in the field of fluid dynamics, and can be defined as the ratio of fluid momentum to frictional forces, which is caused by the channel walls. Based on this concept, fluid flow can be divided into two main regimes: Laminar and

turbulent flows. Fluid flow is laminar if the Reynolds numbers is low and turbulent when it's high, typically above Re=2000. Equation 1 defines the Reynolds number (84,87):

$$\boldsymbol{Re = \frac{\vartheta D_H}{\mu}} \qquad \textbf{Equation 1.1}$$

Where ϑ represents the average velocity of the fluid (m/sec), μ represents the kinematic viscosity (m²/sec) and D_H is the hydraulic diameter (m), which is defined as follows (84,87):

$$\boldsymbol{D_H = \frac{2}{\frac{1}{h}+\frac{1}{w}}} \qquad \textbf{Equation 1.2}$$

Where h represents the square channel height and w represents the width.

1.5.3.2 Surface area to volume ratio

The surface area to volume (SAV) ratio is even more important at the microscale, since it increases dramatically. This is an important factor that was accounted for in the microfluidic work carried out in this Thesis, as acidified oil for example was used in the gelation process of the calcium alginate gel microbeads containing Jurkat cells.

1.5.3.3 Surface energy

Surface tension forces are also an important factor at the microscale. Surface tension occurs at the liquid/gas interphase due to the solidarity between liquid molecules. The amount of tension within a surface can be measured and is known as surface free energy. Moreover, the height at which the water travels through within a capillary is directly proportional to the surface free energy of the water, and is inversely proportional to the capillary's radius. Therefore, since the channels in the microfluidic chip are microns in size, the length that the fluids are driven through the chip is significantly dependant on capillary forces.

A number of approaches have been exploited to study the surface energies within a microfluidic setup, such as the creation of virtual walls (79,88) and pumping mechanisms (79,89). The Young-Laplace equation listed below can be used to calculate the pressure that is caused due the liquid surface which is perpendicular to the radii of the curvature. The Young-Laplace equation is defined as:

$$\Delta \boldsymbol{P} = \boldsymbol{\gamma}\left(\frac{\mathbf{1}}{\boldsymbol{R_1}} + \frac{\mathbf{1}}{\boldsymbol{R_2}}\right) \qquad \textbf{Equation 1.3}$$

Where ΔP represents the pressure, γ represents the liquids surface free energy and R represents the length of the wall. When using virtual walls, R goes to infinity reducing the equation to:

$$\Delta \boldsymbol{P} = \frac{\boldsymbol{\gamma}}{\boldsymbol{R}} \qquad \textbf{Equation 1.4}$$

Pressure is an important factor to be considered because excess pressure can kill the cells (90).

1.5.4 Microencapsulation

Microencapsulation is a simple and inexpensive technique, which was first proposed by Chang in the 1960s to enclose biomaterials such as cells and drugs into minute beads or tubes (91,92), by exploiting temporary three-dimensional scaffolds that provide a steady environment for cell growth and development. These scaffolds are made up of a semi-permeable membrane to shield the encapsulated biomaterials from potentially harmful substances, whilst allowing nutrients and other small molecules such as oxygen, glucose and insulin to be exchanged between the capsule and its outer environment through pores (91,93,94). However, it wasn't until 1980 when Lim and Sun developed a novel microencapsulation procedure using alginate microcapsules, which initiated a new stage in biomaterial encapsulation (94). Since then, remarkable attempts have been made to

introduce and develop microencapsulation in the field of biomedicine, such as in drug delivery and organ transplants, as well as its use in biotechnology, such as large scale cell culturing and fermentation (95). However, despite of the growing development in the use of microencapsulation, and the potential benefits this technique may have in curing a variety of medical conditions such as type-1- diabetes and organ replacements (by protecting cells from immune attack), microencapsulation as it stands today can only provide temporary solutions, given that the beads will most likely need to be changed every few months. This brief solution may be good news for many individuals, for examples those who suffer from conditions such as type-1- diabetes, because of its promising ability to provide patients with an alternative treatment to daily injections. This treatment will involve encapsulating individual insulin-producing cells pancreatic islet beta in a suitable material, which will protect the cells from immune rejection, yet at the same time they can still regulate the glucose level and secrete insulin (96,97). However more development in this area is needed in order for it to be successfully applied in other areas such as transplantations (91).

Microencapsulation as any other technology has some drawbacks associated with it, with the most common drawback being that the scaffolds used must be cell friendly, which in turn limits the amount of materials and formulations that can be used during the process of encapsulation. Despite this, many materials have shown to be biocompatible as described in the following section.

1.5.5 Introduction to hydrogels

Hydrogels are networks of cross-linked hydrophilic polymer chains, which provide a three dimension network. These gels are highly absorbent, providing suitable environments that resemble natural tissues. Hydrogels are therefore suitable candidates for applications in various fields such as tissue engineering and drug delivery (98) Many natural and synthetic

polymeric materials have been used to make hydrogels The choice of materials that are used for cell encapsulation depends largely on the ability to mimic the extracellular matrix, in addition to providing suitable conditions for cell survival and growth (99). These materials can be derived from natural such as collagen and gelatine, hyaluronate, fibrin, agarose, chitosan and alginate (22-47) or synthetic polymers such as poly(acrylic acid) PAA, poly(ethylene oxide) and its copolymers, poly(vinyl alcohol), polyphosphazene and synthetic polypeptides (48-69) and can form hydrogels.

Hydrogels made from natural polymers have gained increased importance for cell encapsulation purposes (100), because of the many advantages that these polymers have to offer including: high porosity (38), biodegradability, biocompatibility, and non-toxicity. In addition natural polymers do not cause undesirable developmental or reproduction effects. However, many commercial natural polymers seem to have different biocompatibilities and properties (22,100,101). Impurities found associated with natural polymers are most likely from the biological sources that they originate from. Some of the common impurities include: proteins, bacterial products, complex carbohydrates, fatty acids and phospholipids (102). It is therefore important to have reliable and standard purification methods in place when using natural polymers as hydrogels, in order to minimise the effect impurities can have when studying in vivo performances.

Furthermore, hydrogels that are formed from natural materials almost resembles the extracellular matrices that are found in a number of human tissues (99). Once formed, the hydrogels exhibit a number of various transport properties depending on: the structure, chemical composition and the degree at which these hydrogels have been crosslinked. This is a vital feature as it determines the ability of the encapsulated cells to obtain nutrients and remove wastes within a 3D network, in turn enhancing cell survival and reducing cell death. Furthermore, the hydrogel matrices act as barriers towards incoming and outgoing

molecules. The molecules that can diffuse through the matrices of these hydrogels have upper size limits. Therefore, when designing a hydrogel system of cell encapsulation, it is vital that oxygen, signalling molecules, nutrients and wastes are able to diffuse through the extracellular membranes, since cell survival and growth depends in the permeability of these components and the removal of waste bi-products. This leads to the generation of different gradient concentrations, such that the cells that are further away from matrix borders will obtain fewer nutrients. Hence, low mass transfer rates of nutrients may be sufficient enough for cells to survive at the border of the matrices but not sufficient enough for cells that are encapsulated within the core of these hydrogels to survive. Thus suggesting that hydrogels such as microbeads with high surface area to volume ratios provide a suitable environment of cell survival (103). The upper size limits of these microbeads are usually 400 μm in diameter (104). In general microbeads provide a more subtle environment for cell survival as the exchange rate of substances, such as nutrients and oxygen between cells and the surrounding environments is higher than that of other standard size beads, which are roughly around 500-1000 μm in diameter (105). Furthermore, the size of the microbeads has a significant effect on their mechanical properties. The smaller the microbeads, the less prone they are to breakages (106). A study carried out on cells that were encapsulated in significantly small beads led to inadequate encapsulation, as the cells protruded from the microbeads (107). However, there is significant evidence that microbeads are generally more biocompatible than larger beads (108,109).

1.5.7 Hydrogels from natural polymers

1.5.7.1 Collagen and Gelatin

The most extensively used tissue-derived polymer is collagen. This natural polymer is the main component that makes up extracellular matrices in mammalian tissues, such as skin, bones and ligaments (110). The subunits of collagen are usually synthesised from free amino acids, which are found in fibroblasts and osteoblasts (111). In nature the most abundant type of collagen is collagen type I. The extraction of Collagen type I is carried out by enzymatic and acid treatments (112).

Collagen proteins contain a triple helix structure; with every third amino acid within this structure being glycine. Glycine is relatively small in size, and therefore the centre of the triple helix structure is occupied by these small amino acids, allowing the three chains to be packed together tightly. Hence, the triple helix sequences of collagen consist of sequences of Gly-Xaa-Yaa residues, where, Xaa and Yaa are any other amino acid residues. Furthermore, 30% of the remaining amino acid residues within the triple helix structure are proline and hydroxyproline. The side chains of these amino acids as opposed to glycine point outwards within the triple helix structure (113).

Collagen hydrogels exhibit poor mechanical properties (114), such as the ease of deformation and degradation, which limits its use in many cell encapsulation studies. Many attempts have been carried out to improve the mechanical properties of these hydrogels for example by cross-linking collagen chemically with glutaraldehyde (27) or diphenylphosphoryl azide (28). Collagen meets numerous design requirements for a number applications other than cell encapsulation studies such as forming tissue culture scaffolds (22) and the reconstruction of vital organs, including: liver (29), and small intestine (30). Collagen gels have also been used as tissue culture scaffolds (22). One the most fundamental elements to the successful use of this natural polymer for such

applications are due to its rapid biodegradability in mammals, which can be controlled via enzymatic treatments or chemical cross-linking. Enzymatic treatment can be applied to collagen since it is made up of amino acid sequences that are recognised by cells and can be broken down by an enzyme called collagenase (115). However, some approaches to improve collagen hydrogels still exhibit limited physical strength, are possibly immunogenic and can be costly (116). Another complication that can arise is the difference of each collagen batch produced from one another. Despite, the drawbacks associated with the use of collagen, the triple helix can be broken down into single stranded molecules, producing gelatin (22,117).

Gelatin is divided into two categories: gelatin A and gelatin B. When collagen is subjected to acidic treatment, followed by thermal denaturation, gelatin A is formed. Gelatin B, on the other hand, is formed when collagen is treated with an alkaline (22). Gelatin is a thermoresponsive polymer (temperature responsive) polymer (99), since the physical properties of these polymers change with a change in temperature (118). In a water based solution, gelatin undergoes a reversible transition from solution to gel when the temperature is cooled to 35^{o}C. The gelation process of gelatin polymers can be reversed by heating up the gelatin gel to physiological temperatures. This physical property has been the basis an attempt to fabricate hydrogels with a gelatin core that can liquefies once the hydrogels are heated up to physiological temperature (119). In addition to this gelatin beads has been used to fabricate porous cell-laden hydrogels, where these beads act as porogen (120). Cell-laden hydrogels are three dimension gel scaffolds that have been fabricated to encapsulate cells within native tissue-like-structures (121). Furthermore, gelatin has been chemically modified with methacrylate groups for example so that gelatin gels are not liquefied at physiological temperature (117,122,123). The biocompatibility of these hydrogels in addition to the ability to control their stability makes modified gelatin

hydrogels a suitable candidate for many cell encapsulation applications encapsulate cells (31,99).

1.5.7.2 Hyaluronate

Hyaluronic acid is a glycosaminoglycan that is found in extracellular matrices of all living organisms, in the majority of connective tissues in addition to being produced by bacteria (124). This glycosaminoglycan polymer is synthesised by membrane bound hyaluronan synthase, which also allows them to be differentiated from that synthesised in the Golgi apparatus. The process of obtaining hyaluronic acid from its native source is typically achieved either by extraction or enzymatic digestion. Furthermore, since the sources and extraction protocols of Hyaluronic acid vary, different behaviours in vivo and in vitro experiments are observed (125,126). The structure of hyaluronic acid is conserved in all living organisms, which is a linear anionic polysaccharide consisting of 1,3-β-D-glucuronic acid and 1,4-β-*N*-acetyl-D-glucosamine (126). This polymer is hydrophilic and highly viscous solutions can be formed at low concentrations (127). Hyaluronic acid has shown to have many potential uses in tissue engineering, for instance in artificial skin (128) wound healing (22), in addition to this it is commonly used as a lubricant (129). In solution, hyaluronic acid molecules are stiffened due a number of factors including: the chemical structure, the internal hydrogen bond in addition to the interactions that occurs with the solvent (130).

In order to form hydrogels from Hyaluronic acid, the polymers need to be subjected to chemical modifications. This procedure can be carried out by modifying the carboxyl or the hydroxyl groups of these polymers by esterification and crosslinking with glutaraldehyde for example (131). Hyaluronic acid polymers have been used to encapsulate

cells once treated with methacrylic anhydride, producing methacrylated hyaluronic acid, which is a photo-cross-linkable polymer (132).

A study carried out by Seidlits *et* al. showed that the mechanical properties of methacrylated hyaluronic acid can be modified to almost resemble the natural central neural tissues (132). As anticipated, the compressive modulus depends on the initial degree of methacrylation (DM), which ranged from 3 to 10 kPa for 1% w/v hyaluronic acid and a molecular weight of 1500 kDa. Moreover, the diffusion of small molecules was noted to be inversely proportional to the DM. Another study that was carried out by Bencherif *et al*. reported that the shear modulus of hyaluronic acid hydrogels increased with an increase in DM. However, this observation was less pronounced when highly methacrylated hyaluronic acid hydrogels were investigated (133). In this study the hyaluronic acid hydrogels with a DM of 14%, 30% and 90% had shear modules of 15, 30 and 90 kPa respectively. Furthermore, it was reported that no significant change in cell attachments and proliferation was observed when cells were encapsulated in hyaluronic acid hydrogels with different DM.

Cell adhesion is not favoured in hyaluronic acid hydrogels but these hydrogels can be modified for such purposes (134). Hyaluronic acid hydrogels are typically used to encapsulate hyaluronic acid itself or glycosaminoglycans rich cell lines (135,136). Hyaluronic acid is rapidly degraded in living organisms by hyaluronidase, β-glucuronidase and β-N-acetyl-glucosaminidase (124).

1.5.7.3 Fibrin

Fibrin has a vital function in natural wound healing and is the key component for clotting blood. Fibrin is formed due the polymerisation of protein (fibrinogen). The fibrinogen in the presence of thrombin at room temperatures forms fibrin gels (32,137). Fibrinogen is a

glycoprotein of 340 kDa and is soluble in water. This glycoprotein is made up from two strands of three polypeptide chains linked by disulphide bonds. Fibrinogen is primarily produced in the liver, is present in human blood and its concentration is known to increase post-trauma (99). Isolating fibrinogen from the plasma can be carried out via precipitation, followed by a series of freeze/thaw cycles or alternatively by using chemicals that decreases the solubility of these proteins (138). Fibrin monomers are formed as a result of thrombin catalysing the cleavage of fibrinopeptides (139). This cleavage takes place at the central N-terminal of the fibrinogen, resulting in the exposure of A and B knob binding sites (140). Insoluble fibrin fibres are produced as a result of these knobs interacting with the A and B holes, which are located at the terminal of the fibrinogen molecule. These fibrin fibres form a three-dimensional network, which can be stabilised in the presence of calcium, which causes transglutaminase factor XIIIa to crosslink. This factor is obtained from the cleavage of factor XIIIa, which is mediated by thrombin. Factor XIIIa is an enzyme, which promotes stem cell adhesion and proliferation (141). The concentrations of the fibrinogen and thrombin have an effect on gel formation and the mechanical properties of the gels (142). Reducing the concertation of thrombin, results in the formation of more compact gels that have thicker fibres and improved mechanical properties. This feature becomes crucial when using fibrin as a matrix to encapsulate cells, since the concentration of thrombin and fibrinogen have significant effects on the rate of cell proliferation and their differentiation (99). Findings from a study carried out by *Catelas et al.*(143) showed that reducing the concentration of fibrinogen to 5 mg ml^{-1} can support cell growth. On the other hand increasing the concentration to 50 mg ml^{-1} resulted cell differentiation.

Fibrin can degrade quite fast in mammals due to the presence of fibrinolysis, which are proteolytic enzymes. As a matter of fact, fibrin degrades slowly during wound healing and

is replace by mature extracellular. The degradation kinetics of fibrin can be controlled by a proteinase inhibitor for example Aprotinin (144,145).

Fibrin hydrogels can be made up from a person's own blood, and can be used as a scaffold for tissue engineering (32). Fibrin hydrogels can be produced *in situ* by injecting a cell suspension in fibrinogen and thrombin. This approach has generated interests in many tissue engineering applications such as regenerating many cells including skeletal (144) and smooth muscle cells (146).

1.5.7.4 Agarose

Agarose is a polysaccharide that is isolated from the cell walls of Rhodophyceae (red algae) (147). Agarose is extracted from these plants after a succession of purification and homogenization steps are carried out (148). Agarose is made up from alternating units of β-D-galactopyranose and 3,6-anhydro-α-L-galactopyranose. The chemical composition of agarose obtained from varying sources may differ, such as a variable substitution of the hydroxyl groups with sulphates. Agarose polymers are responsive; they undergo a solution- gel transition in aqueous solution once cooled. However, when agarose is placed in a solution and the temperature increases above the of the solution-gel temperature, a random-coil confirmation is observed, which once cooled changes into double helix structures. The temperature at which agarose gels are formed depends on a number of factors including: the concentration of the solution containing agarose, the average molecular weight of these polymers and their structure. Therefore, agarose is known to have different physical characteristics such as: different gel strengths and solution-gel transition temperatures. Some of the polymers can be used to encapsulate cells, since the solution-gel transition is around the physiological temperature. The solution-gel transition temperature of agarose like a number of other polymers is reversible; however, there is a large difference in temperature between the gelation and liquefied states of these polymers

(149). As a consequence the average size of agarose hydrogel pores and the mass transport properties are governed by two main factors: the concentration of agarose in solution in addition to the settling temperature (150). A study carried out by Narayanan *et al.* showed that the pore size for a Bio-Rad certified low-melt agarose at a concentration of 1% w/v was 600 nm. However, this value decreased to 100 nm and less when the concentration of the agarose increased to 3% w/v (151). Agarose hydrogels are produced with smaller pores and higher elastic modulus when the settling temperature is reduced. This observation has been reported in another study that was carried out by Aymard *et al.* where they showed a reduction in the elastic modulus for I-A agarose, which was purchased from Sigma and a had gelling temperature of 36^{o}C, from 78 kPa for agarose samples that are cured at 5^{o}C to 53 kPa for samples cured at 35^{o}C (152).

Interactions between adherent cells and the entrapped matrix do not occur because the cells have no receptors for the polymer (153). However, this problem can be tackled by supplementing the agarose hydrogels with extracellular adhesion molecules, for example fibronectin (154) or soluble RGD peptides (155). Agarose degradation is only achieved by specific bacteria, and hence it is not biodegradable in mammals. These hydrogels can be degraded *in vitro* by agarases. These enzymes are divided into three main categories depending on their cleavage pattern, including: α-agarase, β-agarase and β-porphyranase (156-158).

Agarose hydrogels have been used in many applications such as cartilage rapair *in vitro* (159), and in cell encapsulation studies once physiological conditions met (160). However, despite the improvements made to these hydrogels, their use is limited for microencapsulation purposes because they temperature regulated and due to their biodegradability, which in turn inhibits repair processes *in vivo* (161).

1.5.7.5 Chitosan

Chitosan is a polysaccharide extracted from naturally occurring polymers called chitin. Chitin is produced as a structure component of the exoskeleton of many natural species (162). This natural polymer is made up from N-acetyl-D-glucosamine chains that form semi-crystalline structures. The chemical structure of chitin is similar to that of cellulose, which is another structural polysaccharide; the difference being the substitution of a hydroxyl position at C-2 with an acetyl amide group (163). The most common sources of chitin that is available commercially are crab and shrimp shells. Chitin is extracted from these shells by dissolving the minerals with an acid treatment, which is followed by a purification step to remove proteins from the surrounding tissues by an alkaline treatment (164,165). Furthermore, some of the acetyl groups that are bound to the amine can be removed as a result of alkaline treatment (166). When 50% deacetylation or more is achieved, the polymer is then referred to as chitosan. Chitosan is soluble in acid solutions, as a result of the protonation of a primary amine (162). Chitosan has been used in a layer by layer sequential technique, allowing the production of multi-layered thin films, which are made up from opposite charged polymers (167,168). Polyelectrolyte complexes can be rapidly formed using chitosan and other poly-anions such as alginate (169). For example, a number of studies have reported the use of chitosan/alginate multi-layers to coat alginate gel beads containing cells, which results in the production of capsules liquefied core (170,171). The physical, mechanical and biological properties of chitosan polymers are related to the degree of deacetylation (99), which has been shown in a number of studies (172-174). A study carried out by Tomihata & Ikada showed that as the degree of deacetylation increases the rate of degradation decreases (172). The rate of degradation of chitosan was shown to be very low when chitosan was completely deacetylated. These observations were confirmed in another study carried out by Freier and colleagues, where the rate of degradation of chitosan was prolonged when this natural polymer was

completely deacetylated (173). This study investigated the compatibility of chitosan and *N*-acetylated chitosan with neural cells. The findings from these investigations showed that chitosan based films were indeed compatible with neural cells, as good adhesion and proliferation were achieved. Furthermore, another study carried out by Chatelet *et al*. reported that the degree of deacetylation on the *in v*itro compatibility of chitosan had no significant effect on to cell lines (keratinocytes and fibroblasts). Despite these observations, cell adhesion and proliferation of both these cell lines were influenced by the degree of chitosan deacetylation (174). However, the fibroblasts adhered to chitosan twice as much as keratinocytes. Moreover, the fibroblasts did not proliferate irrespective to the numbers of acetyl groups. Chatelet *et al*. suggested that this observation was probably due to a change in the growth rates of fibroblasts as a result of their high affinity for chitosan based materials.

Chitosan gel precipitates are formed when a chitosan acidic solution is alkalinised up to the physiological pH. Once the protonated amine within the chains is neutralised, hydrogen bonding and hydrophilic interactions lead to the formation of a three-dimensional network (175). The addition of phosphate salts within a chitosan solution causes chitosan to become soluble and thermoresponsive at physiological pH, and as a result chitosan gels are formed at physiological temperature (176,177). The solubility of chitosan at neutral pH can be chemically modified without influencing the biocompatibility and biodegradability of these natural polymers. These chemical modifications usually involve covalent binding, which is carried out polymerising the free amino acid or hydroxyl groups (178,179).

1.5.7.6 Alginate

Alginate is one of the most common biomaterials used for drug delivery and tissue engineering due to many factors including its biocompatibility, low toxicity, low cost and its ability to form gels easily in the presence of divalent cations, like Ca^{2+} and Mg^{2+}.

Commercially available alginates are mostly extracted from three different types of brown algae called Laminaria hyperborean, ascophyllum nodosum, and macrocystis pyrifera (48). In nature, alginate exists in the form of blended salts containing many cations that are found in seawater such as Mg^{2+} and Na^{+} (35). Alginate has been used in many applications such as injectable cell delivery, dressing up wounds, dental impressions (37,180) and in treating diabetes (181).

However, despite the advantages offered by alginate gels, alginate in its native form may not be the best choice of material, as it's known to degrade due to divalent ions being lost into surrounding mediums. This degradation process is usually unpredictable and cannot be controlled, and hence many approaches involved alginate being covalently crossed-linked with a variety of molecules in order for the swelling and mechanical properties of alginate gels to be controlled (39). Another disadvantage of using alginate is that its molecular weight is higher than the kidney's clearance threshold (40). However, over the years much effort has been employed to improve the use of alginate beads for biological and medical applications (1,6,26,41,109,182-186).

Alginates are made up from a linear block of consecutive α-l-guluronic and β-d-mannuronic acid residues. The sequences and structure of alginate varies from an alginate molecule to another, depending on the composition of α and β block regions that they consist of (Figure 1.1). Alginate extracted from L. hyperborean has a high number of G-blocks, alginate extracted from A. nodosum has a low amount of G- blocks and alginate extracted from M. pyrifera has an even lower amount of G-blocks than that found in A. nodosum. Therefore, the physical properties of alginates depend on the composition and length of the sequences. (35,42,43).

Another attractive feature for using sodium alginate is the ability to control the degradation process, which can be carried out by isolating the 6000 Da G-blocks from the alginate.

This process is then followed by oxidizing and covalently cross-linking the derivatives with adipic acid dihydrazide. Therefore, the gelation and degradation processes of alginate polymers can be controlled and is subject to the cross-linking density (22).

The sodium alginate used to produce the calcium alginate gel beads in the experimental work carried out in this Thesis, was purchased from Sigma Aldrich and contained approximately 61% M blocks and 30% G blocks.

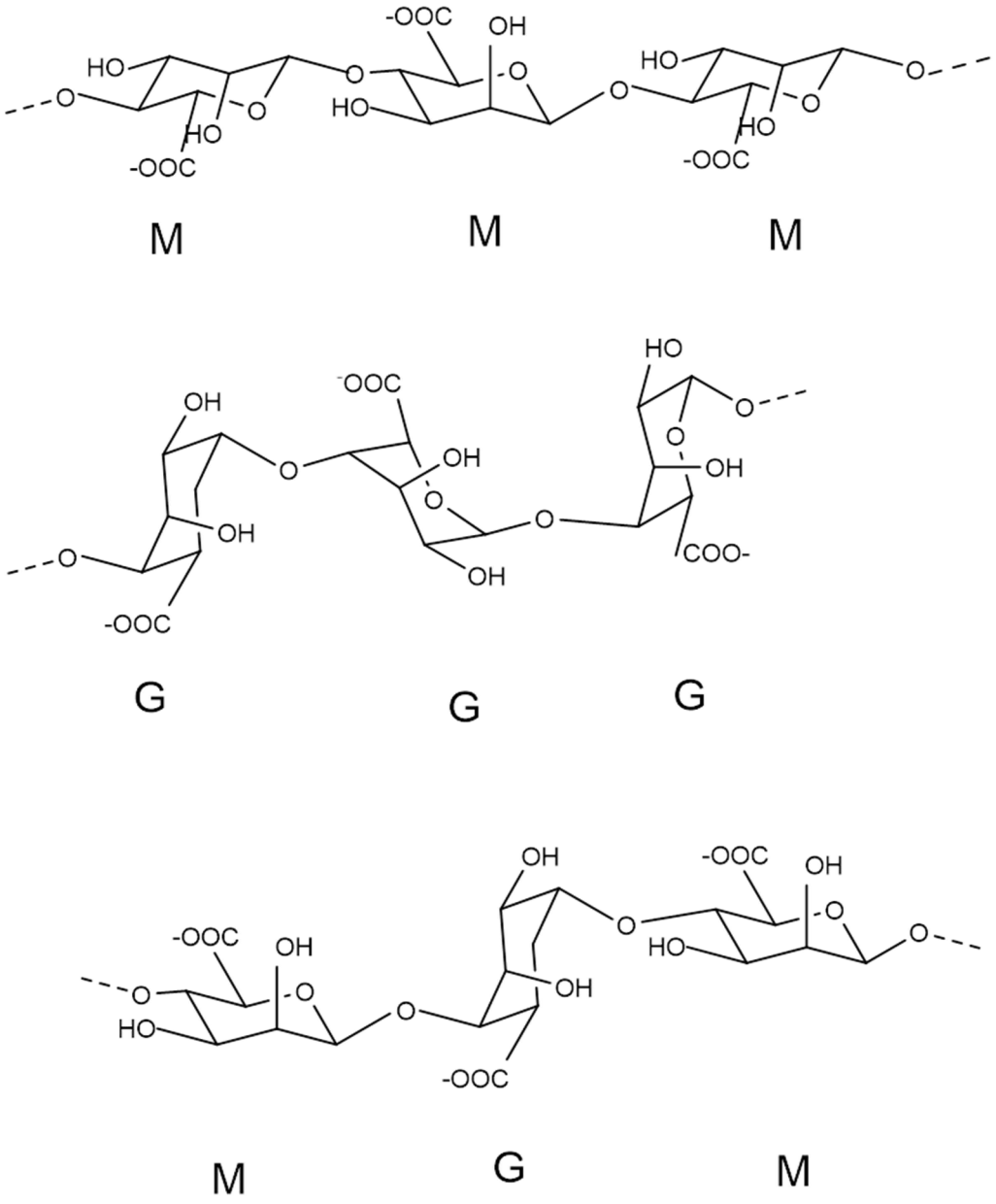

Figure 1.1: The possible configurations of the chemical structure of alginate adapted from [51, 58]

1.5.8 Microbeads

The production of microbeads otherwise known as droplets (187,188), hydrogels (6,189,190) or microspheres (1) for biological (17,191) and medical applications (17) is an emerging field. This is due to the many advantages that microbeads have to offer such as the ability to perform analysis on the single cell level and fast diffusion/ media change without any cell to cell contact. Further advantages include the reduced amount of samples and formulations needed to produce microbeads. Microbeads can be formed in channels, between two plates or on an open surface chip. The work carried out in this Thesis involved producing microbeads in channels. Throughout this Thesis the term microdroplets is used before the gelation process is initiated, the term microbeads is used once the gelation process occurs and the term microparticles is used to describe or refer to either the microdroplets or microbeads depending on the context.

1.5.9 Preparation of spherical microbeads

1.5.9.1 General considerations:

The main function of a hydrogel in the field of cell biology is to provide a three dimensional network environment for cells. A number of important criteria should, therefore be taken into consideration when designing a device for cell encapsulation, including:

- The solvents and materials used should not be harsh to avoid cell damage.
- The gelation process of the gel beads must be mild to avoid cell damage.
- The structure of the gel beads should be compatible with cell division.
- The by-products of degraded gel beads should not have a significant effect on the encapsulated cells (21).
- The gel bead should be permeable to nutrients and allow the release of waste.

A number of cell encapsulating devices have been reported in literature and can be divided into two main classes: macrodevices and microdevices (192).

The use of microbeads in cell encapsulation studies is on the rise since they provide similar conditions to that of cells in tissues and organs. Moreover, in comparison to other scaffold geometries such as microfibers (192), microbeads provide an optimum surface area for nutrients and oxygen to diffuse, which has a positive impact on the percentage cell viability (193).

1.5.9.2 Dimensional, morphological and permeability properties

The dimensional, morphological and permeability properties of microparticles are vital for cell biology applications. These properties influence a number of aspects such as the biocompatibility and diffusion properties (104,194). The ability to mediate the transportation of molecules in and out of microparticles also determines their success for cell encapsulation purposes. Extensive research has been carried out to control the diffusion and porosity properties of microparticles in attempts to prevent immunogenic molecules from entering these particles. For example alginate gel microbeads that are cross-linked with calcium ions usually have pore sizes ranging from 5 to 20 nm. This property prevents only relatively large molecules from entering the microbeads. However, it has been reported in the literature that the porosity of these microbeads can be controlled when layers of polyelectrolyte is formed on the surfaces of alginate hydrogels (104).

The shape of the microparticles used to encapsulate cells is another important property that needs to be taken into consideration, since the shape of these microparticles effect *in vivo* performances. The irregular morphology of microbeads can be due to coalescence, which is the phenomenon used to describe fused or partially fused microparticles (186).

Furthermore, defects in the microparticles due to cracks for example in combination with irregular surfaces can be the underlying cause of unwanted immune responses (104).

1.5.9.3 Microbead characteristics

Microbeads can be used in many cell biology and medical applications for a number of reasons including: the wide range of sizes at which microbeads can be produced, their relatively low masses and well defined shapes. Therefore, many biomolecules such as cells can be encapsulated in microbeads, which is advantageous as reagents are expensive, samples are often scarce and that single cell studies can be performed, since single cells or small groups of cells can be placed in defined positions to each other (195).

1.5.9.4 Microbead shapes and dispersity

Microbeads of various sizes ranging between 1 pL to hundreds of nanoliters have been reported in literature for use in biochemical assays (187,188). Smaller microbeads however can be produced but their use is limited for cell encapsulation applications, particularly if the size of the cells is greater than that of the microbeads. Moreover, challenges arise when smaller microbeads are imaged using standard optical methods such as light microscopes, because they have reached their resolution limits. The size of microbeads can be controlled, depending on the geometry of the microfluidic chip used to produce the microbeads and fluid flow rates applied through the microfluidic setup (187,188). The sizes of cells vary, for example Jurkat, HL60 and Neutrophil cells have diameters roughly around 11.5 12.4 and 8.3 μm respectively (196).

1.5.10 Gelling mechanism

Cell encapsulation is commonly initiated in a water-based solution containing a hydrogel precursor (referred to as the solution flowing phase). The resultant suspension is then subjected to physical, chemical or biochemical processes in order to initiate the gelation process. Each step within the cell encapsulation process should allow cells to survive and

cause minimal stress. Hence the conditions within the hydrogel should mimic the physiological conditions as much as possible (99). However, in some cases these requirements are not feasible, for example photo-cross-linkable polymers. In such cases, it is therefore vital to pay particular attention not only to the toxicity involved in the gelation process, but also to the exposure time (197).

A number of thermoresponsive gels have been used to produce beads. Some of these polymers such as elastin and collagen form gels when they are heated above the transition temperature. These polymers present a lower critical solution temperature (LCST). Decreasing the temperature below the LCST causes the polymers to become miscible with water. In contrast, other polymers such as gelatine and agarose form gels when cooled. These polymers present an upper critical solution temperature (UCST). Increasing the temperature above the UCST causes the polymers to become miscible with water. However, if the temperature drops below the UCST, the polymers' hydrophobicity increases and becomes insoluble in water, which leads to the formation of gels (198,199). Furthermore, dissolving polymers in water can lead to three possible interactions (200): polymer-polymer, polymer-water and water-water. The polymer-water interaction is unfavourable when undergoing a change in temperature. This causes random coils to change into helices in order to reduce the macromolecules' exposure to water. Gel transition temperatures of the thermoresponsive polymers used to encapsulate cells should be around 32^{o}C since this is close to body temperature (201).

Polymers such as alginate and hyaluronic acid form gels when an electrically charged species is present. Such polymers have a net charge on their backbone and are often referred to as polyelectrolytes. The combination of polyelectrolyte polymers and multivalent cations with opposing charges results in the formation of complexes that are insoluble in water (202).

Hydrogels that are cross-linked ionically or thermally are formed as a result of ionic or secondary forces. These hydrogels are easily dissolved under suitable conditions, such as allowing ionically cross-linked hydrogels to be in contact with chelating agents in order to remove the ions that are cross-linked, or by reversing the temperature of thermally cross-linked hydrogels.

1.5.10.1 Internal and external gelation of alginate microdroplets

After the alginate microdroplets are formed using a microfluidic chip, the micro-droplets undergo a gelation process to form alginate gel microbeads. This process usually involves cross-links between the alginate polymer chains with a divalent cation. The affinities of alginate towards the divalent ion vary in the descending order of Pb > Cu > Cd> Ba > Sr > Ca > Co, Ni, Zn > Mn (203). Despite this calcium Ca^{2+} is mainly used in the gelation process of alginate gel microbeads, due its non-toxicity in contrast to the other cations.

Numerous calcium salts can be used in the gelation process of alginate gel microbeads. These salts can be divided into the three categories: readily soluble, partially soluble and insoluble.

A common readily soluble calcium salt used in this gelation process is calcium chloride ($CaCl_2$). $CaCl_2$ allows for instantaneous cross-links to occur between the released Ca^{2+} ions in the solution with the alginate gel micro-droplets, resulting in the formation of alginate gel microbeads. Therefore, these salts are used to externally gelify the alginate gel micro-droplets.

On the other hand, partially soluble calcium salts such as calcium sulphate ($CaSO_4$) can be used when the slow release of Ca^{2+} is required, however, the ability to control this gelation process can be quite challenging (204).

Furthermore insoluble calcium salts such as calcium carbonate ($CaCO_3$) are useful in situations when gradual or controlled crosslinking alginate and Ca^{2+} ions is required. Hence, these salts are typically used when internal gelation of alginate gel microbeads is required. This is achieved by dispersing the calcium salt into the alginate solution prior to emulsification. Once, emulsification takes place, the gelation process of the alginate gel microbeads can be initiated by solubilising the Ca^{2+} salt, thus releasing Ca^{2+} cation which can then be crosslinked with the alginate polymer chains. These crosslinks can be initiated by using a gelling initiator for example an acid or UV radiation, thus causing a reduction in pH. In general, an acid such as glacial acetic acid is added to the emulsion in order to reduce the pH (100). A number of research studies have also shown that gradual gelation of alginate gel beads can be achieved by adding glucono delta-lactone to the alginate solution containing an insoluble calcium salt, which then leads to the slow dissociation of the salt (11,205).

Furthermore, a photo-acid generator was used in a recent study in order to initiate the gelation process of alginate gel microbeads (206). Upon UV irradiation, this gelling initiator initiated the dissociation of hydrogen ions (H^+). The use a photo-acid generator allows for in situ gelation of the alginate microdroplets to occur without the need to migrate within acidified oil, which may eventually lead to the deformation of the alginate gel microbeads in cases where the optimum conditions are not met.

1.5.10.1.1 External gelation

Traditionally alginate gel beads have been gelfied using external gelation methods. This usually involves the introduction of Ca^{2+} ions into alginate droplets in an external Ca^{2+} bath. This causes the diffusion of Ca^{2+} ions inwards into the spaces that are created between the alginate polymer chains, which lead to the formation of cross-linkages. In the case where cells are encapsulated in an alginate gel beads, the alginate solution containing cells is dropped into a Ca^{2+} ion bath as shown in Figure 1.2. Once the alginate polymer chains come in contact with Ca^{2+} ions, cross-linkages at the alginate droplet peripheries begin to form, resulting in the formation of semi solid membranes with liquid cores (207). Extending the incubation time of droplets in a Ca^{2+} ion bath enables the diffusion of more Ca^{2+} ions across the membranes due to the change in concentration gradient and in turn causing the cores of the alginate gel beads to gelate. As a result the cells are encapsulated randomly within the calcium alginate gel beads (208).

The cross-links are initiated at the alginate droplet peripheries, because the alginate polymer chains are attracted towards the peripheries (209). The cores of the droplets become diluted while crosslinking takes place. Once crosslinking is complete, the calcium alginate networks are concentrated at the periphery of the alginate gel beads, causing inhomogeneity within these gels (210). However, the use of these inhomogeneous alginate gel beads for cell applications is limited. This is because necessary solutes such as oxygen and nutrient cannot be exchanged effectively between the core of the alginate beads and the outer environment, due to an increase in the diffusion barrier (211). Furthermore, it is difficult for toxic waste to secrete out of the alginate beads, which eventually leads to cell death. A number of approaches have been conducted to overcome these drawbacks. Some of these approaches include:

- Decreasing the size of the alginate gel beads in order to reduce the diffusion pathway (212),
- Decreasing the concentration of the divalent cations (for example Na^{+}) used in the gelation process to allow for competitive binding of Na^{+} ions to Ca^{2+} ions to occur (209).
- Adopting an internal gelation method, which allows the formation of homogenous hydrogel matrices as discussed in the following section.

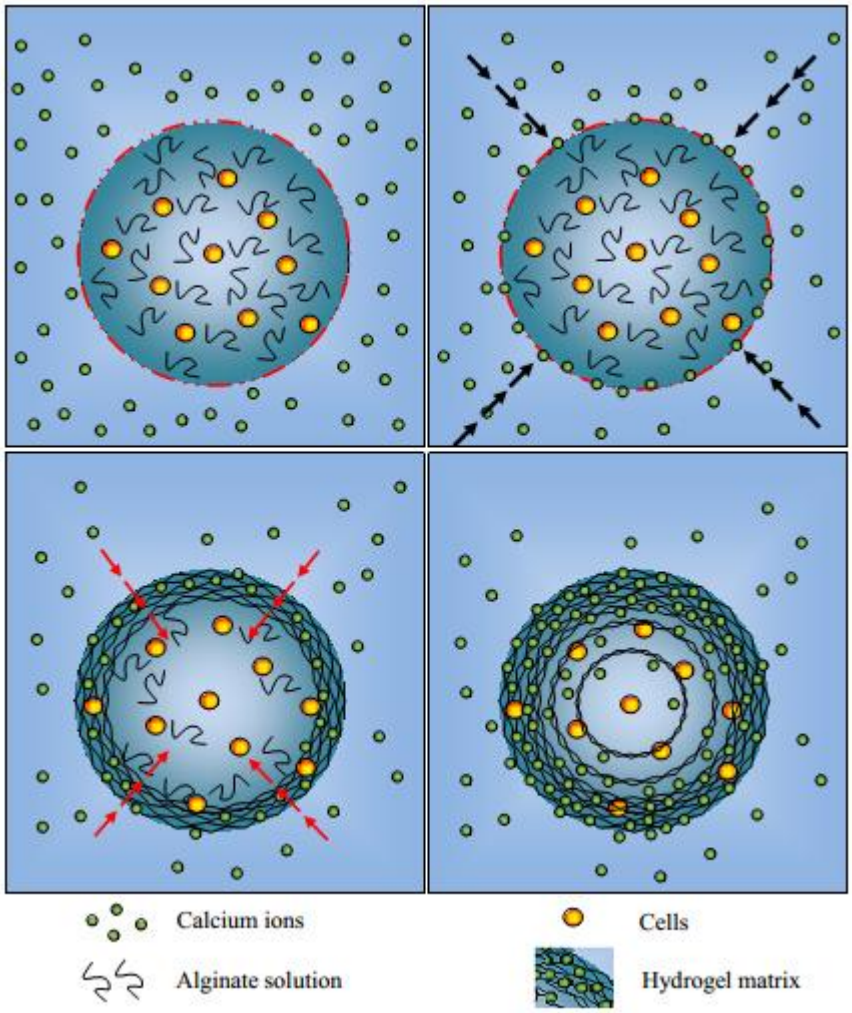

Figure 1.2: Mechanism of an external gelation approach used to encapsulate cells in calcium alginate gel microbeads: (a) sodium alginate microdroplets in contact with a solution containing calcium, (b) calcium ions diffuse into the sodium alginate droplet, (c) inward gelation of alginate droplets and (d) completed gelation of calcium alginate microbeads.

1.5.10.1.2 Internal gelation

The late 1980s was the start of an era where attempts to reduce the size of alginate gel beads and increasing their throughput for industrial took place. Initially, a method involving emulsification was investigated by dispersing an alginate solution into micro-droplets that were then subjected to external gelification, which involved the use of an emulsion containing a calcium solution. This attempt resulted in the mass production of alginate gel beads. However, these beads coagulated into large gel masses, since it was challenging to control the gelation conditions (100). This gelation process was then adapted to control the release of free Ca^{2+} ions (213). This approach involved the use of an alginate solution containing insoluble calcium carbonate particles, which was mixed together into an oil phase as shown in Figure 1.3. This was followed by the addition of acetic acid to reduce the pH, which led to the dissolution of this calcium carbonate into Ca^{2+}, carbon dioxide and water. Consequently, the free Ca^{2+} ions are crosslinked internally with alginate polymer chains, as shown in the chemical equation below:

Acetic acid + calcium carbonate → calcium acetate + carbon dioxide + water

$$\mathbf{2\ CH_3COOH + CaCO_3 \rightarrow Ca\ (CH_3COO)_2 + CO_2 + H_2O} \qquad \textbf{Equation 1.6}$$

The term internal gelation was used to describe this gelation process because the crosslinking and gelation process were initiated within the alginate droplets (214). Insoluble salts are predominantly pH dependant (215). The ability to control the gelation process has enabled the production of alginate gel microbeads with varying sizes ranging from 20-1000 μm (183,215,216).

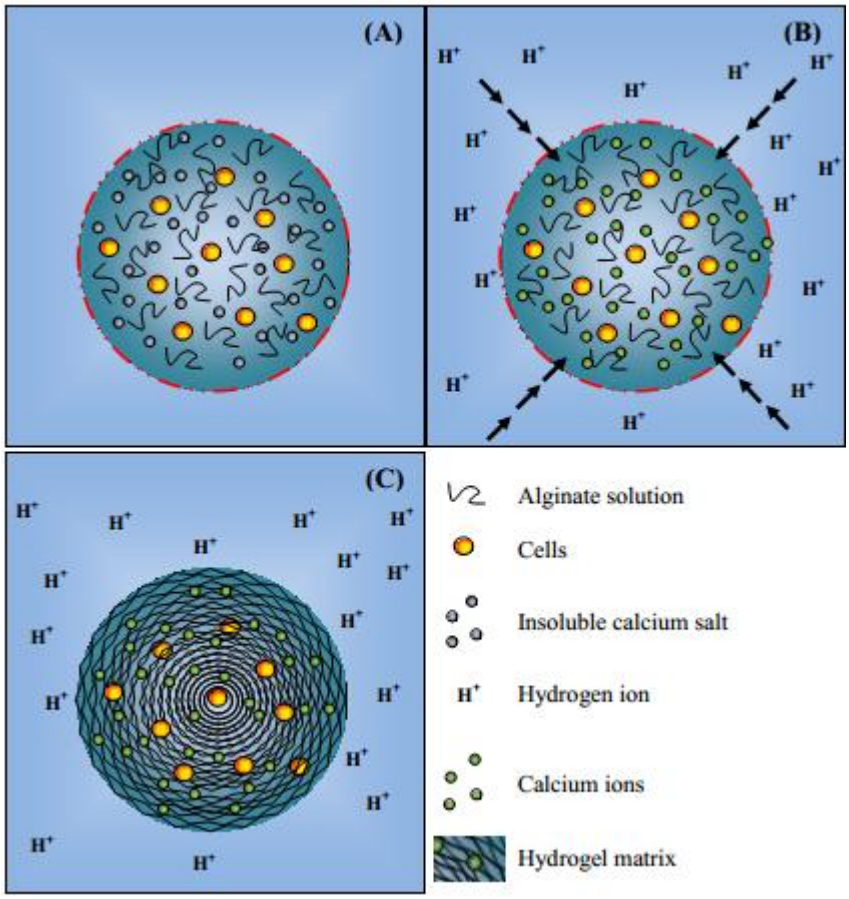

Figure 1.3: Mechanism of an internal gelation approach used to encapsulate cells in calcium alginate gel microbeads: (a) sodium alginate micro-droplets are dispersed in oil, (b) An acid is added to dissolve the insoluble calcium salt and (c) localised gelation of calcium alginate microbeads.

1.5.10.2 Throughput

Choosing the appropriate size to produce microbeads for cell encapsulation purposes is a major contributor to low throughput. Hence the size at which the microbeads are produced should be thought of carefully to ensure that:

- Cells are encapsulated simultaneously in monodisperse microbeads.
- There is sufficient space for cells to grow.
- Enough nutrients can reach the cells and whatever the cells produce can also diffuse away easily (193).

1.5.11 Numerus approaches to encapsulate cells in alginate microbeads

1.5.11.1 Introduction

The production of microparticles can be carried out using a number of different processing methods, such as emulsification, spray drying and electrostatic droplet generation techniques (217,218). The choice of preparation method used to produce microparticles has a significant effect on the physical and chemical properties, including the size, porosity and morphology of the microparticles (193). However, there are three main steps that need to be employed regardless of the choice of method employed to produce the microparticles, including:

- The first step involves the preparation of a suspension containing viable cells and alginate. The concentration of alginate is usually between 1 to 3 % w/v.
- The second step entails the generation of alginate micro-droplets preferably in a controlled manner, in order to produce monodisperse droplets.
- The third step involves a gelation process under mild conditions to produce alginate gel microbeads (193).

The basic principle of a number of droplet preparation methods involves forcing a liquid through a nozzle to produce individual droplets. For examples, the alginate/cell solution can generate a laminar jet that is fragmented into minute droplets either by gravity or other means such as syringe pumps (182,219,220).

The diameters of the micro-droplets can be adjusted by changing a number of experimental parameters, for instance the diameter of the nozzle and the flow rate at which the alginate is pumped through the setup. Nevertheless, the fabrication methods described above lack reproducibility and usually results in the production of large numbers of polydisperse microparticles (193). However, due to an increasing demand to produce homogenous and monodisperse microparticles, new microfluidic techniques emerged (218). This relatively

new emerging field handles fluids in micro/ nano environments, and has been applied in a number of fields such as cell biology, drug screening and biochemical assays (45,79,121,221,222). The use of microfluidic chips can solve a number of challenges that are associated with the use of conversional methods, which are used to produce microparticles, such as the shape and size (223).

Advances in microparticle preparation methods combined with the ability to control the microencapsulation processes, provide promising means for cell encapsulation applications. In addition, microfluidic chips can provide a sterile environment without the need of excessive sterilisation processes (193).

Microfluidic experiments usually entail the production of micro-droplets in a non- miscible phase, which is followed by a gelation process. The gelation procedures vary depending on the polymer, for example ionic crosslinking, thermal gelation and UV radiation (224-227).

The optimal microfluidic setup should enable the production of regular streams of micro-droplets with uniform volumes and rates (228). Microfluidic chips have been designed with different channel geometries for example T-junctions, cross junctions and microcapillary coaxial devices (229-231). Microfluidic chips designed with these three geometries have a common mechanism, which involves dispersing the samples into microchannel that consists of an immiscible carrier that is dispersed through another inlet within the microfluidic chip. The fluids then meet at a junction that has been designed to generate reproducible micro-droplets. Moreover, the geometry of the microfluidic chips, flow rates and physical properties (e.g. interfacial tension) of the fluids dispersed through the channels, causes droplets to pinch off (232). Furthermore, the flow rate ratio of fluids that are pumped through the microchannels, control the size of microparticles, meaning that microparticles of almost any size can be produced. In addition, microparticles with

various shapes can be produced depending on the geometry of the microchannels (233,234).

The following section provides a critical review on the different approaches reported to encapsulate cells in alginate gel microbeads. This review was divided based on the different types of geometries used to produce the alginate gel microbeads, followed by a number of examples on other natural materials used to produce microbeads containing cells.

1.5.11.2 T-junction microfluidic chips

T-junction microfluidic chips are simple design that are widely spread for many the production of microparticles. In T-junction chips, the dispersed phase becomes in contact with the continuous phase at the T-shaped junction, which is located at a 90^{o} angle. As the microdroplets that are formed in the dispersed phase grow, they hinder the microfluidic channel, causing a restriction to the flow of the continuous phase. This hindrance leads to a relatively large increase in pressure, resulting in the formation of microdroplets (235). Due to its simplicity, T-junctions have been reported to be the most effective geometry for the formation of microdroplets in a continuous phase (236-238). Furthermore, the chance that coalescence of two consecutive micro-droplets occurs is minimal, and depends on the flow rate applied through the microchannels, since the micro-droplets tend to exit the main microchannel individually (193).

Microfluidic chips that are designed with T-junction microchannels are usually fabricated from glass or polydimethylsiloxane (PDMS) (239), although PMMA has also been used (240). To fabricate a chip made from PDMS for example, both soft lithography and photolithography can be used so that minute customised microchannels can be embedded (239).

The use of T-junction microfluidic chips for cell encapsulation studies reported in literature mainly focuses on the experimental setups without providing much detailed analysis on the encapsulated cells. A paper published by Chang-Hyung Choi and colleagues (241), describes a microfluidic approach to encapsulate yeast cells in alginate gel microbeads, using a microfluidic chip with a T-junction and four inlets (alginate, yeast cell suspension, calcium chloride and hexadecane), and is shown in Figure 1.4.

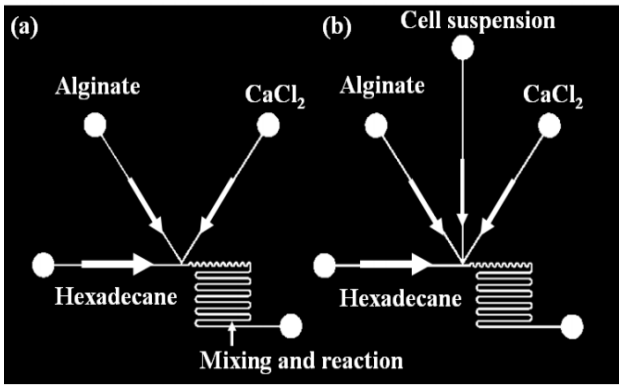

Figure 1.4: Schematics of the microfluidic chip fabricated by Chang-Hyung Choi et al. to encapsulate cells in alginate gel microbeads (239).

The alginate microdroplets formed were then subjected to an external gelation protocol, resulting in the encapsulation of yeast cells in alginate microbeads with diameters ranging from 60 and 95 μm. The sizes of the microbeads were controlled by changing the flow rate, viscosity and the interfacial tension. Hexadecane was used as the immiscible phase, and was injected into the main microfluidic channel of the chip; the other three side inlets were used to inject the yeast cells (stained with green fluorescent protein (GFP)), $CaCl_2$ solution and alginate independently. This microfluidic approach enabled the production of monodisperse alginate gel microbeads both with and without and yeast cells. The paper showed fluorescence images of viable encapsulated yeast cells immediately after encapsulation (figure 1.5). However, the long term cell viability was not detailed.

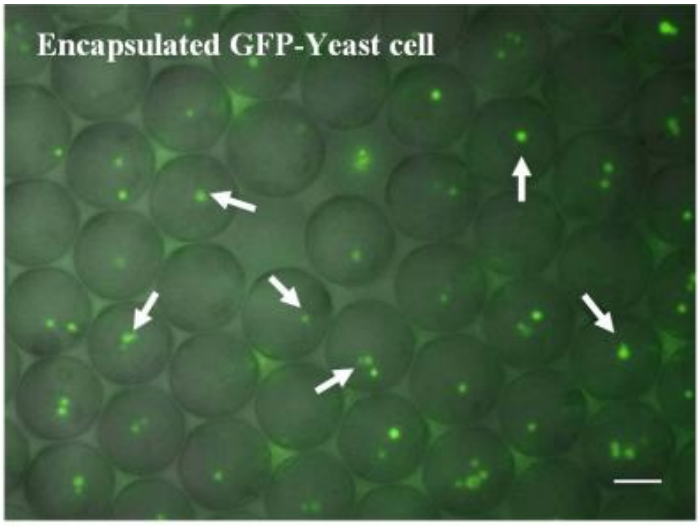

Figure 1.5: A snapshot of the alginate gel microbeads that was produced by Chang-Hyung Choi et al. to encapsulate GFP-Yeast cells in alginate gel microbeads; scale bar is 50 µm (241).

A different example from the literature that demonstrates the use of T-junction microfluidic chips for encapsulating Jurkat, Clone E6-1 cells in alginate gel microbeads, was described in a communication published by Wei-Heong Tan and colleagues (6). These microbeads were produced by an internal gelation mechanism and ranged between 94 - 150 µm in size. In order for the internal gelation to occur, calcium chloride was added to the alginate solution, ensuring a homogenous solution was achieved, in addition to preventing blockages within the microchannels. The microfluidic chip used to produce the alginate gel microparticles was fabricated from PDMS and a T-junction was cooperated into the design (Figure 1.6). The alginate microdroplets become in contact with corn oil that contained acetic acid, which were injected into the microfluidic chip prior to this via a side inlet. On this contact, Ca^{2+} ions are released due a reduction in pH, causing the gelation of the alginate gel microparticles.

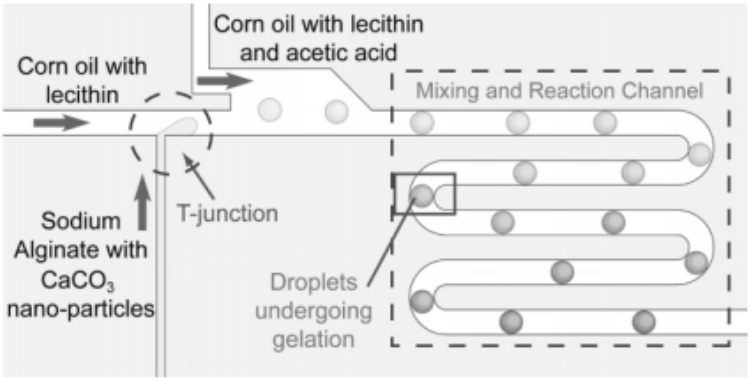

Figure 1.6: Schematic of the microfluidic chip fabricated by Wei-Heong Tan et al. to encapsulate cells in alginate gel microbeads (5).

Wei-Heong Tan and colleagues described the microparticles produced by this microfluidic method as beads. The results obtained indicated that no single cells were encapsulated and that there was an inhomogeneous distribution of Jurkat cells, since a significant number of alginate gel microbeads were empty (Figure 1.7). Furthermore, the percentage viability of Jurkat cells increased from 19.3% to 74.3%, with a higher concentration of $CaCO_3$. However, there were no results reported regarding the long term survival and percentage viability of the Jurkat cells.

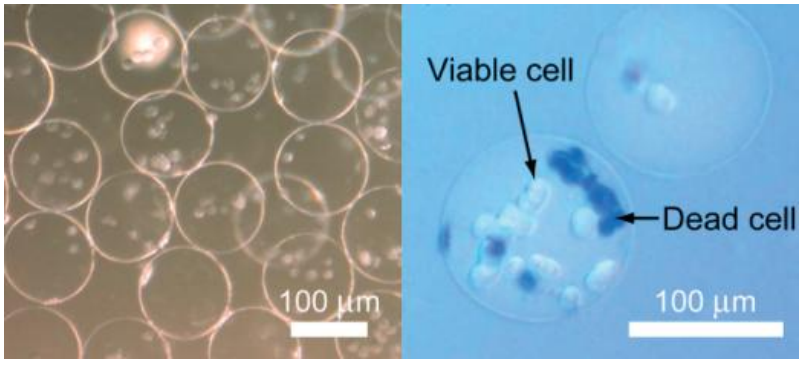

Figure 1.7: (a) Jurkat cells encapsulated in alginate gel microbeads produced by Wei-Heong Tan et al. (6) (b) The Jurkat cells with trypan blue, a live/dead staining technique to distinguish between the live and dead encapsulated cells. The cells stained blue are dead.

Capretto and colleagues were the first to publish an article that described the use of a microfluidic system to form alginate microparticles. The gelation process was the main focus of this article (242). The main aim of this study was to obtain alginate microparticles that had optimal characteristics in terms of their morphology and dimension, i.e. sphere in shape and almost monodisperse. In addition, a comparison of different gelation methods including: external, internal and partial gelation was carried out. The microfluidic chip that was used to encapsulate primary eukaryotic cells in this study was a commercially available chip that was designed embedded with a Y junction, which is very similar to that of a T-junction and is shown in Figure 1.8.

Capretto and colleagues first attempt to produce alginate gel microbeads, involved an external gelation method, where alginate was used as the water phase (WP) and sunflower seed oil was used as the oil phase (OP). The two immiscible phases (WP and OP) were injected into the microchannels at the relevant flow rates. This was followed by the multiphase dripping into a gelling bath containing Barium chloride ($BaCl_2$), which resulted in the gelation of the alginate microdroplets. The resultant alginate gel microdroplets produced appeared as tail-shaped microbeads and polydispersed. These observations were due to the slow introduction of the alginate suspension into the OP/ $BaCl_2$ gelling bath interphase. Attempts to overcome these drawbacks included either the addition of an oil layer above the $BaCl_2$ gelling bath or the addition of a thickener to the WP, such as glycerol. These attempts reduced the tails formed on the alginate gel microbeads, although the microbeads still had tails.

Following on from these experiments, Capretto and colleagues produced alginate microdroplets by adopting an internal gelation process. This gelation process was carried out by the dispersion of an insoluble or partially soluble barium carbonate into the WP that contained the pre-prepared Na-alginate solution. The microdroplets were then gelified by

the adding an oil soluble acid (acetic acid 0.15% v/v) to the OP. Lowering the pH caused the release of barium ions (Ba^{2+}) and the formation of Ba-alginate microparticles. Microphotographs of the microbeads produced using this internal gelation approach showed the characteristics of the microbeads were greatly influenced by the concentration of $BaCO_3$. At lower concentrations of $BaCO_3$, the alginate microbeads appeared to be highly dispersed, with a strong tail-shape, in addition, the microphotographs also revealed that coalescences occurred. In contrast, the alginate gel microbeads exposed to a higher concentration of $BaCO_3$ were spherical although coalescences also occurred. The morphology of the microbeads was improved significantly by adding a stabiliser (span 80) to the OP. These alginate microbeads appeared to be almost spherical and the presence of coalescences reduced significantly. However, the major drawback of this approach was that barium is toxic.

A new gelation method (partial gelation) was the investigated for the purpose of producing monodisperse sphere shaped microbeads. This approach involved increasing the viscosity of the WP by adding minute amounts of $BaCl_2$ into the alginate solution, prior to injecting the solution into the microfluidic chip. The microphotographs obtained showed that alginate gel microbeads produced by this approach were spherical in shape, in addition to the absence of coalescence and tails.

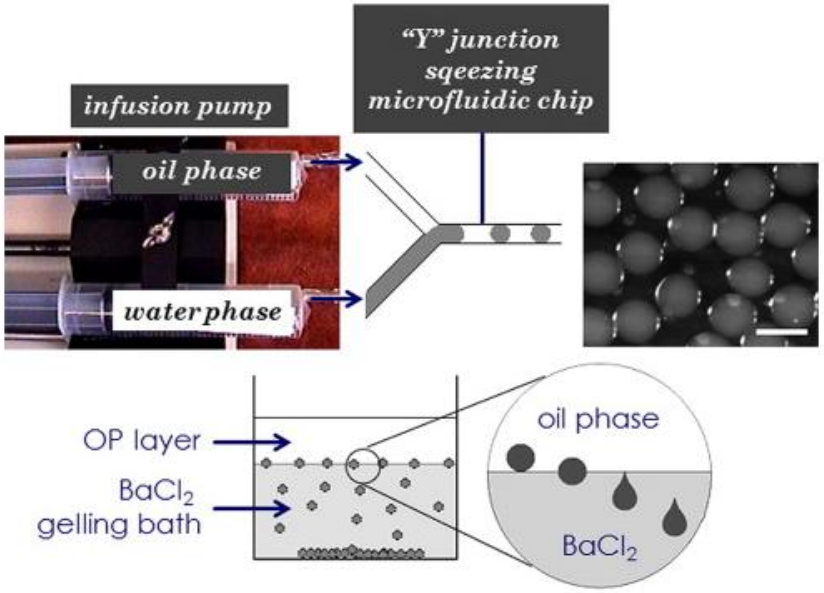

Figure 1.8: The upper figer shows the microfluidic setup Capertto et al. designed for the production of alginate micrdoplets using a Y-Junction squeezed based microfludici chip (242). On the other hand the lower part of this figure shows the the alginate microdroplets travel though the water/oil interphases, allowing the formation of alginate gel microparticles with tail like sturctures. The photomicrograph on the left handside shows the alginate gel microbeads that were produce when they underwent partial gelation. These microbeads were sphere and had a narrow size distribution. Scale 500 µm.

Another paper published by the same group, confirmed that gel microbeads produced using the described partial gelation method can be used to encapsulate cells (243). Capretto and colleagues produced partial gelated microbeads by mixing two natural polymers (alginate and agarose). The gelation mechanisms for both these polymers differ; ionic gelation and thermal gelation are used for alginate and agarose respectively, resulting in the production of alginate/agarose hybrid microbeads. These microbeads had an excellent morphology and were almost monodisperse. In order to validate the use of the hybrid alginate/ agarose microbeads for cell encapsulation purposes, Capretto and colleagues encapsulated pig Sertoli cells, primary eukaryotic cells. The process of encapsulating cells can have an effect on the percentage cell viability and their functions. Therefore, this study investigated both of these aspects and confirmed that the encapsulated cells had high percentage viabilities over a period of 16 days. Furthermore, investigations into the effect of cell encapsulation on functionality demonstrated that the encapsulated cells exhibited similar

functionality to that of free cells. Lastly, high biocompatibility of the hybrid microbeads was achieved when *in vivo* studies were carried out in NOD mice.

Another microfluidic study carried out by Um and colleagues saw the development of a microfluidic chip that consisted of a focusing zone where alginate microdroplets are formed by the use of oil and a double T-junction (244). The gelation process of the microdroplets took place when they became in touch with $CaCl_2$ solution at the first T-junction (Figure 1.9). Once gelified, the microbeads travel through the microfluidic chip and reach the second T-junction where an additional liquid is mixed with the microbeads. Alginic acid (polymer) and Puramatrix (peptide) were used to fabricate these microbeads. Microscope images of these microbeads are shown in Figure 1.10.

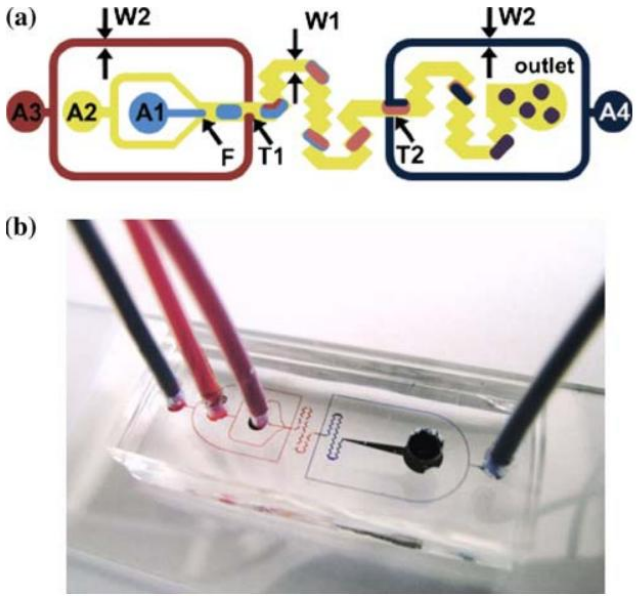

Figure 1.9: (a) A schematic diagram of the microfluidic chip fabricated by Um et al. for the formation of hydrogel microdroplets using two T-junction channels (T1 and T2) and four inlets (A1-A4), F is the hydrogel solution focusing region with and immiscible oil, and W1 and W2 represent the widths of the main channel and branches of the T channels respectively. (b) A photograph of the microfluidic chip. The microchannels were filled with dyes for visualisation purposes (244).The authors claimed that the alginate microbeads they produced were shaped either like almonds or rods, because the initiation of the gelation procedure occurs in the microchannels of the microfluidic chips. These peptide based microparticles were used to encapsulate a hepatocellular carcinoma cell line (HepG2), which was treated prior to encapsulation with CellTracker Green for fluorescence to occur. The fluorescence intensity of the encapsulated cells was then analysed 15 minutes after encapsulation occurred. Um and colleagues concluded that the microfluidic approach that they have adopted has great potential in cell-cell and protein-protein interaction studies, yet they provided no evidence to support these conclusions.

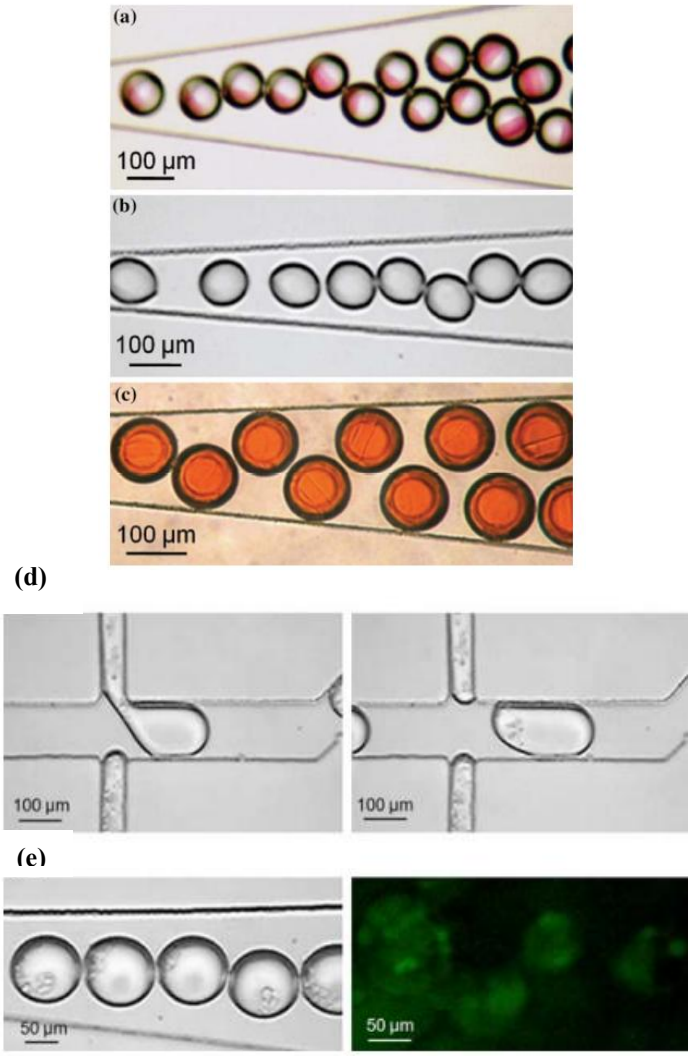

Figure 1.10: Microscopic images of the microbeads produced by Um et al. (244). (a) The Puramatrix microdroplets once they have passed through the first T-junction, (b) the gelation process of alginate gel microdroplets when they become in contact with $CaCl_2$ solution, (c) rod-shaped microparticles confined in yellow solution microdroplets, (e) the process of combining the HepG2 cells with Puramatrix microdroplets and (f) encapsulated fluorescent HepG2 cells.

Another microfluidic attempt to encapsulate cells in alginate microbeads was reported by Wu and Pan (245). The microfluidic chip described in their research was fabricated from PDMS, in which alginate microdroplets were formed by a pulsed airflow as an alternative to a liquid stream. In detail, this microfluidic chip (Figure 1.11) consisted of one main microchannel for the alginate/cell solution, in addition to a T-shaped pneumatic (air-filled) microchannel with two inlets (one of the pulsed airflow and the other or constant pneumatic pressure, which is needed to prevent the backflow of the alginate/ cell solution

towards the T-shaped pneumatic microchannels). The alginate gel microdroplets that are produced in the microchannels are then delivered by a microcapillary tube into a sterile $CaCl_2$ solution for gelation to take place. Controlling the flow rate of the alginate/cell solution enables to production of size-controlled alginate gel microbeads (ranging between 150 to 370 μm in diameter).

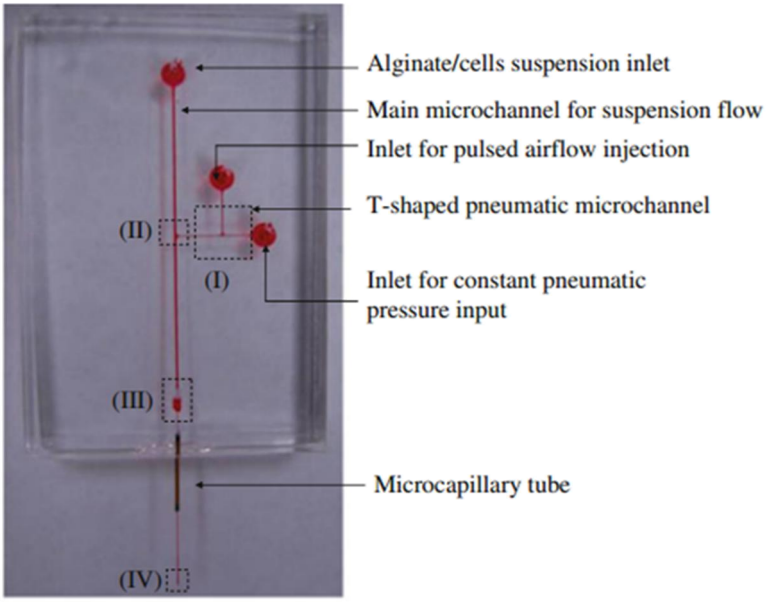

Figure 1.11: A top view photograph of the microfluidic chip fabricated by Wu and Pan used to encapsulate cells in alginate gel microbeads (245).

Once the microfluidic setup was optimised, this microfluidic approach was used to encapsulate primary chondrocytes that were isolated from the metacarpal–phalangeal joint of steers. The novelty in this microfluidic approach is the use of air as a squeezing stream for the continuous phase instead of a typical immiscible fluid (Figure 1.11). This approach can possibly reduce the chances of cross contamination from occurring. However, the results presented in the paper showed that the number of cells embedded into the alginate gel microbeads was relatively low comparing to the initial cell count. Microscope images of the alginate microbeads are shown in Figure 1.12. The reported percentage cell viability of encapsulated cells in the alginate gel microbeads was roughly around 96%.

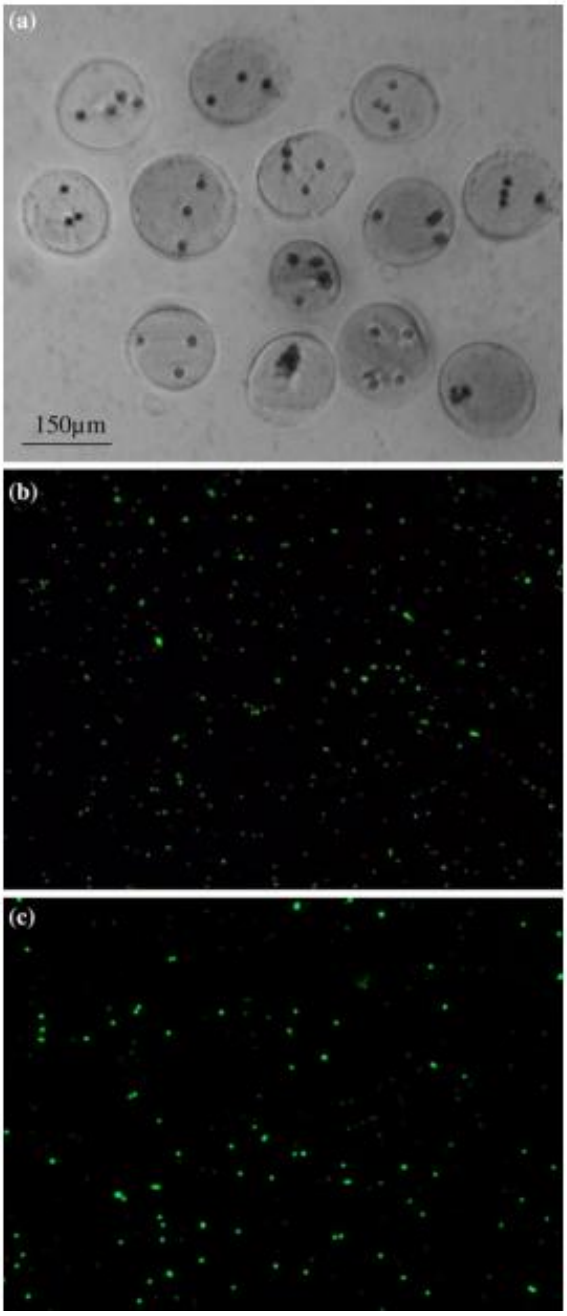

Figure 1.12: (a) Light microscope image of encapsulated primary chondrocytes in alginate gel microbeads using the microfluidic approach developed by Wu and Pan (245), (b) fluorescence microscope image of encapsulated primary chondrocytes cells in alginate gel microbeads and (c) fluorescence image of primary chondrocytes in cell suspension stained. Both the encapsulated and non-encapsulated cells were stained with live/dead dye, so that live cells fluoresce green and dead cells fluoresce red.

Another microfluidic approach that incorporated the use of a T-junction geometry to encapsulate cells in alginate microparticles was reported in a communication published by

Jongin Hong et al. (246). This microfluidic approach was based on the coupling of biological electrospraying and a microfluidicplatform. Biological electrospraying is a technology that involves charging the liquid medium to several hundred volts, which is then allowed to pass through a needle so that the droplets can be fragmented. This technology can be used for fragmenting living cell suspensions into microdroplets of cells, without causing any apparent effect on cell percentage viability and function. However, this technology is unable to control the distribution of cells or their distances within the droplets. Therefore, Jongin Hong et al. developed a microfluidic setup that combined a biological electrospray single-nozzle with droplet based microfluidic systems, in order to encapsulate and compartmentalise cells in microparticles. The microfluidic setup described in this communication consisted of a microfluidic chip, with two inlets (oil and aqueous inlets) and an outlet that was connected to the single-needle biological electrospraying (Figure 1.13). The authors considered both T-junction and flow focusing geometries for the purpose of producing alginate microdroplets. The results showed that the chip embedded with a flow focusing geometry resulted in the encapsulation of a smaller number of cells. The fluid flow rates were then investigated so to that a stable jet of microdroplets containing cells can be obtained. Upon the formation of the microdroplets, the gelation process took place when the microdroplets came in contact with a calcium chloride solution, which was place at both electrodes.

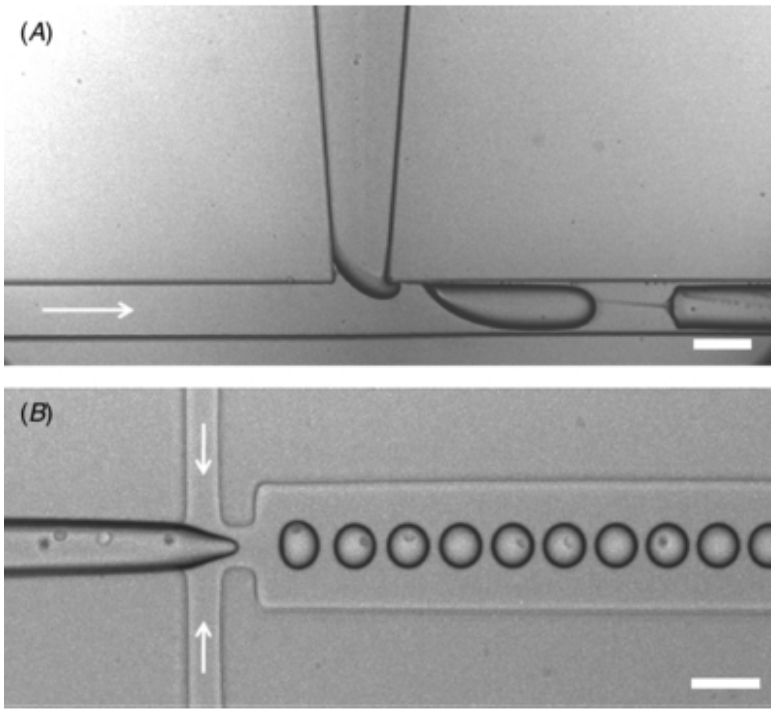

Figure 1.13: Images of the alginate gel microdroplets formed using two microfluidic chips that were fabricated by Jongin Hong el al. (246). (A) the alginate microdroplets were formed in a microfluidic chip with an embedded T-junction and (B) the alginate microdroplets were formed in flow-focusing microfluidic chip. The white arrows demonstrate the flow of the oil phase and 100 µm respectively.

Jongin Hong et al. reported their ability to encapsulate of one, two or multiple Jurkat cells in alginate gel microbeads using the described microfluidic setup, and that the number of cells encapsulated in these microbeads can be controlled by altering the flow ratio of the fluids (aqueous solution and oil). However, referring back to the microscopic images reported in this communication (Figure 1.14), regularity in the shape of the alginate microbeads is not observed. Furthermore, the microscopic image of the proposed single cell that was encapsulated in an alginate gel microbead was not conclusive. The percentage cell viability of the encapsulated cells was then evaluated using a flow cytometer followed by a microscope.

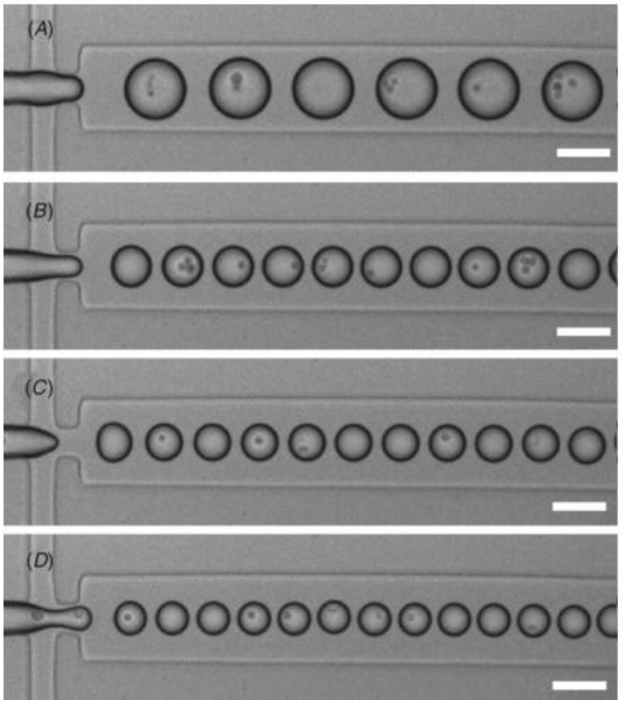

Figure 1.14: Single and multiple cells encapsulated in alginate microdroplets that were produced by Jongin Hong et al. via a number of different flow focusing configurations (244). The scale bar shown on the image represents 100 µm.

1.5.11.3 Cross junction microfluidic chips

Cross junction microfluidic chips work on the basis of creating a stream of the dispersed phases, which is then broken up by flow focusing with an immiscible carrier fluid (the continuous phase). Once the two phases meet, droplets are formed one at a time due to the shear force caused by the continuous phase stream. In such microfluidic chips, the dispersed phase is always introduced into the middle inlet and the second immiscible fluid is introduced into the side inlets. In order to produce gel microbeads, the uniform microdroplets that are formed at the cross junction are subsequently gelated via different gelation mechanisms (193).

Zhang et al. reported the use of a cross junction microfluidic chip to produce microparticles at ambient conditions. The particles produced were monodisperse and spherical (207). This paper is the first to describe the curing process of alginate gel

microdroplets within the microchannels of the microfluidic chip. As shown in Figure 1.15, the alginate gel microbeads were produced by the emulsification an aqueous alginate solution in an organic phase consisting of calcium iodide (CaI_2) as a cross-linker. Calcium ions then diffused from the undecanol containing CaI_2 in the downstream channel, leading to the gelation of the alginate gel microdroplets. The sizes of the alginate microbeads produced using this microfluidic approach ranged from 30 to 230 µm, with a reported polydispersity of 0.2%.

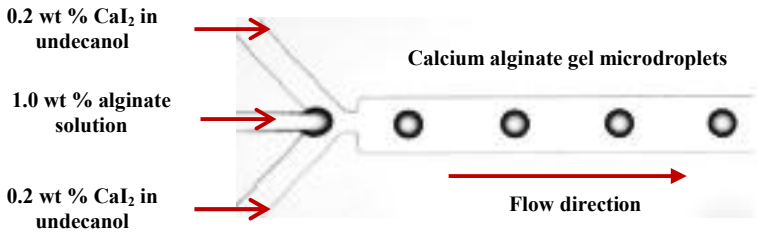

Figure 1.15: The cross junction microfluidic chip used by Zhang et al. to produce alginate gel microdroplets (203).

A dye fluo-3 was mixed with the alginate solution in order to enable the analysis of Ca^{2+} distribution within the alginate gel microbeads, which were then subsequently analysed using a confocal fluorescence microscope. The results showed that an increase in the concentration of CaI_2 in addition to an increase in the exposure time to the Ca^{2+} ions resulted in a uniform distribution of Ca^{2+} within the alginate gel microbeads. Unfortunately, this microfluidic approach was used to encapsulate polystyrene (PS) beads as a cell model. Therefore, although this approach can be used to control the amount of particles that are encapsulated per alginate gel microbeads, PS is not true representative of living cells. Furthermore, the organic phase used in this microfluidic approach is toxic to cells and should therefore be substituted (247).

Another approach to gelify alginate gel microdroplets was described by Shintaku et al. (248). This approach involved the fabrication of novel microfluidic chip consisting of a cross junction and T-junction as shown in Figure 1.16. The formation of alginate microdroplets using this microfluidic approach was analysed both experimentally and theoretically in terms of the fluid dynamic process.

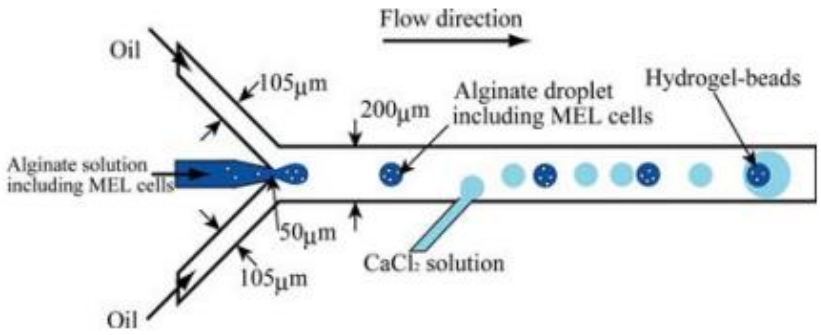

Figure 1.16: Schematic diagram of the microfluidic chip developed by Shintaku et al. in order to produce alginate gel microbeads containing living MEL cells (246).

An alginate/ cell (mouse erythroleukemia cells (MEL)) solution was introduced to the microfluidic chip via the central inlet of the cross junction. The oil continues phase subsequently caused the alginate/cell solution to break-up into monodisperse alginate microdroplets containing MEL cells. This was followed by the gelation process of the alginate microdroplets, once they became in contact with the merging $CaCl_2$ solution, which was introduced into the chip via T-junction that was referred to as a nozzle by Shintaku et al. (248). The diameters of the alginate microdroplets were measured at varying flow rates and ranged between 104 to 167 μm. Findings from this study showed that the higher the flow rates the smaller the diameters of the microdroplets due to the drag force, which causes the breakup of the alginate microdroplets. Furthermore, the alginate gel microbeads containing MEL cells were not spherical and had defects within their

surfaces as seen in Figure 1. 17. In addition to this the viability and functionality of the encapsulated MEL cells were not tested.

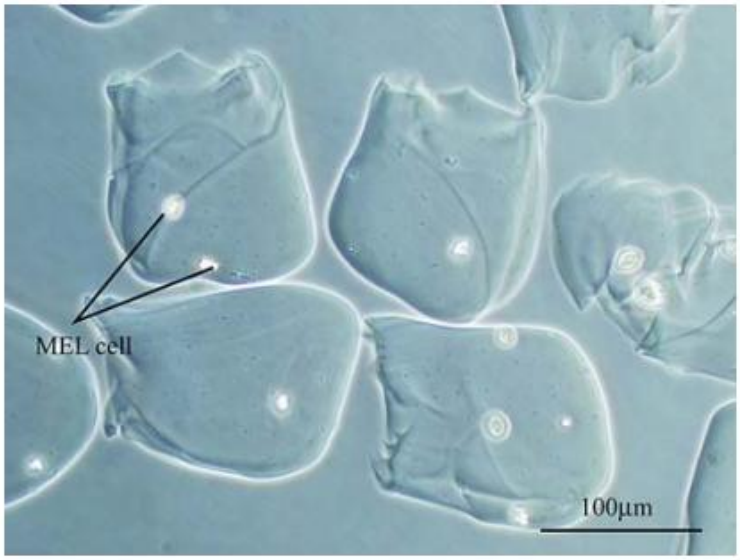

Figure 1.17: A photograph of the alginate gel microbeads containing MEL cells. These microbeads were formed by the microfluidic chip, which was developed by Shintaku et al. (246).

A different study carried out by Workman et al. (249) described the production of alginate gel microbeads containing cells. These microbeads were produced by a non-conventional approach, liquid chromatography fluid connectors were introduced equatorially into a 316 stainless steel manifold. Nitrile rubber O rings were used to seal the vertical through rigs, which directed the fluid flow toward the top of the surface of polytetrafluorethylene (PTFE) located on the 316 stainless steel manifold. The microchannels in this microfluidic approach were machined into the PTFE discs. An internal gelation process was adopted to produce alginate gel microbeads containing living cells. Nanocrystalline calcium carbonate was added to the sodium alginate solution (internal aqueous phase), whereas acetic acid was added to sunflower oil (external oil phase). The acetic acid and calcium carbonate react almost immediately, which can lead to the main channel clogging up. In order to overcome this drawback, Workman and colleagues developed a novel geometry that

protected the alginate solution containing calcium carbonate from the acetic acid until the alginate microdroplets were formed and enter the main microchannel (Figure 1.18). The shielding flow described in this study to protect the alginate solution containing calcium carbonate involved the addition of two inlets to pump sunflower oil into the microfluidic setup. Therefore, the alginate microdroplets formed were enclosed in a shielding fluid. The subsequent diffusion of protons from the external oil phase, allowed the alginate microdroplets to acidify. This approach prevented the gelation process from occurring at the junction, in addition to having more control over the diffusion rate of acetic acid into the alginate microdroplets. This microfluidic approach allowed the formation of monodisperse alginate gel microbeads with diameters ranging from 80 – 400 µm, depending on the experimental setup.

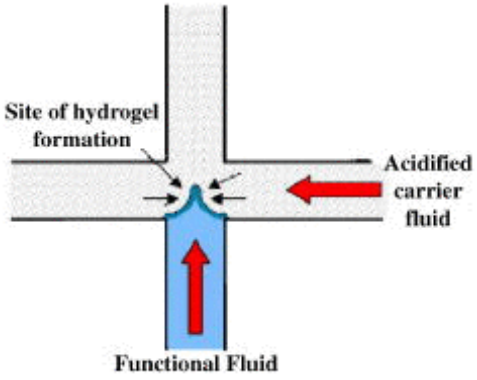

Figure 1.18: Schematic diagram of the microfluidic chip fabricated by Workman et al. (247) to encapsulate cells in alginate gel microbeads.

The alginate gel microbeads produced in this study were then used to encapsulate human embryonic kidney cell line HEK 293. The percentage viability of encapsulated HEK 293 cells in alginate gel microbeads was measured over a period of 12 weeks. Workman and colleagues reported that clusters of cells started to form after day 15 of encapsulation, and that these clusters consisted of live cells. On the contrary, single encapsulated cells died 15

days after encapsulation. However, all the encapsulated cells died 12 weeks later (Figure 1.19).

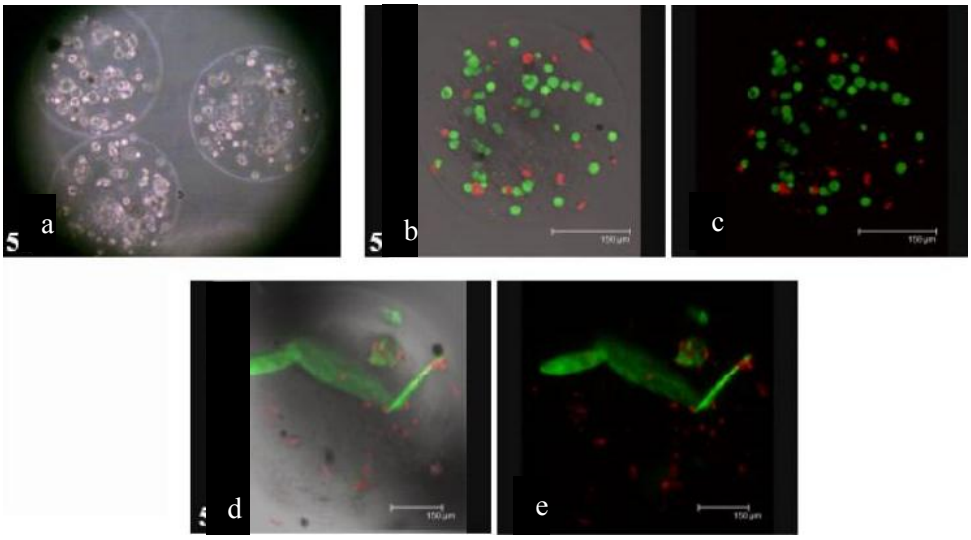

Figure 1.19: Microscope images of encapsulated HEK 293 cells reported by Workman et al. (a) light microscope image of three alginate gel microbeads containing HEK 293 cells, (b and c) are confocal images of encapsulated HEK 293 cells in an alginate microdroplet 24 hours after encapsulation, and (d and e) are confocal images of encapsulated HEK 293 cells in an alginate microdroplet 24 hours after encapsulation. The encapsulated live HEK 293 cells were stained with a green dye and the dead cells were stained with a red dye (249).

The same microfluidic approach was later reported in another study by the same group for encapsulating a number of other cell lines, including: human: human osteosarcoma cell line (U-2OS) and a cell line derived from a pheochromocytoma of the rat adrenal medulla (PC 12 cells) (1). Moreover, since calcium carbonate and glacial acetic acid are potentially toxic to living cells, cytotoxicity tests were carried out. These tests revealed that the concentrations at which both chemicals were used caused no significant damage to cells. Workman and colleagues concluded that the microfluidic approach they developed had minimal effect on the encapsulated cell viability, despite providing a limited detailed viability test with regards to the amount of alginate gel microbeads.

A study carried out by Choong Kim et al. described an interesting microfluidic approach to encapsulate cells in alginate gel microbeads by an external gelation mechanism (247). This

approach involved the use of calcified oleic acid for in situ gelation to occur, which proved harmful to cells. In order to combat this challenge and improve the percentage cell viability of encapsulated cells, the authors designed the microfluidic chip with an outlet specifically for flushing out the toxic oil as soon as the alginate microdroplets gelated. The PDMS microfluidic chip consisted of two main regions: the microdroplet generation part and the fluid exchange part. In the inlets located in the microdroplet region, a water-glycerol (80% v/v) was mixed with the alginate solution due to hydrodynamic focusing. The resultant water-glycol solution enclosed by the alginate solution was then broken up into microdroplets by a solution consisting of oleic acid and calcium chloride. The gelation process of the alginate solution occurred due to the presence of calcium chloride, which led to the formation of core-shell microcapsules. Whereas, solid alginate gel microbeads were produced by substituting the water-glycerol solution with a sodium alginate solution.

1.5.11.4 Capillary microfluidic devices

Capillary microfluidic devices usually involves the alignment of glass tubes (a cylindrical internal tube and either a cylindrical or rectangular out channels). The most attractive features of using glass microfluidic devices reside in the potential to create three dimensional flows in addition to being highly resistant to chemicals. Besides this, the glass surface can be treated to create either a hydrophobic or hydrophilic surface depending on the surface modifier used. Cylindrical capillaries with outer diameters of approximately 1 mm are typically used in order to fabricate microcapillary devices. The glass capillary is then heated and pulled to achieve a narrowing shape with a fine orifice, which is then inserted into other glass capillary (characterised with square cross sections) in order to build up the final microfluidic device. In order to align both glass capillaries (rounded and squared), the outer diameters of both capillaries are the same. Pumping a fluid through the circular capillary and an immiscible fluid through the square capillary, with both fluids flowing in the same direction allows a coaxial flow to be achieved (250) (Figure 1.20).

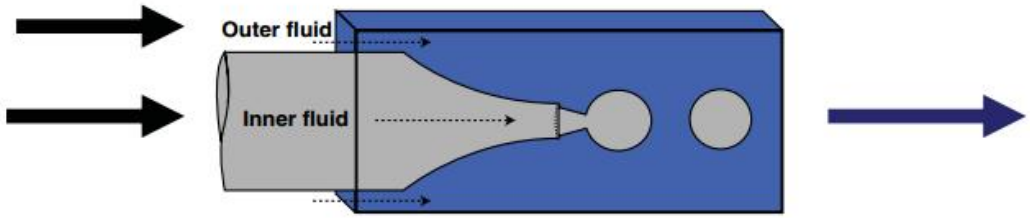

Figure 1.20: A schematic diagram of a co-flow microfluidic device fabricated for the production of microdroplets (251). The arrows represent the direction of the flow of fluids and the generated microdroplets.

In contrast, a flow focusing mechanism is achieved when the two immiscible fluids are introduced in opposite flow directions into the device at the ends of the same square capillary (Figure 1.21). The inner fluid is hydrodynamically focused by the outer fluid by the small orifice of the round capillary, which leads to the formation of a regular steam of microdroplets.

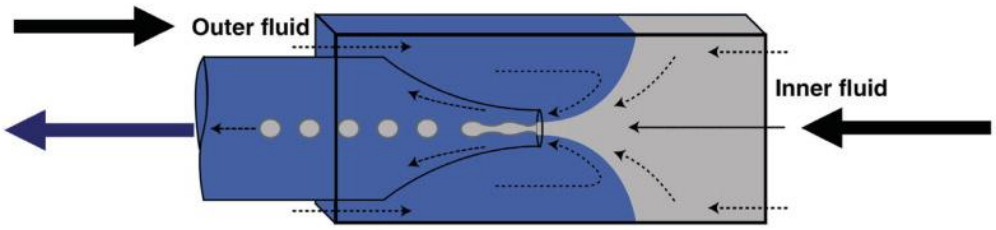

Figure 1.21: A schematic diagram of a flow focusing microfluidic device fabricated for the production of microdroplets (251). The arrows represent the direction of the flow of fluids and the generated microdroplets.

Morimoto et al. were the first to describe the use of microcapillary coaxial devices for producing alginate-poly-L-Lysine (PLL) gel microcapsules containing cells (11). The microfluidic device described in this study was developed by stereolithography for the production of monodisperse alginate water/oil microdroplets. The gelation process involved a modified internal gelation method, where $CaCO_3$ was added to the alginate solution; however, acetic acid was replaced with Glucono delta-lactone (GDL) as an acidifier. The authors reported a gradual reduction in pH when using GDL and the use of this acid was gentle enough on cells. Corn oil that contained 2% (w/v) lectin was used as the outer fluid, and an alginate/ $CaCO_3$ nanoparticle solution containing Chlamydomonas in addition to GDL represented the inner fluid. The outer and inner fluids then mixed at the orifice, resulting in the production of alginate gel microdroplets, which were subsequently gelated by the slow pH reduction caused by the release of Ca^{2+} ions.

Once the corn oil was removed, the alginate gel microbeads were coated with PLL, forming a poly-ion complex with alginate (negatively charged). Lastly, a thin layer of alginate was used to create another external layer in order to improve the strength of the membrane. The resultant alginate gel microbeads were referred to as "semi-permeable membrane cages". These microbeads were then studied to show that they can be manipulated and investigated in dynamic microarray devices (11). The microarray was then used to assess and evaluate the capsular membrane permselectivity and the viability of

the encapsulated cells. Although the results from this study seemed promising, a more complex cell model rather than a unicellular alga should be used to conclude the suitability of this microfluidic approach for future mammalian cell encapsulation studies.

Microfluidic devices have been known to generate multiple emulsions, in which microdroplets containing smaller microdroplets represent the dispersed phase (250). The multiple emulsions can be produced in glass microcapillaries by consecutive or concurrent co-flow and flow focusing.

Martinez et al. (252) described a microfluidic approach to encapsulate living cells in monodisperse alginate hydrogel microparticles, which were produced by a monodisperse double-emulsion intermediate. The inner water phase (water in oil in water double emulsion) consisted of alginate microdroplets coated by an oil phase consisting of a mineral oil layer, which was then further dispersed in an external water phase comprising an aqueous solution containing $CaCl_2$. The authors used a microfluidic device that was built up from round capillaries that were inserted into a square capillary (the coaxial geometry), combining the co-flow and flow focusing, and in turn enabling the double emulsions are fabricated in a single step (Figure 1.22).

The alginate solution (inner water phase) is pumped into one of the inner capillaries, whereas the mixture containing the surfactant, glycerol and deionized water (external water phase) in addition to the mineral water phase are pumped into the squared capillary from the opposite direction. The double emulsion microdroplets are then formed at the entrance of the second capillary. These microdroplets

undergo an external gelation process once they are collected in a calcium bath. However, due to the low interfacial tension observed between the two aqueous solutions, there was

an insufficient driving force to enable the restoration of the spherical shape of the alginate microdroplets.

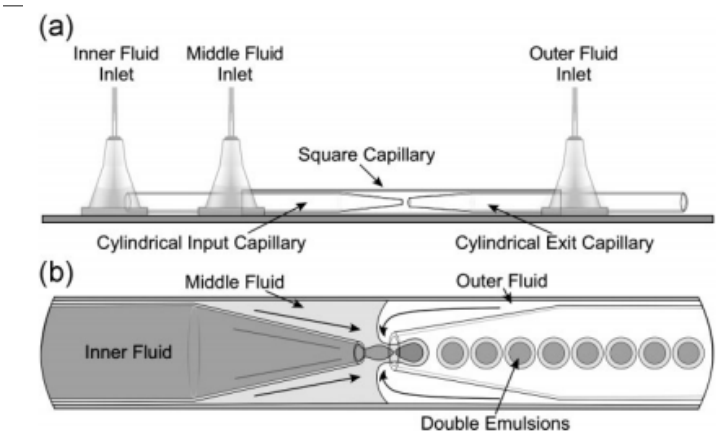

Figure 1.22: Schematic diagrams of (a) the microfluidic device used by Martinez et al. (250), (b) The area of the microfluidic device showing the intersection of the input and exit capillaries.

This microfluidic approach led to production of alginate microparticles characterised with tear-drop shapes (Figure 1.23). The lack of sphericity of the microdroplets produced using this microfluidic method, limits its application in in-vivo studies, since regular spherical microbeads and smooth surfaces are vital requirements. Furthermore with regards to cell encapsulation applications, yeast cells were encapsulated in the alginate gel microparticles and cell viability was subsequently monitored over a week.

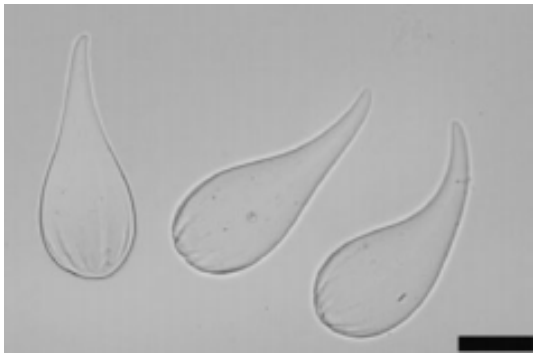

Figure 1.23: Bright field image of alginate microparticles produced by Martinez et al. (250). The inner dimeters of these microparticles were 226 µm.

Recently, the use of agarose gel microbeads has been investigated for a number of applications such as the food industry, medicine and cell encapsulation studies (253,254). Luo et al. described one of the first microfluidic approaches to encapsulate cells in agarose microcapsules (255). This approach involved the use of a microfluidic chip (microfluidic device) fabricated from PDMS with a flow focusing geometry. The agarose solution containing yeast cells (aqueous phase) was pumped through to the middle of the flow focusing geometry, whereas the oil phase was pumped though by two side inlets as shown in Figure 1.24.

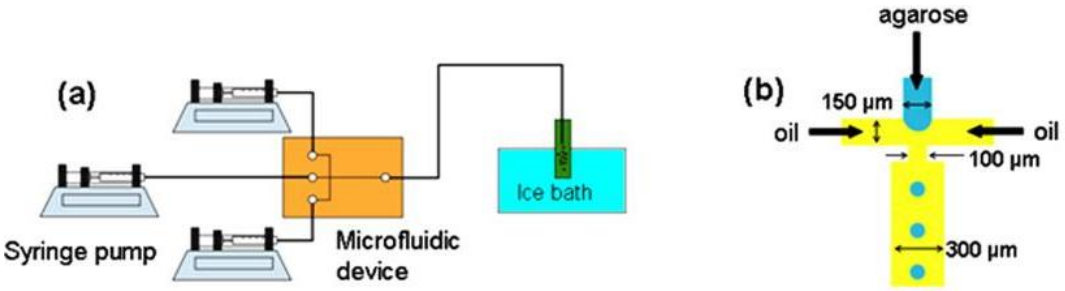

Figure 1.24: (a) experimental setup described by Luo et al. et al for the production of agarose gel microparticles containing live yeast cells. (b) A schematic diagram of the microfluidic chip fabricated by Luo et al. for the production of agarose gel microparticles containing live yeast cells (255).

The microdroplets produced were then cooled externally using an ice bath for the gelation process of the agarose particles. The results obtained from this study showed that the higher the flow rates of the oil and aqueous phases the smaller the sizes of the microdroplets produced. Furthermore, this letter describes the effectiveness of agarose microparticles to encapsulate living yeast cells. However, long term cell viability was not tested, and yeast cells were used as a model. Yeast cells are smaller and have a cell wall. The microfluidic chip described in this study was not reusable and it would have been hard to use by lay-people.

Another microfluidic attempt to encapsulate cells in agarose microparticles was described by Eun et al. (256). The microfluidic device used in this study was fabricated from PDMS and entailed a flow focusing geometry in addition to three inlets and one outlet as shown in Figure 1.25. The agarose solution containing cells were dispersed into the microfluidic chip via the horizontal inlet, whereas the mineral oil streams were pumped into the microfluidic device via two orthogonally oriented microchannels, resulting in the formation of agarose microdroplets. Furthermore, so that the premature gelation of the microdroplets was avoided, the syringes attached to the pumps were heated up to 40^{o}C using a heating tape, whereas the microfluidic chip was maintained at 37^{o}C.

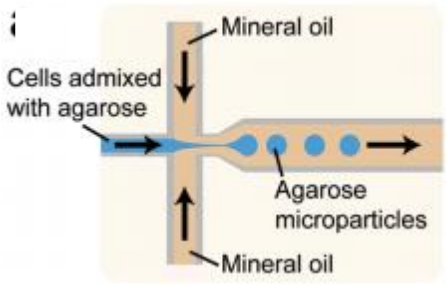

Figure 1.25: A schematic diagram of the PDMS microfluidic device fabricate by Eun et al. to produce agarose microdroplets containing E.coli (254).

This microfluidic approach was developed as a pioneering substrate for bacterial cell culture instead of using agar plates for routine screening, selecting and isolating bacteria cells. The agarose microparticles produced in this study enabled the bacteria cells to be located easily upon encapsulation and nutrients and oxygen were exchanged between the encapsulated bacteria cells the medium. Eun and colleagues proposed the potential the use of this microfluidics approach for biological screening purposes. Therefore, to validate this concept the authors encapsulated E.coli in agarose microparticles. The encapsulated E.coli cells were then tested in the presence of bacterial RNA inhibitor rifampicin at different concentrations. Microscope images obtained from these experiments showed that the

authors encapsulated single E.coli cells in agarose microparticles. Although single cells encapsulation was achieved, a significant amount of the agarose microparticles remained empty (Figure 1.26). This signifies the need to improve the fluid flow rates pumped through the microfluidic chip in order to produce reproducible, constant and continuous agarose microparticles containing single bacteria cells.

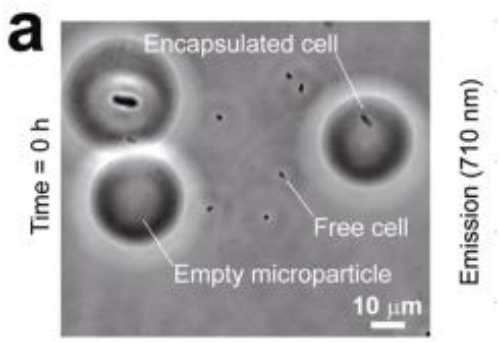

Figure 1.26: Image of agarose microbeads produced by Eun et al. (254) in order to encapsulate E.coli at time 0.

An example of a microfluidic chip with a T-junction droplet generator fabricated to produce agarose hydrogels with different mechanical properties was described by Kumachev et al. (257) (Figure 1.27). This approach saw the formation of the agarose aqueous phase above the T-junction by a curvy shape mixing microchannel and two inlets to pump in different concentrations of agarose solutions. The syringe pumps were maintained 37^{o}C to heat up the agarose solution. However, upon emulsification the temperature was reduced to 32^{o}C. After the agarose solution travelled through the curvy mixing channel, the stream of alginate solution was broken down into microdroplets by mineral oil, which represents the continuous squeezing phase. The agarose concentration within the microdroplets differed depending on the flow rates employed for both of the agarose solutions, which leads to the production of agarose hydrogel microparticles with varying characteristics. This microfluidic approach can be used to investigate different mechanical properties and their effect on cellular responses of the encapsulated cells.

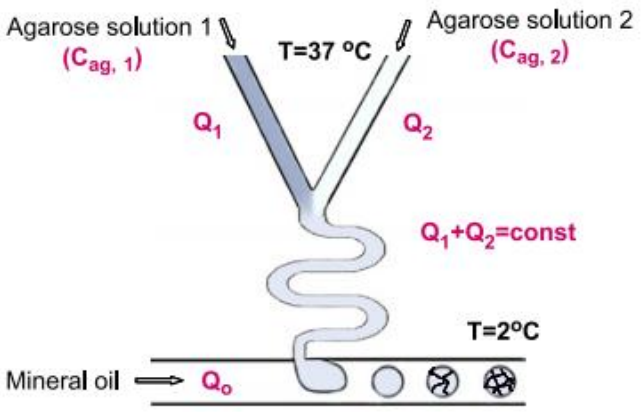

Figure 1.27: Schematic diagram of the microfluidic chip fabricated by Kumachev et al. (257).

The cells encapsulated in the agarose microparticles described in this study were two murine embryonic cell lines. Images of the encapsulated cells indicated that the cell distribution within the microparticles were homogeneous (Figure 1.28).

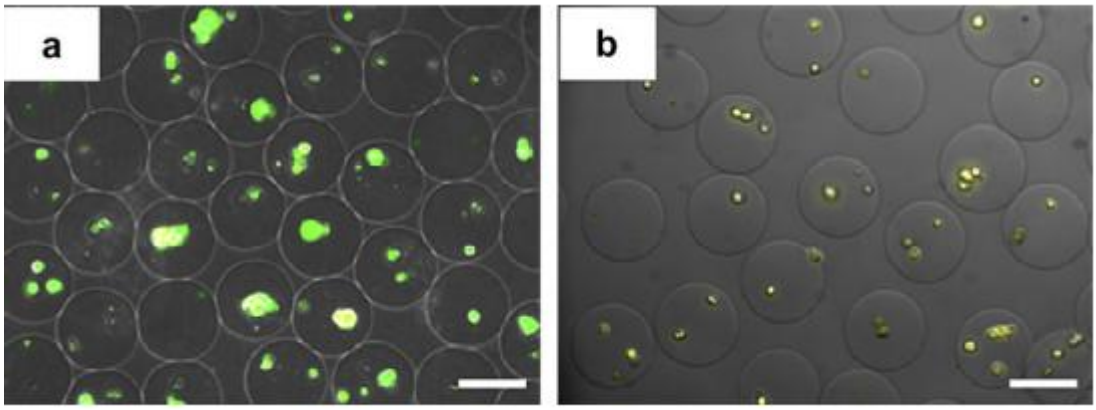

Figure 1.28: The fluorescence microscopy images obtained by Kumachev et al. of agarose microparticles containing (a) R1 and (b) YC5-YFP-NEO murine embryonic cells in Hanks Balanced Salt Solution buffer (255).

1.5.11.5 Other polymer microparticles

A significant number of articles published the use of polymers other than alginate and agarose to produce microparticles for cell encapsulation studies. Examples of polymers that have been used as encapsulating materials include gelatine, pectin xanthan and PEG.

Sakai et al. (119) reported the production of gelatine core-shell capsules to encapsulate rat adipose-derived stem cells using a flow-focusing droplet generator. These gelatine microparticles were produced by emulsifying a gelatine/ cell solution in paraffin. The resultant gelatine microparticles were suspended in a cross-linkable solution made up from a gelatine solution containing phenolic hydroxyl groups and horseradish peroxidase, resulting in the formation of a shell layer. Upon coating, the microcapsules were then passed through the same microfluidic setup, allowing the formation of multi-layered microcapsules which were then treated with the gelatine solution containing phenolic hydroxyl groups and horseradish peroxidase to all for the cross-linking reaction to occur.

The purpose of the outer layer shell described in this study was to acquire a bioadhesive surface, which can potentially be used to add an adherent cell layer to the microcapsules containing cells. Sakai et al. (119) investigated the adhesiveness of the microcapsules that they have developed by using adherent L929 fibroblast cells. Results showed that one day after in vitro culture took place, the seeded L929 fibroblast cells formed cell layers on the gelatine microcapsules containing HepG2 cells.

Pectin is a natural polymer that exhibits similar gelling behaviour to alginate. This natural polymer has been used in a variety of fields such as the food and pharmaceutical industries because it is biocompatible and versatile. Pectin is known to have a complex structure which generally consists of linear (1–4) linked α-D-galacturonic acid units, with some of the carboxyl groups presented in the form of methyl ester. Pectins can be classified as

either low methoxyl or high methoxyl depending on the degree of methyl esterification. Both classes of pectins can form gels however, their gelling mechanisms vary.

A study carried out by Yang et al. took advantage of the low methoxyl pectin gelling properties (258). This study involved the use of a flow focusing microfluidic system to produce pectin microparticles. The external focusing phase consisted of mineral oil whereas the water phase consisted of three aqueous steams including: a pectin solution, calcium chloride solution and water. Pectin hydrogels were formed once the low methoxyl pectin solution in mineral oil was cross-linked with calcium ions. These hydrogels appeared to be polydisperse and their sizes ranged from 40 to 100 μm in diameter. Yang et al. suggested that this microfluidic approach may potentially be used for a number of applications including drug delivery associated with controlled release. In order to provide proof of principle, this study involved the encapsulation of bovine serum album as a model protein. Table 1.1. shows a direct comparison of the different approaches described in section 1.5.11.

Table 1.1: A comparison between numerous approaches reported in literature to encapsulate cells in alginate gel microbeads.

Encapsulated cell	Material of microfluidic chip	Gelation mechanism	Crosslinking mechanism	Junction geometry	Cell viability	Microbead morphology
Yeast (241)	PDMS	External	Ionic crosslinking/ calcium chloride.	T-junction	Long term viability not detailed.	60- 95 µm Sphere.
Jurkat (E6-1) (6)	PDMS	Internal	Ionic crosslinking/ calcium chloride, and corn oil containing acetic acid.	T-junction	19.3% to 74.3% viable immediately after encapsulation. Long term viability not detailed.	94- 150 µm Sphere.
NOD mice (243)	Cyclo-olefin co-polymer	Partial	Ionic crosslinking for crosslinking the alginate/ barium ions.	Y-Junction	Reported to be highly viable after 16 days. However, the % cell viability was not reported.	~ 233 - 249.3 µm depending on the employed parameters. Alginate/agarose microbeads were spherical.
HepG2 (244)	PDMS	Internal	Ionic crosslinking/ calcium chloride, and corn oil containing acetic acid.	Double T-junction	Cells were analysed 15 minutes after encapsulation, and long term viability was not detailed.	40-100 µm. Almond like shaped.
Primary chondrocytes (245)	PDMS	External	Ionic crosslinking/ calcium chloride.	T-juncrion	Cell viability was ~ 96% and long term viability was not reported.	150-370 µm. Oval.
Jurkats (246)	PDMS	External	Ionic crosslinking/ calcium chloride.	T-junction and flow focusing	Reported to be highly viable but no specific time mentioned.	The size was not indicated. A distorted shape.
Polystyrene beads (207)	PDMS	Internal	Ionic crosslinking/ calcium iodide.	Cross junction	Cells were not encapsulated.	30- 230 µm. Spherical and distorted shapes.
MEL (248)	PDMS	Internal	Ionic crosslinking/ calcium carbonate.	Cross junction and T-junction	Cell viability was not considered.	104- 167 µm. Lacked sphericity
HEK 293(249)	PTFE	Internal	Ionic crosslinking/ calcium carbonate.	Cross junction	Cell viability was measured over 12 weeks, and was reported to have no significant effect on cell viability.	80- 400 µm. Sphere.
Three different cell types (247)	PDMS	External	Ionic crosslinking/ calcium chloride.	Cross junction	Cells remained viable for up to 7days.	Spheres.
Chlamydomonas (11)	PDMS	Internal	Ionic crosslinking/ Calcium carbonate.	Coaxial	Cells remained viable 22 hours after encapsulation	Sphere.
Yeast cells (250)	Glass	External	Ionic crosslinking/ calcium chloride.	Coaxial	65% of cells remained viable a week after encapsulation.	Lacked sphericity- appeared liked tear drops.

1.5.12 Jurkat cells

Jurkat cells were first established from peripheral blood of a 14 year old boy who suffered from acute lymphoblastic leukemia (ALL). The boy was treated with chemotherapy and preventative irradiation to the skull, but then suffered four relapses within a span of 7 months, and his condition deteriorated and he passed away during the fourth relapse. These cells lines were established during the first relapse (16). Jurkat cells are transformed cancer cells and can be cultivated using standard flasks and culture medium. Therefore, these cells have become an acceptable model for many biological and medical research studies (259). Jurkat cells were used as a cell model for the encapsulation studies carried out throughout this Thesis.

1.5.13 Digital detection of encapsulated cells using fluorescence microscopy

The ability to understand cell functions and fate is vital in many fields such as cell biology, biotechnology and medicine. Therefore, a number of tools such as florescence microscopy have been developed to help manipulate and characterise cells, which in turn has enhanced our understanding of cell functioning. The cells that were encapsulated using the optimised microfluidic chip and setup described in Chapter 4 were imaged using florescence microscopy to monitor cell growth.

Fluorescence microscopy is a powerful tool that enables instant and detailed visualisation of cells, cellular components and tissues. Visualisation of these biomolecules is achieved since fluorescent labels, such as propidium iodide (PI), bind to specific cellular components and allows real time images to be taken. Furthermore, taking snapshots of cells allows for stationary optical information to be obtained. On the other hand, operating the microscope in the dynamic mode enables various cellular functions such as cell growth and division to be monitored (260).

1.5.13.1 Fluorescent dyes

There is a broad range of fluorescent dyes that are commercially available to stain different cellular components. These dyes have different colours, which make it easier to differentiate between cellular components in addition to assessing whether cells are alive or dead. For instance, the ability to label cell nuclei with propidium iodide (PI) can facilitate with tracking single cells both manually and automatically (260,261). Furthermore, calcein acetoxymethyl ester (calcein-AM) is another useful dye, which is used for time-lapse microscopy. Calcein-AM is a naturally non fluorescent molecule, which is able to penetrate cell membranes. However, the green signal emitted from calcein-AM is caused due to the modification it incurs by intercellular esterases found in living cells, which results in the production of a green fluorescent product that is trapped in the cytoplasm. Hence calcein-AM is beneficial both as a tracking dye and for monitoring cell viability during living imaging (261).

1.5.13.2 Maintaining healthy cells for continuous imaging

The ability to maintain live cells is the most important parameter for long term time lapse imaging. Hence, there is a need to recreate the cells native environment as much as possible. To recreate such an environment many factors need to be considered. The medium used should be able to supply cells with the relevant nutrients, the temperature and pH, the supply of oxygen and carbon dioxide, in addition to maintaining cell osmolarity (261).

The concentration of CO_2 is usually higher in cell culture media than in the atmosphere, this is because a higher concentration is needed in order to maintain cell processes and pH (261,262). Cell cultures are usually maintained in humidified incubators that are set at 37^oC and are supplied with 5% CO_2. However, the CO_2 can evaporate quite rapidly due to the constant exchange of gases. Removing cells from the incubators can reduce cell

viability due to fast changes in pH. Therefore many buffers, such as 25 mM HEPES [4-(2-hydroxyethyl)-1-piperazineethanesulfonic acid], are routinely used in cell culture laboratories (261,263).

The best approach to maintain the desired pH for cell viability when carrying out time-lapse experiments is to ensure the microscope used is equipped with an incubator, which allows both the temperature and CO_2 to be monitored and altered when needed. Alternatively, the culture medium can be equilibrated at 5% CO_2 and the incubation chambers used should be sealed. It important to remember that most plastic ware used for cell culturing purposes is permeable to gas (261).

1.6 Conclusion

Microfluidic technology plays a fundamental role in reducing samples and formulations needed for a wide range of biological and medical applications. Numerous approaches have been carried out to encapsulate live cells in microbeads to conduct further biological experiments such as monitoring cell growth and fate. However, there is a need to optimise existing approaches to produce an ideal microbead for cell encapsulation so that further biological and medical applications can be carried out. A comparison between natural and synthetic materials that have been used in literature to encapsulate cells, reveal that a number of materials maybe suitable for cell encapsulation once modified. Moreover, a comparison of different materials used to fabricate microfluidic chips was also carried out, and showed that a number of materials can be used but some are more suitable than others.

The low cost, biocompatibility and easiness to form gels makes alginate one of the most popular materials used for cell encapsulation. Cells still remain viable and grow upon encapsulation in alginate gel microbeads. This is most probably due to the advantages that this natural material has to offer in addition to allowing nutrients and oxygen to enter the microbeads when needed. Furthermore, the ability to degrade alginate gel microbeads using relatively mild techniques, offers many potential advantages for medical applications such as releasing insulin in diabetic patients.

A number of areas that required more understanding and improving were identified and can be summarised as follows:

- There is no detailed report on the effect of encapsulating cells in alginate gel microbeads, in terms of cell growth.
- There is also no detailed report on the effect of reagents and formulations used to solidify and degrade alginate gel microbeads.

- There is a need to optimise a microfluidic setup and chip to produce alginate gel microbeads, which are easy to use, design and generate reproducible microbeads, which can then be used for cell encapsulation.

The following Chapter (Chapter Two) details investigations that were carried out to determine the suitability of alginate as an encapsulating material for live Jurkat cells. In summary, these investigations included studying the effect of reagents used to solidify and degrade the alginate beads on cell growth, in addition to monitoring cell growth in the alginate gel beads over a period of seven days. Based on the results obtained alginate was used to produce gel microbeads containing cells in further investigations, which were carried out in Chapters three and four.

2 Chapter TWO
Calcium Alginate as an encapsulating material

2.1 Introduction

Extensive research has been carried out in the field of cell biology to enhance the development of three-dimensional (3D) cell cultures. The significant increase in interest of studying cells in 3D culture is due to the fact that 2D cultures are unable to mimic cellular activities *in vivo* (13,14). Moreover, cells interact with each other and with matrices, regulate signalling pathways and cell survival in 3D environments (14,264). Hence, findings obtained from 2D culture systems could be misleading (13) and unreliable. The development of a stable and reliable 3D culture will therefore improve our current knowledge of many cellular processes.

The main aims of this chapter were to encapsulate live Jurkat Clone E6-1 cell lines (T-lymphocytes) in calcium alginate gel beads, in addition to determining the effect of the formulations used to solidify and dissolve these beads. Jurkat cells were chosen for the work carried out in this Thesis as they are an acceptable cell model for many biological and medical research studies (16), in addition they are easy to maintain and was readily available from Dr. Anne-Marie Buckle's research group.

Alginates are composed of blocks of α-l-guluronic and β-d-mannuronic acid residues. The sequences and structures of alginate vary from one type to another, depending on the composition of α and β block regions that they consist of (48). Alginate was used as the encapsulating material in the work described in this PhD thesis for several reasons including: its biocompatibility (265), low toxicity, inexpensive (265) and its ability to form gels easily in the presence of divalent cations, for example Ca^{2+} and Mg^{2+} (48,265).

The calcium alginate gel beads were produced using a 25 Gauge × 25.4 mm needle that was attached to a syringe containing the sodium alginate/cell solution. This solution was

then dispersed gently into a cross-linking bath consisting of 10% calcium chloride solution, resulting in the gelation of the alginate droplets. It was vital that the alginate solution was dispersed into the 10% calcium chloride solution gently in order to prevent unwanted coalescences of the alginate gel beads (220).

The materials, methods, and formulations used to produce calcium alginate gel beads containing Jurkat cells and to dissolve them if needed are discussed in this Chapter. The effect of calcium chloride and sodium citrate on cell viability and cell growth was studied to determine their compatibility with live cell studies, in particular for the process of microencapsulation. Findings showed that these formulations had a relatively low impact on cell viability and that encapsulated Jurkat cells were 100% viable over a period of 7 days.

2.2 Materials, methodologies and instrumentation

2.2.1 Materials

The materials used for cell culturing, cell encapsulation and dissolution calcium alginate gel beads are listed in Table 2. below.

Table 2.1: Materials used for initial studies on cell encapsulation in alginate gel beads

Reagents and materials	**Purity/ concentration**	**Product code**	**Supplier**
Alginic acid sodium salt from brown algae (sodium alginate)		A2033	Sigma Aldrich
Calcium chloride, anhydrous	≥97%	746495	Sigma Aldrich
Corning® cell culture flasks surface area 25 cm^2, angled neck, cap (vented)	NA	CLS3056	Sigma Aldrich
Corning® cell culture flasks surface area 75 cm^2, canted neck, cap (vented)	NA	CLS430641	Sigma Aldrich
Corning® Costar® cell culture plates 24 well, flat bottom (individually wrapped)	NA	CLS3524	Sigma Aldrich
Corning® Costar® Stripette® serological pipettes, individually paper/plastic wrapped. Capacity 5 mL	NA	CLS4487	Sigma Aldrich
Corning® Costar® Stripette® serological pipettes, individually paper/plastic wrapped. Capacity 10 Ml	NA	CLS4488	Sigma Aldrich
Corning® Costar® Stripette® serological pipettes, individually paper/plastic wrapped. Capacity 25 mL	NA	CLS4489	Sigma Aldrich
Dimethyl sulfoxide	≥99.9%	472301	Sigma Aldrich
Fetal Bovine Serum USA origin, sterile-filtered, suitable for cell culture, suitable for hybridoma	Impurities ≤10 EU/mL endotoxin	F2442	Sigma Aldrich

Glacial acetic acid	≥99.7%	695092	Sigma Aldrich
Gelatine from bovine skin		G9391	Sigma Aldrich
Hydrochloric acid (HCl)	36.5-38.0%	H1758	Sigma Aldrich
Gilson micropipettes	NA	10736825	Thermo Fisher Scientific, Inc
(4-(2-hydroxyethyl)-1-piperazineethanesulfonic acid) (HEPES)	≥99.5%	H4034	Sigma Aldrich
Isopropanol	70% in H_2O	563935	Sigma Aldrich
L-Glutamine solution, sterile-filtered, BioXtra, suitable for cell culture	200 mM,	G7513	Sigma Aldrich
25 Gauge × 25.4 mm needle	NA	BD305125	VWR
Micropipette tips (20, 100 and 1000 µl)	NA	15287783 and 10123002	Fisher Scientific
Penicillin-Streptomycin. Solution stabilised, with 10,000 units penicillin and 10 mg streptomycin/mL, sterile-filtered, BioReagent, suitable for cell culture	100 ×	P4333	Sigma-Aldrich
Dulbecco's Phosphate Buffered Saline (PBS) With MgCl2 and $CaCl_2$, liquid, sterile-filtered, suitable for cell culture		D8662	Sigma-Aldrich
RPMI-1640 (with sodium bicarbonate, without L-glutamine)		R6504	Sigma-Aldrich
Sodium hydroxide (NaOH)	≥97.0%	221465	Sigma-Aldrich
Trisodium citrate		S1804	Sigma-Aldrich
Trypan blue 0.4%, liquid, sterile-filtered, suitable for cell culture		T8154	Sigma-Aldrich
Mr Frosty (cell freezing container)	NA	5100-0001	Fischer Scientific

2.3 Methodology

2.3.1 Cell culturing, maintenance, freezing and recovery procedures for Jurkat cell lines

The Jurkat cells used for investigations carried out in this Chapter were obtained from Dr. Anne-Marie Buckle's research group at the University of Manchester. Jurkat cell lines were sub-cultured in a class II biohazard cabinet under a laminar flow (purchased from Walker Safety Cabinet Ltd, Glossop, UK). The cells were maintained in RPMI-1640 medium (with sodium bicarbonate, without L-glutamine), and were incubated in a Galaxy® S Series CO_2 Incubator (Walker safety cabinets, Glossop, UK) at 37°C and in a 5% CO_2 atmospheric environment. The RMPI-1640 medium was supplemented with 5% (v/v) foetal bovine serum (FBS), 1 mM L-glutamine and 1% (v/v) Penicillin-Streptomycin (10,000 units of penicillin and 10 mg of streptomycin/ mL). The supplemented RPMI-1640 medium was stored at 4°C until needed. The Jurkat cells were routinely sub-cultured three times a week in fresh complete RPMI-1640 medium so that the initial seeding density was never allowed to exceed 2×10^5 cells/ mL and was not allowed to exceed 3×10^6 cells/ mL. The cells were transferred into a 15 mL universal tube every two weeks and were centrifuged at 1800 rpm for 5 minutes forming cell pellets that was re-suspended in 9 mL of RPMI-1640 medium to remove any build up of old RPMI-medium and cell debris.

The Jurkat cells were preserved by freezing using liquid nitrogen in a pre-prepared freezing medium consisting of 80% FBS with 20% Dimethyl sulfoxide (DMSO). The cells were centrifuged at 1800rpm for 5 minutes, and the supernatant was removed. The cell pellet was then re-suspended in the freezing media to a concentration of 3×10^6 cells/ mL and aliquoted into 1 mL cryogenic vials. DMSO is hazardous at 37^oC or room temperature so this step needs to be carried out on ice. Once the cryogenic vials were filled, they were placed into a cell freezing container with isopropanol. The Jurkat cells were then stored in

a - 80°C freezer for two days before being transferred to liquid nitrogen for long term storage.

The cells were thawed by rolling the cryogenic vial in the hands and were pipetted out as quickly as possible. The cells were subsequently transferred into 10mL of chilled fresh complete RPMI-1640 medium as soon as the ice had almost thawed, and were spun down in a universal centrifuge tube at 1800rpm for 5 minutes. The supernatant was removed and the cell pellet was re-suspended in 10mL of complete RMPI-1640 medium (room temperature) and was placed into the incubator.

2.3.2 Cell count

Trypan blue exclusion method was used to count the number of Jurkat cells (viable and dead cells) in suspension. This traditional cell biology staining method works by staining the cytoplasm of dead cells blue, while the cytoplasms of the live cells remain clear because trypan blue does not penetrate viable cell membranes (266). To carry out this test, 5µl of Jurkat cell suspension was mixed with 5µl of pre-filtered 0.05% trypan blue dye, and was then examined immediately using a haemocytometer under a microscope. Figure 2.1 shows a light microscope image of Jurkat cells that have been stained with 0.05% trypan blue.

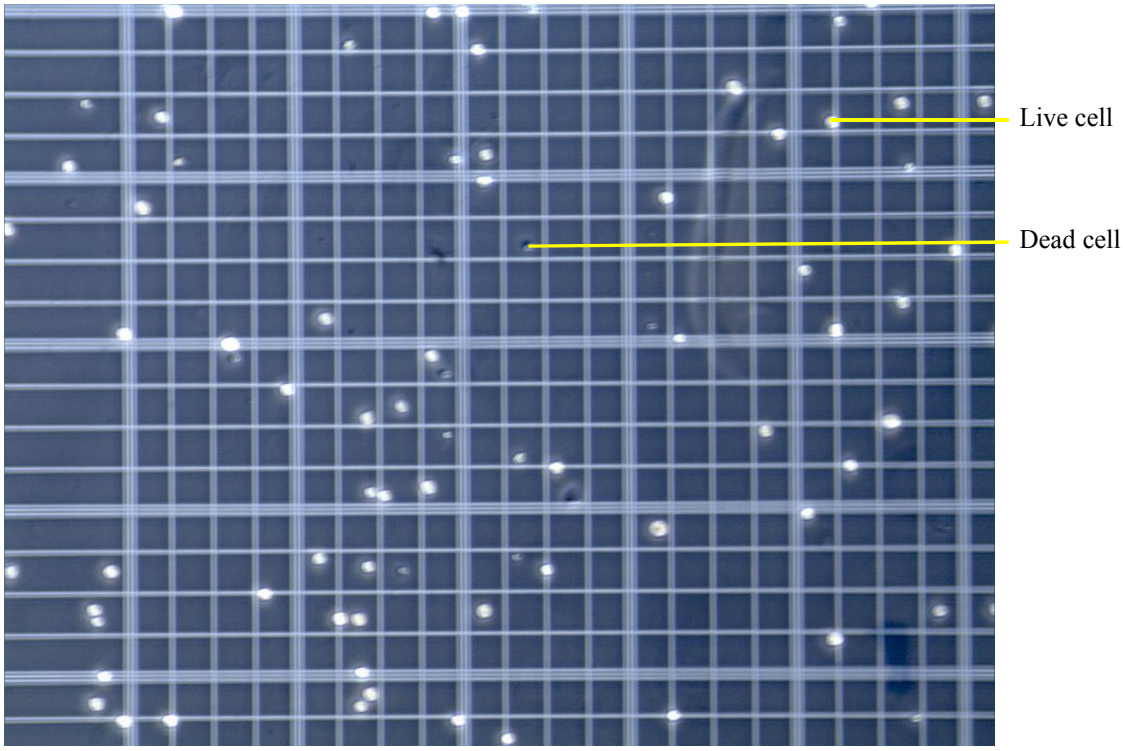

Figure 2.1: Cells stained with trypan blue visualised using a light microscope. The bright (white) cells are live and the dark blue cells are dead.

A haemocytometer is a thick microscope slide that is made up of two polished sub-divided grid surfaces and two wells. These grids have nine primary squares, with each primary square sub-divided into secondary squares, each measuring 0.0625mm^2. An image of the haemocytometer grids is shown in Figure 2.2. A haemocytometer coverslip was used to mount the microscope slide to resist any surface tension from liquid. The coverslip is 0.1mm above the grid and thus give a volume of 0.1 mm^3 allowing the calculation of cell count per ml.

$$\boldsymbol{Cell\ count\ per\ ml = counted\ number\ of\ cells \times 10000} \qquad \textbf{Equation 2.1}$$

Each time the haemocytometer and coverslips were used they were carefully cleaned with 80% ethanol and lens paper. The coverslip was then placed over the haemocytometer before the cell suspension was introduced. Subsequently enough cell suspension was

gradually pipetted into one of the wells, filling up the polished gridded surface under the coverslip by capillary action. In case of chamber overloading, filter paper was used to remove any unwanted cell suspension. The haemocytometer was then placed under the microscope for cell counting using the x20 magnification objective. The cells that occupied the upper or left boundaries of the grid were included in the cell count, whereas cells that occupied the bottom or right boundaries were excluded.

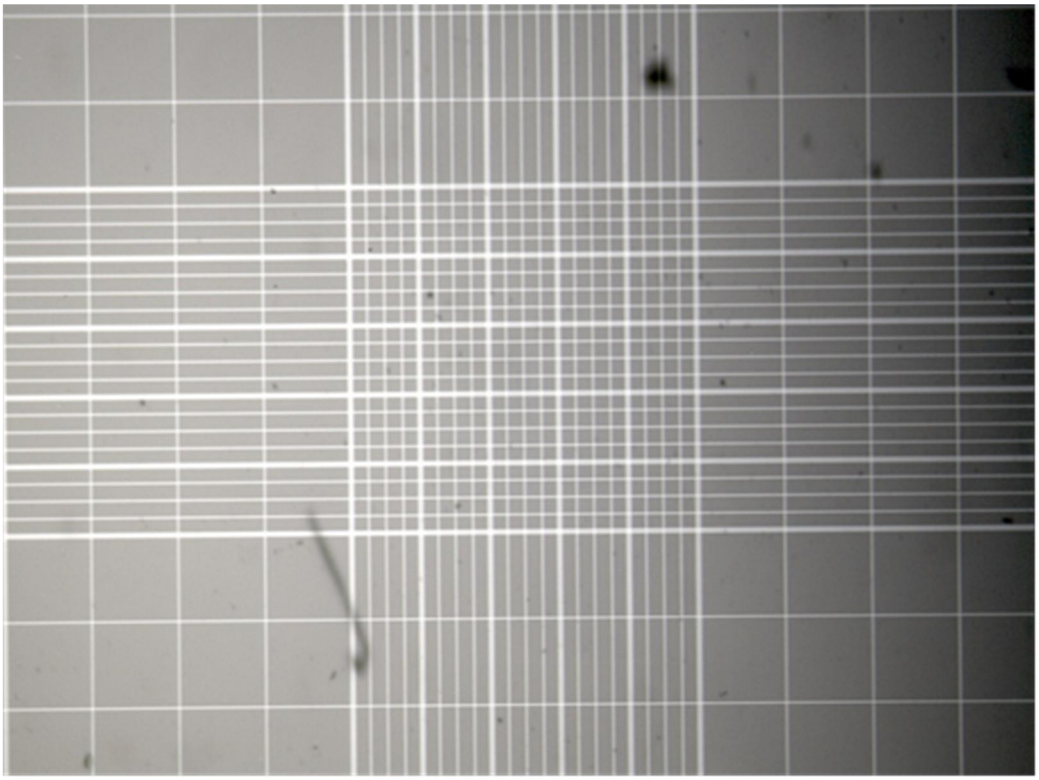

Figure 2.2: Image of the sub-divided grid surface of the haemocytometer used to count cells using the trypan blue exclusion method.

The trypan blue exclusion method was not only used to count cells, but was also used to determine the percentage viability of cells, the live and dead cells as described above in this section. Percentage viability of cells was calculated using equation 2.2.

$$\%\ \boldsymbol{Cell\ Viability} = \frac{\boldsymbol{number\ of\ live\ cells}}{\boldsymbol{total\ cell\ count}} \times \mathbf{100} \qquad \text{Equation 2.2}$$

2.3.3 Calcium chloride solution preparation

Firstly a stock solution of 10% (w/v) calcium chloride ($CaCl_2$) was prepared using deionised water, and the solution was autoclaved. Subsequently, 1M HEPES (4-(2-hydroxyethyl)-1-piperazineethanesulfonic acid) solution was made up. To make a 100 mL of $CaCl_2$ solution, the following solutions were mixed together: 11 mL $CaCl_2$ stock solution, 100 µl of 10% Tween 20 and 1 mL of 1M HEPES solution. Deionised water was then added to the solution to make a total volume of 100 mL, and the pH was adjusted to 7.4 with HCl and/ or NaOH.

2.3.4 Preparation of sodium alginate solution

A 1.1% sodium alginate solution was prepared for cell encapsulation by adding 0.55 g of alginate powder to 47.5 mL of sterile PBS (267) and 2.5 mL gelatin 2% v/w. Gelatin was added to the alginate solution to enhance its biodegradability (122) and to stimulate cell attachment (268).

2.3.5 Encapsulation of cells in calcium alginate gel beads using a syringe

Firstly, the cells were counted using the trypan blue exclusion method described above, and were then centrifuged to remove any old medium and cell debris. The cell pellet was then resuspended in 1 mL of 1.1% alginate solution. 1 mL of 10% $CaCl_2$ solution was transferred into the wells of a 24 well plate using a 1 mL micropipette. The alginate and cells were then aspirated carefully using a 1 mL syringe to prevent air bubbles. The aspirated alginate/cell suspension was then released into the well containing 10% $CaCl_2$ solution in a dropwise manner using a 25 Gauge x 25.4 mm needle to form the beads. The

distance between the needle and the suspension was about 2 cm, as this was the ideal distance to produce alginate microbeads with sizes nearing 2 mm in diameter.

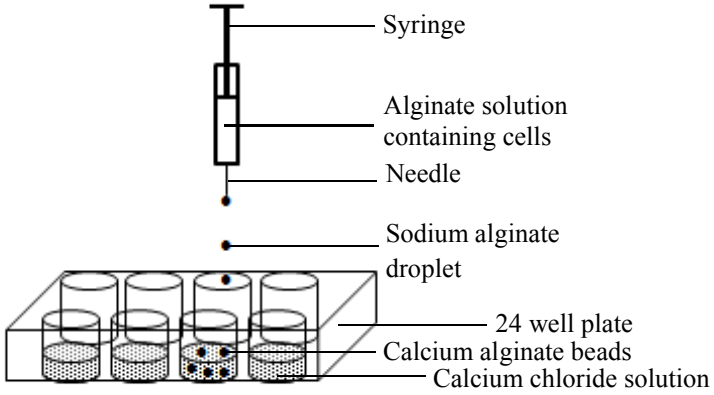

Figure 2.3: Schematic diagram showing the experimental setup used to encapsulate Jurkat cells in huge calcium alginate beads.

The volume of each bead produced was estimated to be approximately 13 µl (approximate radius of 1.5 µm), since 80 beads were produced per 1 mL of alginate/cell solution. The beads were left to incubate for 10 minutes in 10% $CaCl_2$ solution. Excess/ unreacted 10% $CaCl_2$ solution was then removed carefully using a 1 mL micropipette ensuring that the beads were not pipetted out during this process. The beads were washed three times with 1 mL of PBS per well. Once the beads were washed, 1 mL of complete RPMI-1640 media was finally added to each well, and the 24-well plate was left to incubate in a Galaxy® S Series CO_2 Incubator at 37°C and in a 5% CO_2 atmospheric environment. The medium was changed every 4-5 days. Photographs of some of hollow alginate gel beads produced using the syringe method were taken and are shown in Figure 2.4. These beads were stained with amaranth dye in order to help visualise the beads under a microscope using the phase contrast setting.

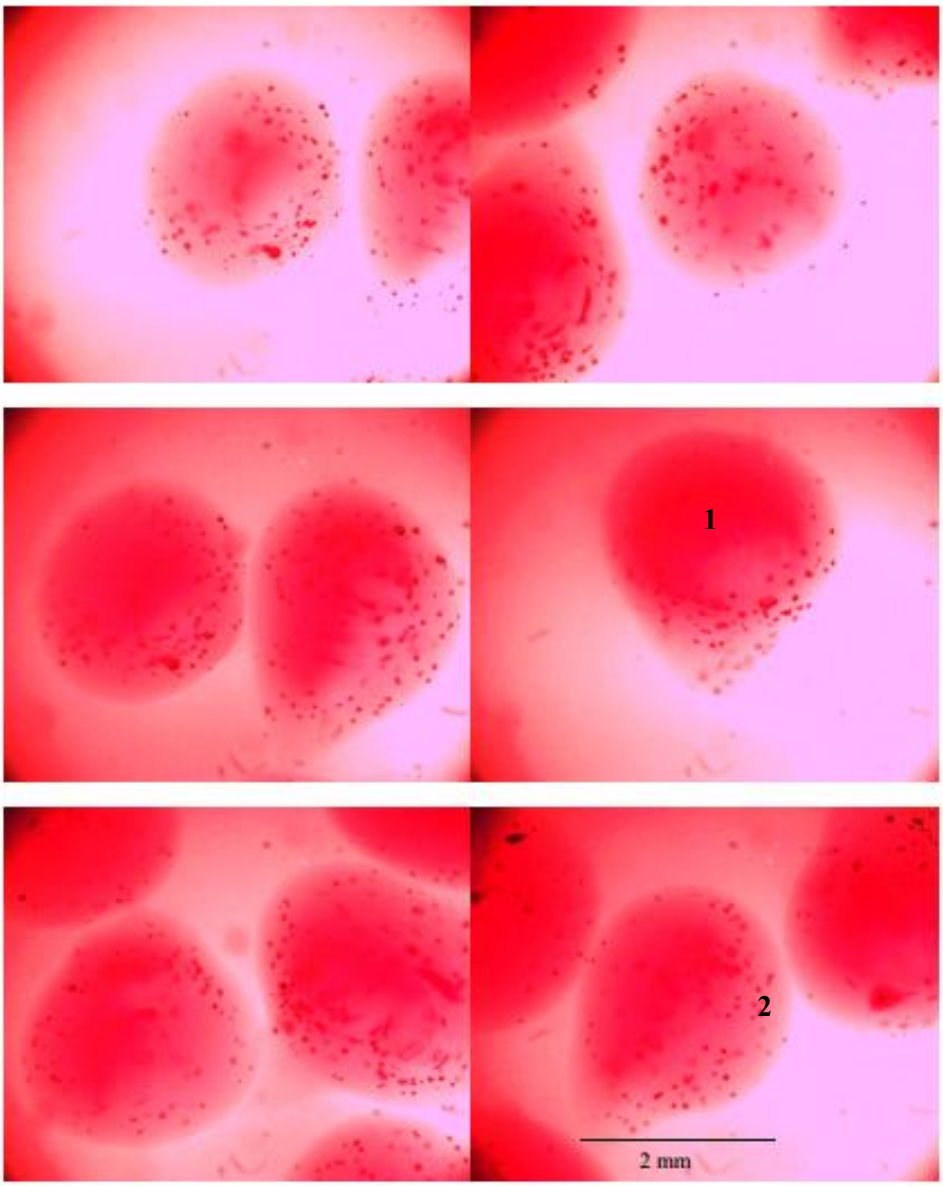

Figure 2.4: Single frame images of alginate gel beads produced using a syringe and 25 Gauge × 25.4 mm needle. The beads were stained using amaranth dye to help visualise the beads under the microscope. These images were taken using a mono camera on a Zeiss Primo Star microscope at x 40 magnification using the phase contrast setting. 1: An empty calcium alginate gel microbead and 2: Inconsistency within the alginate gel.

2.3.6 Measurements of the calcium alginate beads

The calcium alginate beads containing cells were examined using a light microscope at ×20 magnification. The diameters of these beads were then measured using a stage micrometer.

2.3.7 Preparation of sodium citrate buffer at varying concentrations

The dissolution buffer chosen to release the cells from the calcium alginate gel beads was sodium citrate. The buffer was made up initially at a concentration of 50 mM by adding 14.8 g of sodium chloride, 2.4 g of HEPES and 14.8 g tri sodium citrate to distilled water. This was followed by adjusting the pH of the buffer to 7.33. The buffer was then autoclaved.

Another two concentrations (100 mM and 200 mM) of sodium citrate buffer were also prepared in order to study the effect of increasing the concentration of sodium citrate buffer on the time needed to dissolve the calcium alginate gel beads containing cells.

2.3.8 Sodium citrate as a dissolution buffer

The calcium alginate gel beads were dissolved using sodium citrate buffer (dissolution buffer). Firstly, the RPMI-1640 medium was removed from the wells containing beads, and the beads were washed twice with PBS buffer. Next the beads were left to incubate at room temperature in 1 mL of dissolution buffer for 10 minutes. Then 1 mL of PBS was added to each well. The cell suspension containing sodium citrate buffer was then centrifuged at 1800rpm for 5 minutes. The supernatant was removed carefully using a 1 mL micropipette. This was followed by adding l mL of RPMI-1640 medium to the cell pellet. The cell pellet/medium mixture was mixed thoroughly by pipetting the mixture up and down using a blue 1 mL micropipette tip in preparation for cell counting section 2.3.2.

2.3.9 Cytotoxicity testing

A series of cytotoxicity tests were conducted to study the effect of the solutions and the buffer needed to encapsulate the cells in calcium alginate gel beads and to dissolve the beads. To carry out these tests 10 mL of samples containing Jurkat cells in RPMI medium (2×10^6 cells per mL) was centrifuged at 1800 rpm for 5 minutes. The medium was removed and the cell pellet was gently resuspended in 1 mL of the substance to be tested,

and was incubated for 10 minutes at 37°C and in a 5% CO_2 atmospheric environment. The substances tested in the initial studies conducted were the calcium chloride solution and sodium citrate buffer. The cells were resuspended in 1 mL of either calcium chloride solution or sodium citrate buffer depending on the test required. Once the incubation period was over, 10 µl of the resuspended cells was added to 100 µl of complete RMP1-1640 medium. This was carried out at different time points to study the effect of exposing the Jurkat cells to these substances over a period. The time points used in these experiments were 0 (control), 2, 4, 6, 8 and 10 minutes. Cell numbers were then counted using the trypan blue exclusion method as described in section 2.3.2. Cell numbers of each sample were also counted at longer time points including: 10 minutes, 30 minutes, 1 hour, 8 hours, 24 hours and 48 hours after incubation. Jurkat cells grown in a traditional 2D cell culture flask was used as a control in all of the cytoxicity tests.

2.3.10 Cell growth in calcium alginate gel beads

Jurkat cells were encapsulated in alginate gel beads as described in section 2.3.5. The beads were incubated at 37°C upto seven days in an incubator supplied with 5% CO_2. The alginate gel beads were dissolved in preparation for cell counting using the sodium citrate buffer prepared in section 2.3.8. The cells were then counted over five different time points to study cell growth using the trypan blue exclusion method described in section 2.3.2. The time points were: 30 minutes, 24 hours, 3days, 5 days and 7 days after encapsulation.

2.3.11 Effect of sodium citrate on alginate gel bead dissolution under varying volume and temperature conditions

Alginate gel beads containing cells were dissolved using three different concentrations of sodium citrate dissolution buffer. The concentration of sodium citrate was increased to 100 mM and 200 mM compared to the 50 mM used to make up the dissolution buffer described in section 2.3.7. The beads were dissolved using the three dissolution buffers at two distinct temperatures, 25°C and 37°C, and the time needed to dissolve them was measured

using a stop watch. The purpose of increasing the concentration of sodium citrate was to determine whether or not an increase in concentration increased the speed of gel dissolution. The alginate gel beads were also exposed to three different volumes (6 µl, 10 µl and 13 µl) of the three dissolution buffers, in order to determine the minimum volume and time needed to dissolve alginate gel beads.

2.3.12 The effect of three different concentrations of sodium citrate dissolution buffer on Jurkat cells

Jurkat cells were seeded at 2×10^5, and were directly exposed to the three dissolution buffers containing different sodium citrate concentrations; in order to determine the effect of increasing the concentration of sodium citrate in the dissolution buffer on cell growth. This was carried out using the experimental design described in section 2.3.9.

2.4 Results

2.4.1 The effect of 10% calcium chloride ($CaCl_2$) solution on Jurkat cells

The calcium alginate gel beads produced to encapsulate Jurkat cells in this chapter were gelified as mentioned above using a calcium chloride solution. Therefore, toxicity tests were carried out to determine the effect of 10% $CaCl_2$ solution on cell growth. The results from these trials were plotted into two separate graphs. Each point on the scattered plot represents an average of three experiments that were carried on three different days.

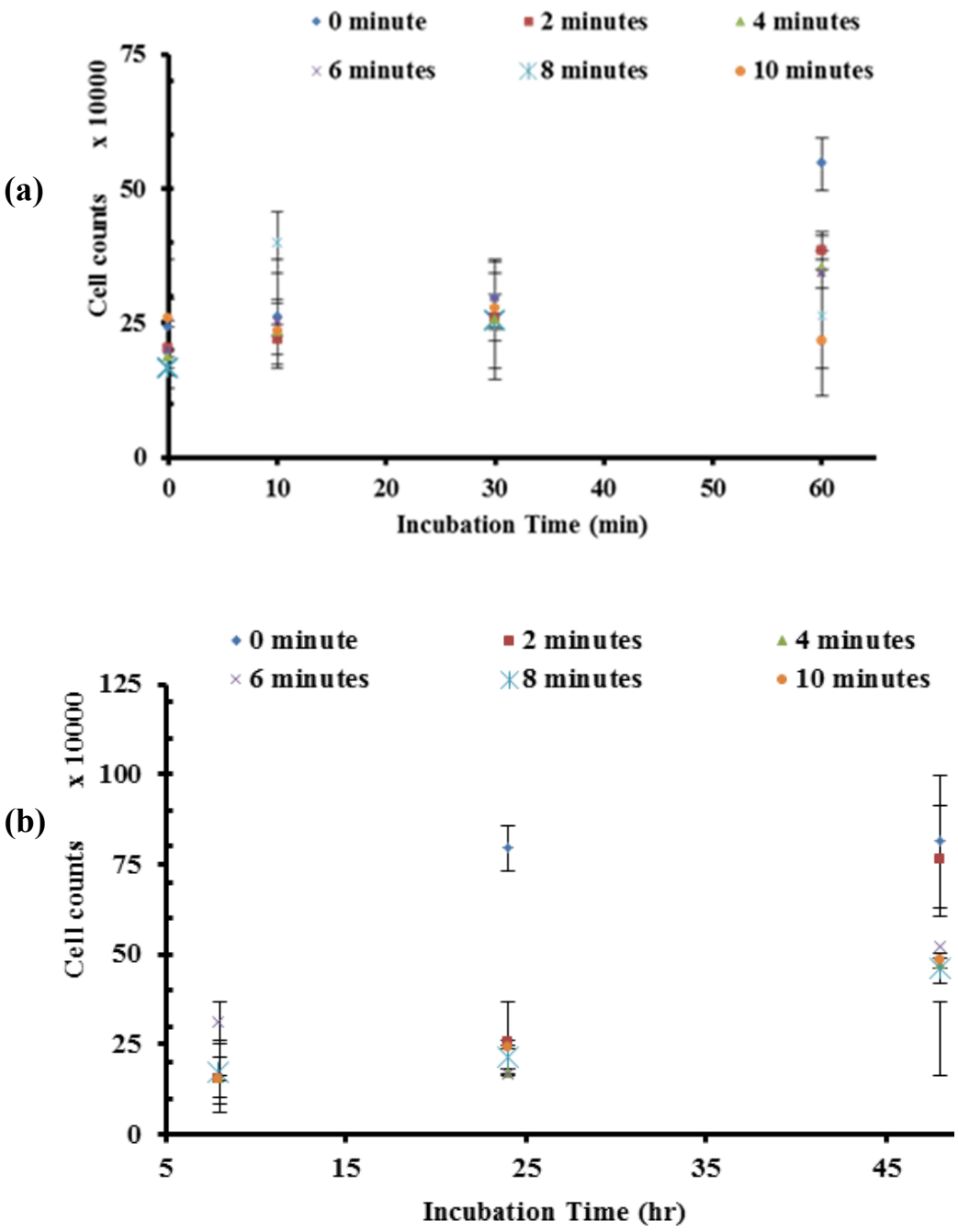

Figure 2.5: The effect of 10% $CaCl_2$ treatment used to gelify the calcium alginate gel beads on cell count over a period of up to: (a) 60 minutes and (b) 48 hours. The error bars indicate the standard error of the mean of three sample replicates.

In general, there is no significant effect of 10% $CaCl_2$ solution on cell growth for the first 30 minutes. However, after 30 minutes of incubation a trend starts to appear, whereby cell counts decrease with an increase in exposure time to 10% $CaCl_2$ solution as shown in Figure 2.5.a Moreover, extended incubations beyond the initial 1 hour and up to 48 hours was carried out to investigate whether varying exposure times to 10% $CaCl_2$ solution has any potential effect on cell division. Figure 2.5.b shows that there is an increase in the number of cells at incubation time 24 hours and 48 hours (these two incubation times are enough for cell division), which was almost double in comparison to the control. However, the rate at which cells divide seems to be affected by 10% $CaCl_2$ exposure since untreated cells divide at a faster rate over 48 hours incubation. Thus, it can be concluded that the initial cell growth inhibition by 10% $CaCl_2$ has a lasting and prolonged effect on cells and exposure to 10% $CaCl_2$ should be kept to a minimum. Similar observations have also been reported in the literature (269,270).

2.4.2 The effect of 10% $CaCl_2$ on cell viability

The effect of 10% $CaCl_2$ on the viability of the Jurkat cells was also investigated. The results were plotted into two separate graphs (Figures 2.6.a and 2.6.b). Each point on the scattered plots represents an average of three experiments that were carried on three different days.

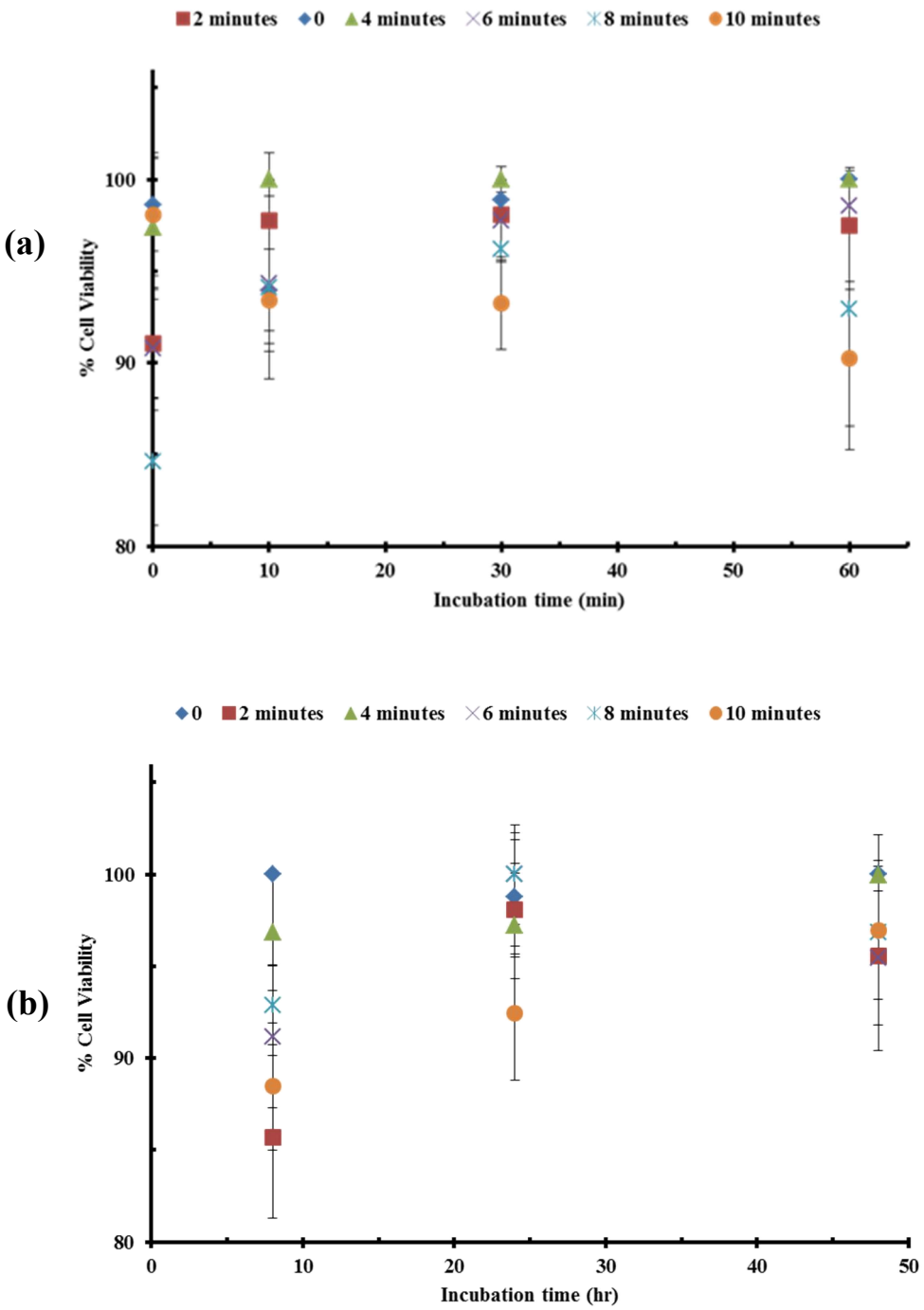

Figure 2.6: The effect of 10% $CaCl_2$ treatment used to gelify the alginate gel beads on cell viability over a period of: (a) 60 minutes and (b) 48 hours. The error bars indicate the standard error of the mean of three sample replicates.

Figure 2.6.a shows the viability of Jurkat cells that have been exposed to 10% $CaCl_2$ for a number of incubation time points: 0, 2, 4, 6, 8 and 10 minutes respectively. In general over 90% of the Jurkat cells were viable for the first 60 minute, and the % viability was mostly between 94% - 99% with only two percentages as low as 84 and 87%. The % cell viability

of Jurkat cells when exposed to 10% $CaCl_2$ solution initially decreases a little. These lower percentages were found in cell populations that were exposed to 10% $CaCl_2$ solution for an initial time of 8 and 10 minutes. On closer analysis it was observed that a trend in exposure time to 10% $CaCl_2$ to % cell viability is evident; the longer the exposure time to 10% $CaCl_2$, the less viable were the cells.

Figure 2.6 shows the results obtained on Jurkat cells exposed to 10% $CaCl_2$ over 2,4,6,8 and 10 minutes and incubated up to 48 hours. Similar trend to that observed for the incubation of up to 1 hour was observed (Fig. 2.5 for up to 60 mins) on prolonged exposures for up to 48 hours. There isn't a clear pattern in the viability of the cells in the function of exposure to 10% $CaCl_2$.

In summary, the percentage viability of the Jurkat cells treated with 10% $CaCl_2$ did not decrease significantly over the first 10 minutes (~90% cell viability), with the lowest number of viable cells observed after 8 hours. The effect of $CaCl_2$ on cell viability was clear. Instead of the expected 200% increase in cell numbers, 50% increase in cell was only observed, indicating that the ability of Jurkat cells to grow clearly deteriorated when exposed to $CaCl_2$. Similar findings have been reported in a number of published articles. Gyun Min Lee et al. reported no significant effect of calcium chloride treatment on cell viability in the first hour of exposure; nevertheless cell growth appeared to deteriorate (269). Therefore, the authors suggested that is it desirable to limit the time that the cells are exposed to calcium chloride treatment. In another study carried out by Kim M. McGinnis et al. (270) , cells were treated with 5 mM calcium chloride to study the effect of calcium chloride on cell viability. The results obtained indicated that indeed excess exposure of cells to calcium chloride stimulates cell death. Moreover, a more recent study reported by Gudapati H et al. (271), concluded that the recoverability of cells encapsulated in alginate gel beads decreased as the exposure time to calcium chloride (used for the gelation

process) increased. One of the possible explanations for this observation is that the excess calcium ions induced cell injury (269,270), which is not surprising since calcium is the main internal messenger in the cell.

2.4.3 The size of the alginate gel beads produced

Alginate gel beads are widely used for encapsulating many biomaterials such as cells, enzymes and hormones (37,104,182,208,271). The successful encapsulation of such materials prompted many research groups to investigate the importance of bead characteristics (such as size and shape) on the materials to be encapsulated (37,272-275). Owing to the importance of these characteristics, the size distribution of a number of the alginate gel beads produced for work carried out in this chapter was evaluated over three different trials Figure 2.7.

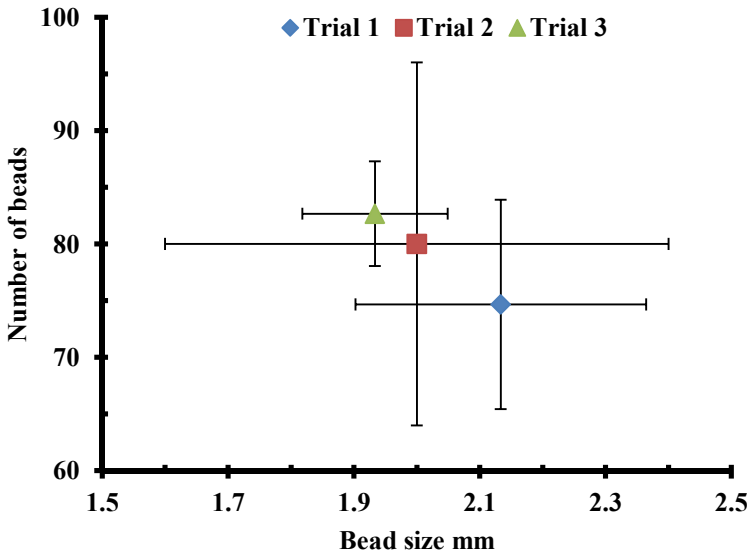

Figure 2.7: A graphical representation showing the relationship between the numbers of alginate beads produced using the dripping method described in this chapter verse the sizes of these beads. The error bars indicate the standard error of the mean of three sample replicates.

The results in Figure 2.7 shows that the alginate gel beads produced using the conventional dripping method described in this chapter had an undesirable wide size distribution range (1.6-2.4). Similar observations in term of producing polydisperse alginate beads have also been reported in the literature (242,276,277). One of the studies that were carried out by Ranganath and colleagues involved the encapsulation of PLGA-paclitaxel in alginate beads using two different dripping approaches: manual and electrospray dripping. The manual

dripping approach they adopted generated polydisperse and non-spherical beads. These characteristics were later improved using the electrospraying dipping method, which led to the production of alginate beads containing PLGA-paclitaxel. The size of the bead produced using this method is too large for any application and therefore using microfluidic chips is guaranteed to decrease the size.

2.4.4 The speed of alginate beads dissolution at three different concentrations of sodium citrate at two distinct temperatures.

The use of sodium citrate buffer to dissolve alginate gel beads has been reported in numerous papers (278-280). Excess exposure of calcium alginate gel beads to sodium citrate causes decrosslinks within calcium alginate gels, which is due to the chelation of calcium. As a result weaker and less stable alginate gels are formed, or if the concentration of the sodium citrate is significant enough, the alginate gels can be dissolved (279). The experiments described in this section were carried out to determine how quickly alginate gel beads dissolve in three different sodium citrate volumes (50 µM, 100 µM and 200 µM) at two different temperatures (room temperature (25^{o}C) and 37^{o}C). The results are summarized in Figure 2.8 below.

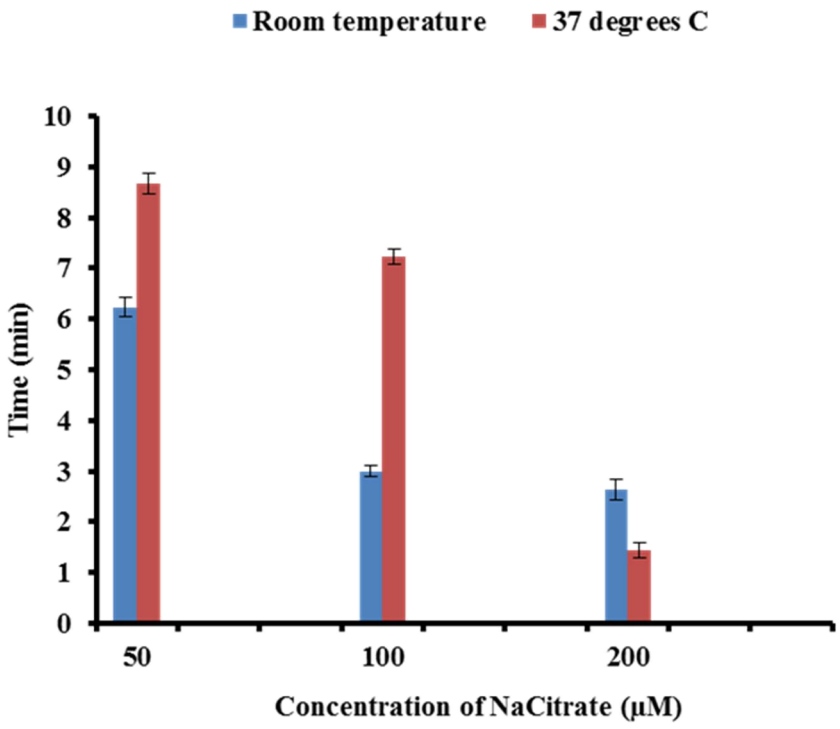

Figure 2.8: Effect of temperature on alginate beads dissolution in varying concentration of sodium citrate. The error bars indicate the standard error of the mean of three sample replicates.

The speed at which the alginate gel beads were dissolved at room temperature (25^{o}C) increased with an increase in the concentration of sodium citrate. In other words, the time required to dissolve the alginate gel beads incubated in 50 μM or100 μM sodium citrate increased when the temperature was raised to 37^{o}C, but decreased when they were incubated in 200 μM. Remarkably to our knowledge there are no other studies that reported the time needed to dissolve alginate beads at the aforementioned concentrations of sodium citrate and at two distinct temperatures. Hence, following on from this investigation, it was vital to study the effect of increasing the concentration of sodium citrate in the dissolution buffer on Jurkat cells, both in terms of viability and cell count.

2.4.5 The effect of varying the concentration sodium citrate dissolution buffer on Jurkat cells

Jurkat cells were incubated in three different sodium citrate dissolution buffers for 10 minutes at buffer concentrations 50 μM, 100 μM and 200 μM respectively in order to determine the effect of sodium citrate buffer on Jurkat cell growth. Following exposure to sodium citrate, the Jurkat cells were then incubated for a period of time spanning from 0 to 48 hours. The results are presented in Figures 2.9(a) (incubation time of 0 to 60 minutes) and Figure 2.8(b) (incubation time of 8 to 48 hours) respectively.

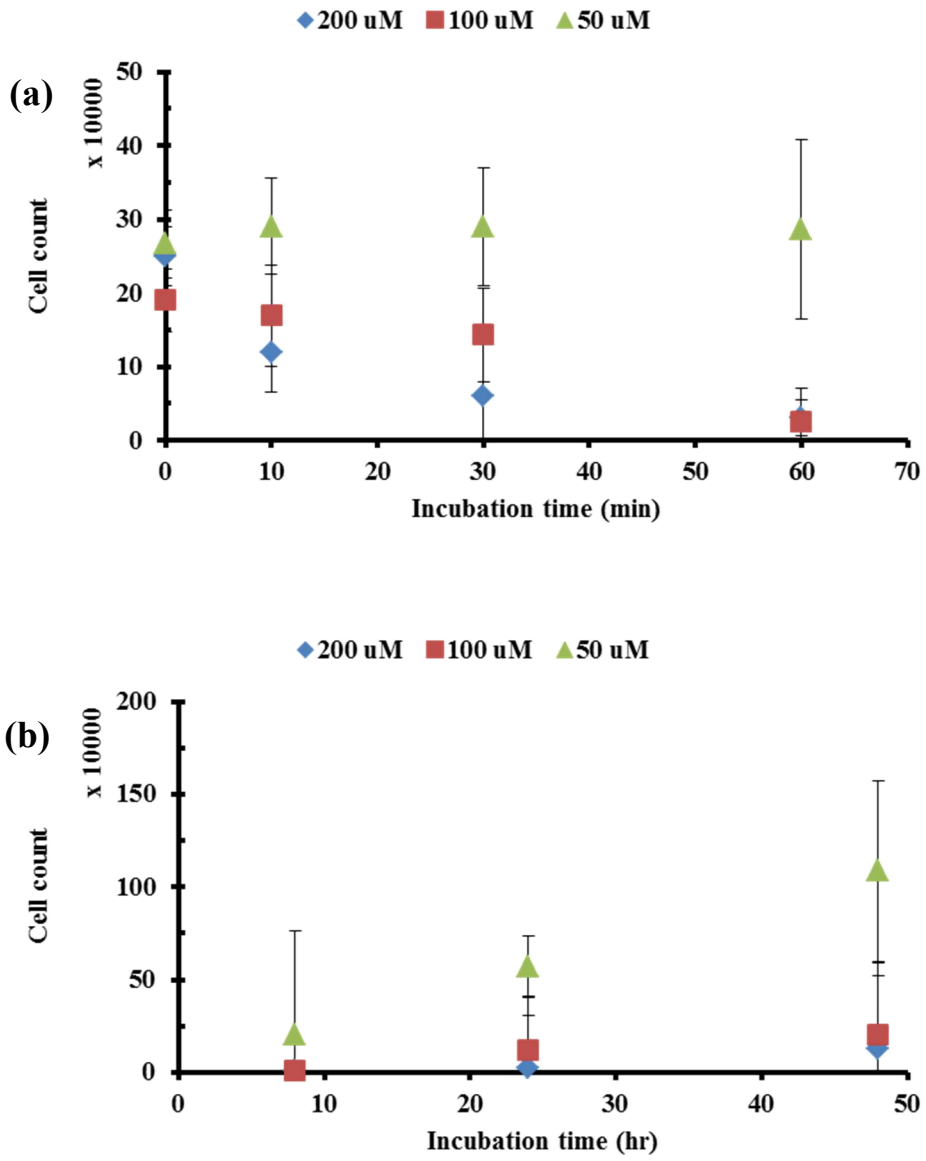

Figure 2.9: Effect of varying sodium citrate buffer concentrations of 200 µM, 100 µM and 50 µM on Jurkat cell growth for up to: (a) 60 minutes and (b) 48 hours. The error bars indicate the standard error of the mean of three sample replicates.

Figure 2.9(a) shows the effect of varying concentrations of sodium citrate buffer solution on Jurkat cell growth and initial finding shows that over 60 minutes there is a linear decrease in cell count for buffer concentrations of 100 µM and 200 µM. At 50 µM sodium citrate concentration there is no significant change in cell count indicating that this concentration does not affect cells incubated in it for 60 minutes.

Figure 2.9(b) shows the effect of varying buffer concentrations on Jurkat cells over prolonged incubation of up to 48 hours which would indicate if varying the concentrations of sodium citrate buffer has any potential effect not only on cell growth but on cell division. In all cases, from 8 hours exposure to 48 hours show an increase in cell counts. However, the rate of cell division reduced at higher buffer concentrations of 100 μM and 200 μM. At sodium citrate concentration of 50 μM the cell count almost doubled for each 24 hours exposure; showing that at this buffer concentration cell division is not impaired. This result is in line with what was observed over shorter exposure of up to 60 minutes (Figure 2.9(a)). Based on these results all further experiments with sodium citrate buffer were carried out at a concentration of 50 μM.

2.4.6 The effect of varying exposure time to 50 μM sodium citrate dissolution buffer on Jurkat cells

Jurkat cells were incubated in 50 μM sodium citrate dissolution buffer with different incubation times, in order to study the effect of exposure time to sodium citrate dissolution buffer solution on cell growth. Exposure time to sodium citrate buffer was varied from 0 to 10 minutes and for each exposure time, the Jurkat cells were incubated for a period of time spanning from 0 to 48 hours. Figure 2.10(a) shows the results obtained when incubating Jurkat cells for 60 minutes after being exposed to sodium citrate for various times (up to 10 minutes).

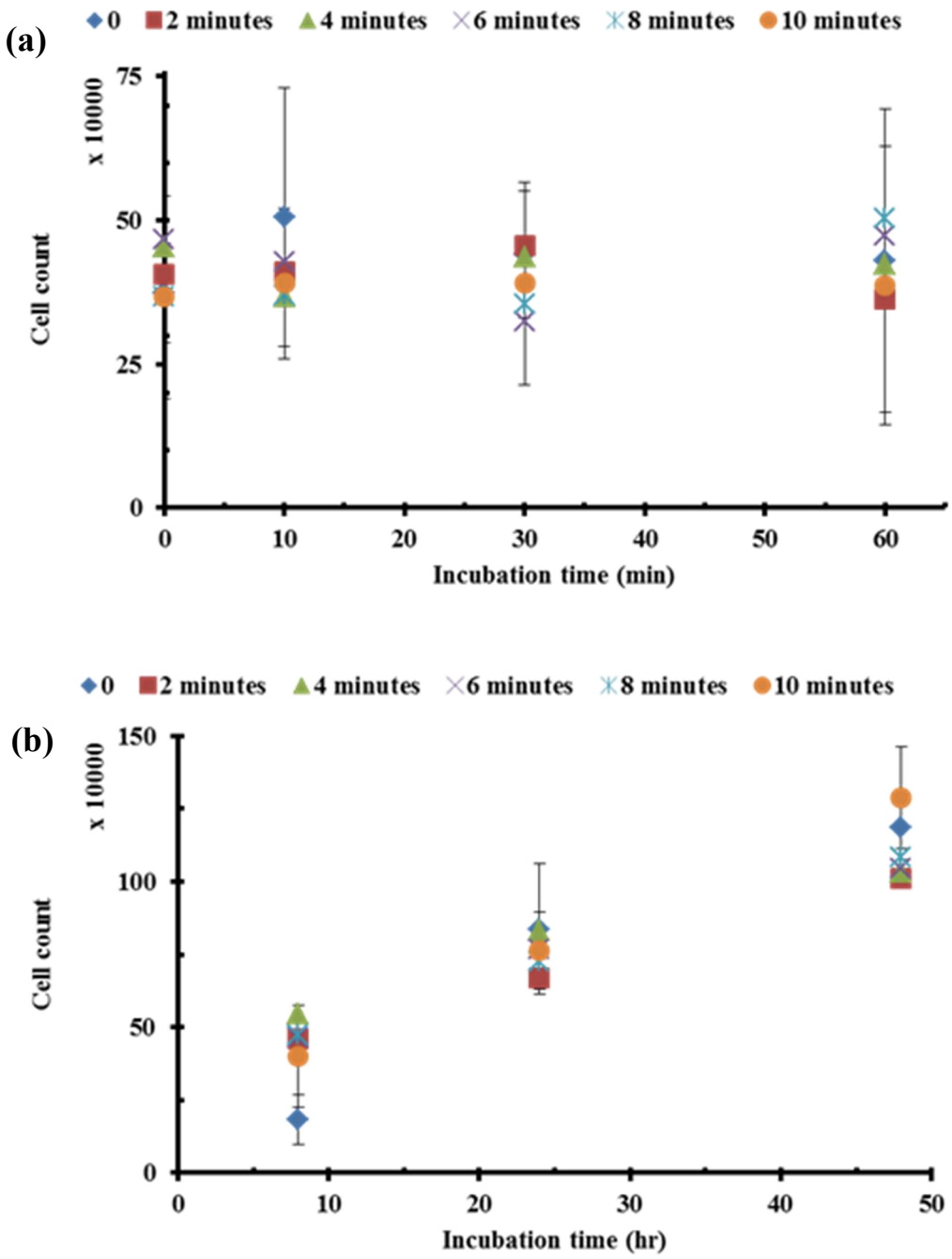

Figure 2.10: The effect of sodium citrate treatment used to dissolve the alginate gel beads on cell counts over a period of: (a) 60 minutes and (b) 48 hours. The error bars indicate the standard error of the mean of three sample replicates.

The main finding from Figure 2.10(a) is that the exposure to sodium citrate buffer does not have a significant effect on Jurkat cell numbers for up to 60 minutes. This is a very positive result and shows as well as confirms the suitability of sodium citrate as a dissolution buffer for Jurkat cells. The effect of a prolonged incubation time (48 hours) is presented in Figure

2.10(b). The results obtained from this test showed that there is a significant increase in cell count from 8 to 48 hours incubation. Thus these tests showed the suitability of sodium citrate as a dissolution buffer at a concentration of 50 µM.

2.4.7 The effect of 50 µM sodium citrate dissolution buffer on cell viability

Jurkat cells were incubated in sodium citrate dissolution buffer with different incubation times (0 to 48 hours), in order to study the effect of the dissolution buffer on % cell viability.

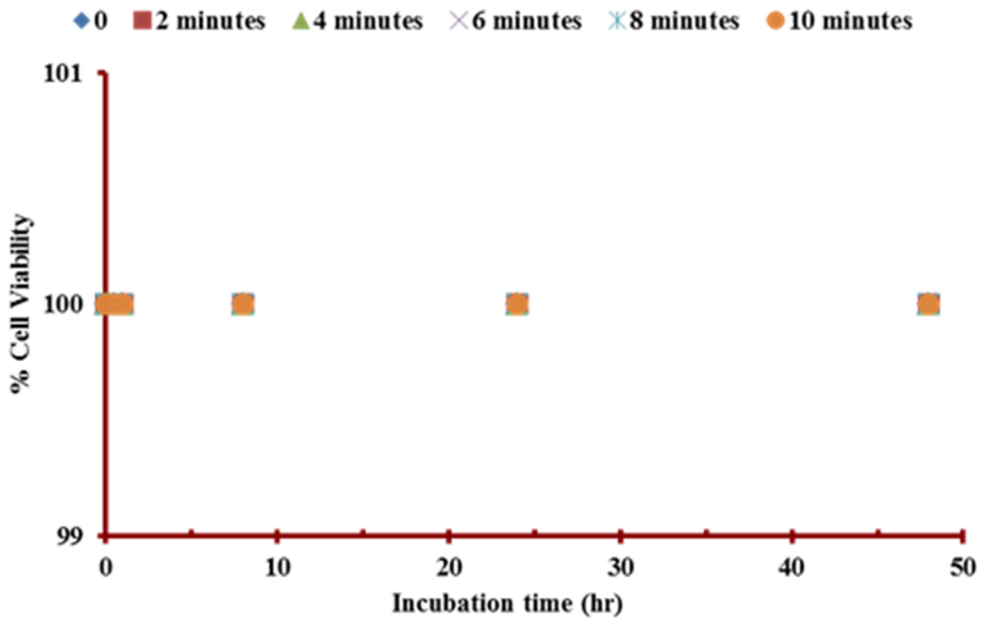

Figure 2.11: The effect of 50 µM sodium citrate treatment used to dissolve the calcium alginate gel beads on percentage cell viability over a period of 48 hours. Each point on the scattered plot represents an average of three experiments that were carried out on different days. Bars indicate the error; when they are not visible the error bar is smaller than the symbol used.

Figure 2.11 shows the effect of exposing Jurkat cells to varying times (2 to 10 minutes) to 50 µM sodium citrate and incubating over 48 hours. The results obtained are in agreement to those presented in Figure 2.9 and 2.10 (Cell growth) and shows that almost 100% (percentage viabilities range between 99.99% - 100%) of cells were viable over the 48 hours incubation showing the suitability of this buffer concentration.

In summary, the experiments conducted in sections 2.5.5- 2.4.7 clearly showed that neither cell growth nor the cell viability was affected significantly by 50 μM sodium citrate treatment. Hence, the sodium citrate buffer was used to dissolve encapsulated cells when needed.

In summary, these findings indicate that a high concentration of sodium is toxic to living cells. Similar conclusions have been reported in the literature. Garland et al. investigated a number of calcium and sodium compounds at different concentrations, including sodium citrate (281). Another study reported by Scaglia and colleagues, 10 mM sodium citrate had minimal effect on mock-transfected control cells (282).

2.4.8 Cell growth in alginate gel beads

Jurkat cells were encapsulated in alginate gel beads, and were incubated in complete RPMI media at 37°C and in a 5% CO_2 atmospheric environment. The encapsulated cells were removed from calcium alginate beads using sodium citrate buffer at four different time points to study the rate of encapsulated cell growth over a period of 7 days. Figure 2.12 summarises the average cell counts of three different encapsulated Jurkat cells beads over 7 days. These experiments were carried out three times to validate the results alongside with a control (Jurkat cells in complete RPMI-140 media on tissue culture plastic).

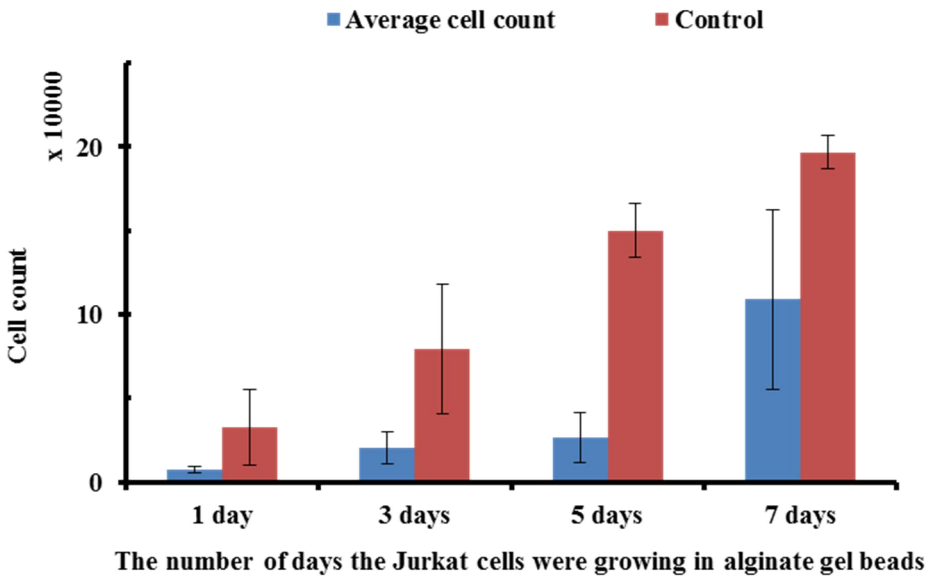

Figure 2.12: Jurkat cells encapsulation in alginate gel beads studied over 7 days compared to a control test. The control is a cell count of Jurkat cells in complete RPMI-1640 media on TCP.

Figure 2.12 shows the results obtained on Jurkat cells encapsulated in alginate beads and cell counts measured for a period of 7 days. This was compared to a control test in which Jurkat cells were not encapsulated (a standard cell culture method). Initial encapsulation on day 1 shows that there is a significant decrease in the cell count which could be attributed to cell damage. As the number of incubation days increased, the encapsulated cell count also increased with a significant increase observed on day 7. This could have been due to

the cells recovering from the initial cell damage of the encapsulation process and that the Jurkat cells started to divide. However, compared to the control, encapsulated Jurkat cells grew at a slower rate.

The standard control test in this investigation was chosen despite the different dimensions, as it is difficult to produce a growth control test in a 3D environment, in addition 2D cultures have been used a as a gold standard reference for decades (283). Moreover similar comparisons (growth of cells in 2D cultures verses 3D cultures) have also been reported by numerous research groups (283,284). Wang and colleagues carried out an investigation on the use of alginate beads as a means to support the differentiation of embryonic stem cells into insulin producing cells (284). This study provided a direct comparison between the viability of cells in 2D cultures and 3D cultures. In another published study, Shih et al. conducted a series of studies were carried out to investigate to viability of HepG2 liver cells encapsulated in two different alginate based hydrogels. The viability tests were compared whenever possible to a standard 2D control (283).

2.5 Conclusion

Alginate is a polysaccharide used to fabricate 3D scaffolds for cell encapsulation. Alginate has gained interest by many researchers due to the many advantages it has to offer including biocompatibility, reproducibility, ability to form gels, low toxicity levels, easy to handle and store in addition to being relatively inexpensive.

This chapter focuses on determining the effect of formulation used to produce and degrade the alginate gel beads on cell growth and viability. The alginate chains were cross-linked with 10% $CaCl_2$ to causing the gelation of the sodium alginate droplets, and in turn producing calcium alginate gel beads. The cells were mixed with sodium alginate solution prior to crosslinking with 10% $CaCl_2$ allowing cell encapsulation. The effect of 10% $CaCl_2$ on cell growth and percentage cell viability was determined. The results showed that 10% $CaCl_2$ had a significant effect on cell growth and viability, since cell division (controls doubled) did not occur after 24 hours and they only increased by 50% after 48 hours. This solution was used to solidify the alginate beads in further studies. Furthermore, it was observed that by using the dripping method described in this chapter, the alginate gel beads were highly dispersed and large. In addition a huge amount of cells per Jurkat cells were encapsulated in each alginate gel bead.

The alginate gel beads were dissolved in a subsequent set of experiments using a sodium citrate buffer at three different concentrations to release the encapsulated cells. Sodium citrate buffer concentrations of 50 μM, 100 μM and 200 μM were investigated to determine the optimum buffer concentration that has minimum impact on cell numbers, growth and cell division over period of time spanning from 0 to 48 hours. Both at the short incubation time (less than 60 minutes) and prolonged incubation time (up to 48 hours), the use of 50 μM sodium citrate was sufficient enough to dissolve the alginate gel beads. Further tests at this concentration revealed a high percentage of cell viability (percentage

viability being between 99.9%-100%). The effect of temperature on alginate beads dissolution was also investigated and the findings showed that alginate gel beads dissolved faster in 200μM sodium citrate at 37^{o}C. However, the cell count decreased when the alginate gel beads were dissolved using this high concentration of sodium citrate. The same negative effect was observed when the gel beads were dissolved in 100μM sodium citrate. Hence, it was decided that 50μM sodium citrate was used in later experiments to dissolve the alginate gel beads at room temperature (25^{o}C).

In summary, the dripping method described in this chapter resulted in the formation of polydisperse huge beads. Therefore in order to overcome this drawback further optimisation towards encapsulating cells in small monodisperse beads was needed. The two following chapters describe two novel approaches to encapsulate cells in small alginate microbeads with a narrow size distribution.

3 Chapter THREE
Methodology and Preliminary Microfluidic Study

3.1 Introduction

The growing interest in microfluidic technology for numerous applications is attributed to its desirable features, such as reducing the amount of consumables (samples, reagents, etc.), time and costs (285,286).

The work carried out in this chapter described the encapsulation of Jurkat cells in alginate gel microbeads using a simple microfluidic setup driven be gravity. The microfluidic chip that was used in this setup was fabricated by a moulding method carried out by Dr Stephan Mohr and the material used was PMMA. PMMA is transparent (287), which makes it easier to visualise the calcium alginate gel microbeads in the microchannels. Moreover, PMMA is biocompatible, inexpensive and is easy to machine in comparison to other substrates such as glass and silicon, fabricate and mould (188,287,288). By adapting this approach, Jurkat cells have been successfully encapsulated in alginate gel microbeads using a microfluidic chip, which consisted of two flow focusing junctions, characterised with pinched segments and rectangular cross section. Furthermore, this microfluidic approach allows the fluids (sample, oil and acidified oil) to flow through a continuous and laminar regime, which eases the injection of fluids into the microfluidic chip. Moreover surface tension developed at the flow focusing junctions, which in combination with external shearing initiated by the carrier oil, contributed towards the pinch-off of spherical alginate microdroplets at the first junction and spherical calcium alginate microbeads at the second junction.

This microfluidic approach allowed the production of calcium alginate gel microbeads containing Jurkat cells. Similar microfluidic approaches in terms of using flow focusing junctions to facilitate the formation of microdroplets have been reported in the literature

(289,290). Furthermore, the results obtained demonstrated the ability to use the gravity-based microfluidic approach described in this chapter for the successful production of alginate gel microbeads containing Jurkat cells.

3.2 Materials, instrumentation and methodologies

The materials used to culture and encapsulate cells described in this chapter were similar to that described in the previous chapter (Chapter 2), with a few exceptions. Firstly the calcium source was substituted with nano precipitated calcium carbonate (NPPC). Secondly ionic crosslinking of the calcium alginate occurred as a result of being in contact with a low concentration of glacial acetic acid. Finally, other materials were needed to construct the microfluidic setup and encapsulate Jurkat cell in calcium gel microbeads using microfluidics, these materials are listed in Table 3.1.

Table 3.1: summarises the materials used for the initial setup to encapsulate cells in alginate gel beads.

Reagents and materials	**Purity, concentration or model**	**Product code**	**Supplier**
BD luer-lok sterile 1 mL syringe (disposable)	NA	309628	Interfax Acuflow Ltd.
BD luer-lok sterile 10 mL syringe (disposable)	NA	300912	Interfax Acuflow Ltd.
Uninsulated Bootlace ferrules, diameter: 1.2 mm	NA	2509492988	RS Components Ltd, Corby.
Camera		LU165M	Lumenera Co. Ottawa, Canada
Computers × 2	NA	NA	Dell
Navitar light source	NA		Navitar Inc., Rochester, NY, USA

Microbore polytetrafluoroethylene PTFE Tubing, 0.012"ID x 0.030"OD, 100 ft/roll OU-06417-11	NA	EW-06417-11	Cole-Parmer Instrument Co. Ltd
Nano participated Calcium Carbonate			China Daysun Fireworks & Trading Co., LTD, China.
Polymethyl methacrylate (2 mm sheet of)	NA		Bayplastics
Transparent self-adhesive polyester +laminate (100 μm thick)	NA		Bayplastics
Vegetable oil	100%	NA	Sainsburys
Polyvinylchloride tubing	NA		Portex
CAD package (Inventor Autodesk software (v 10.00))			Autodesk Inc
Datron CAT3D milling machine			Datron CAT3D.

3.2.1 Instrumentation

3.2.1.1 Microfluidic setup for the production of alginate gel micro-beads

The microfluidic setup used to produce alginate gel microbeads in this chapter is shown in Figure 3.1. This setup consisted of a clamp that held three syringes containing the fluids (carrier oil, acidified oil and samples containing cells) in upright (vertical) positions, which were attached to the microfluidic tubing to allow the fluids to travel through the syringes and into the microfluidic chip. Moreover, the fluids travelling through the tubes were controlled using valves.

A few aspects needed to be considered when constructing the microfluidic setup to produce alginate gel microbeads containing Jurkat cells, including:

- The fluid injection method: fluids were injected into the microfluidic chip by gravity.
- The microfluidic chip: The PMMA microfluidic chip was fabricated with three connections to allow for internal gelation of alginate gel microbeads.
- Acidified oil: Tests were also carried out on the acidified oil to determine the lowest concentration of glacial acetic acid needed to gelify the alginate gel microbeads containing Jurkat cells.

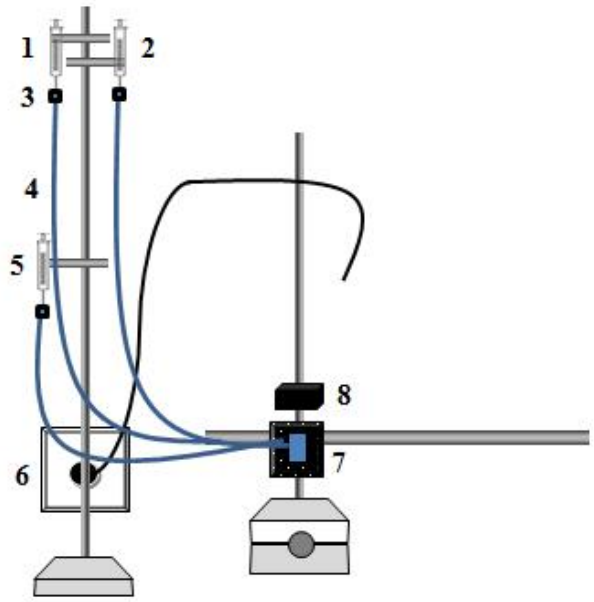

Figure 3.1: A schematic diagram of the microfluidic setup used for producing alginate gel microbeads using gravity for fluid injection. 1: Acidified oil, 2: carrier oil, 3: valve, 4: microfluidic tubing, 5: sample containing alginate solution and Jurkat cells, 6: light source, 7: microfluidic chip and 8: Camera.

3.2.1.2 Microfluidic device and fabrication

A microfluidic device (chip) PMMA MC1 was fabricated from PMMA to encapsulate Jurkat cells in calcium alginate gel microbead. Schematic diagrams and a digital image of the chip used to encapsulate Jurkat cells are shown in Figure 3.2 and Figure 3.3 respectively. PMMA MC1 consisted of a sample inlet and two laminar flow inlets for the carrier and acidified oils, which flowed together into the main microchannel of the chip. In addition, two pinch flow junctions were incorporated to produce calcium alginate gel microbeads containing Jurkat cells and to allow the acidified oil to feed into the mixing area of the chip respectively. Upon contact with the glacial acetic acid (GAA), the alginate gel microbeads underwent gelification, and the Jurkat cells were encapsulated stochastically (at random distribution) (291). The carrier oil, from its name, was used as a carrying medium that surrounds the microbeads in the microfluidic chip. The size of the microbeads formed depended on the carrier oil and sample flow rates applied through the microchannels of the chip (292).

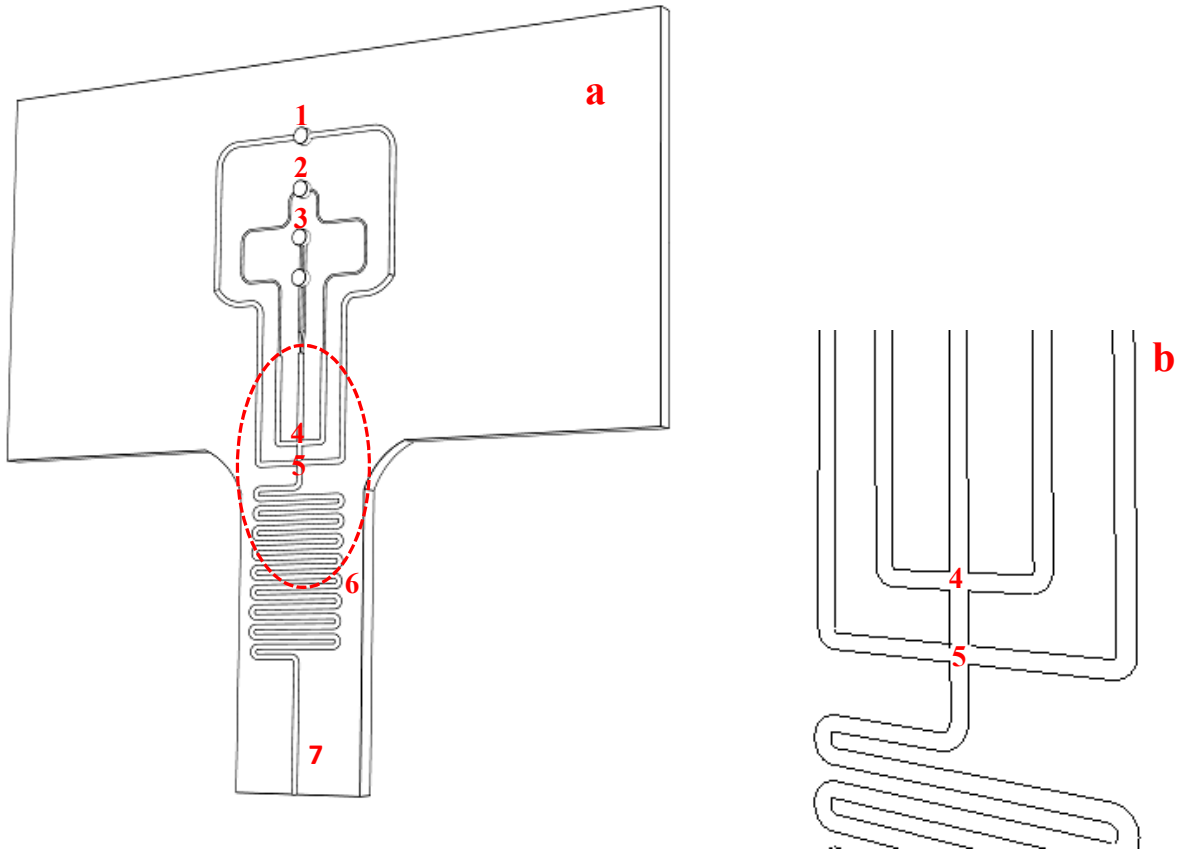

Figure 3.2: (a) A schematic diagram of PMMA MC1 fabricated to produce calcium gel alginate microbeads containing Jurkat cells. The crucial features within the chip were numbered as follows: 1: acidified oil inlet, 2: carrier oil inlet, 3: sample inlet, 4: microbead production area, 5: acidified oil feed, 6: mixing area and 7: outlet. (b) An amplified region of the PMMA MC1 showing the pinch flow junctions.

PMMA MC1 was made using a 2mm sheet of polymethyl methacrylate and was sealed with a 100 μm thick self-adhesive polyester laminate, which was transparent to allow channels to be visualised and monitored when the alginate gel micro-beads were forming and solidifying. The microfluidic chip was deep cleansed prior to applying the seal, using deionised water and was subsequently dried in an oven at 40^{o}C for 30 minutes, in order to allow the water to evaporate. The seal was then applied smoothly to prevent trapping bubbles between the sealant and the microfluidic chip. A digital image of this chip was taken and is shown in Figure 3.3.

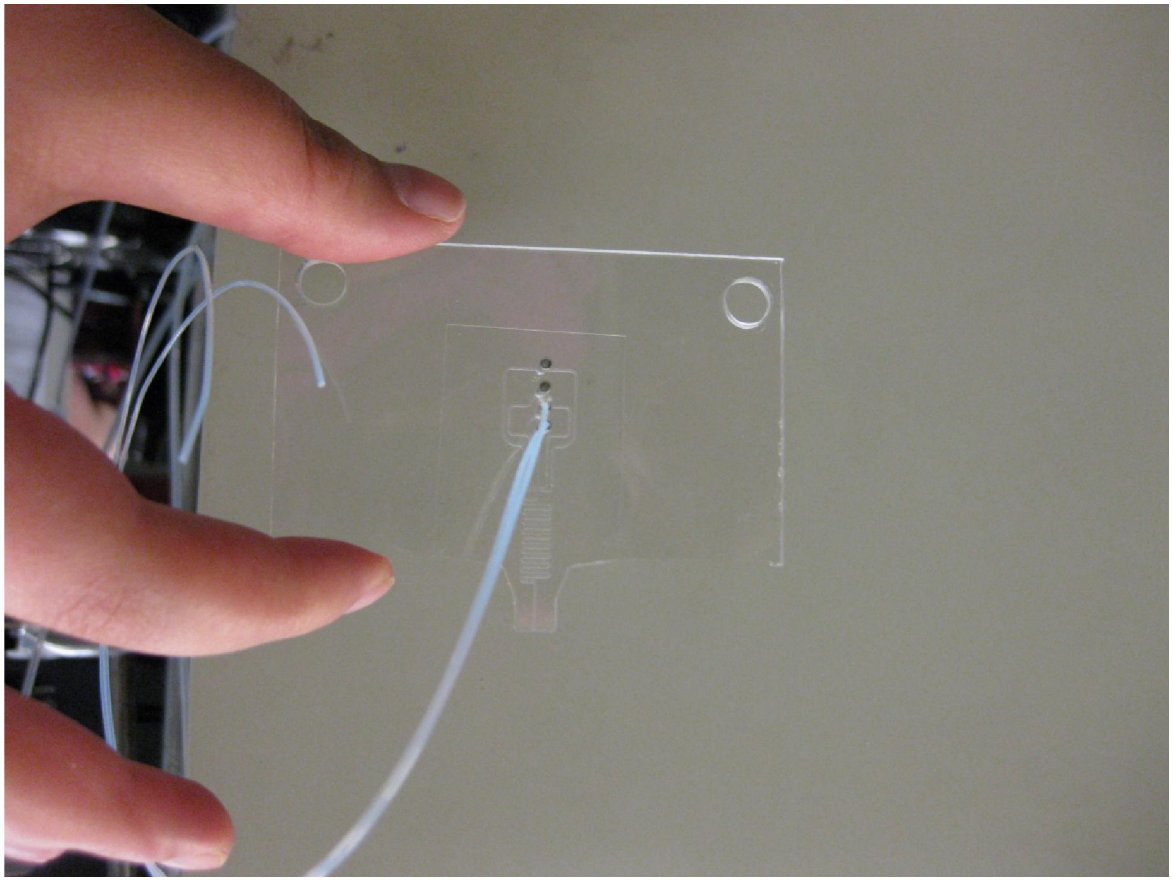

Figure 3.3: Microfluidic chip (PMMA MC1) that was used to encapsulate Jurkat cells in calcium alginate gel microbeads.

3.2.1.3 Fluid injection

The fluids (oil, acidified oil and samples) were injected into the microfluidic setup by gravity to encapsulate Jurkat cells in calcium alginate gel microbeads. This approach was adapted from previous work carried out by Dr. M P Carreas Romeo in collaboration with Dr. Stephan Mohr and Dr. Louise Carney. The oils were introduced into two 10 mL sterile disposable luer-lok syringes and the samples were introduced into a 1 mL sterile disposable luer-lok syringe. These three syringes were fixed to a clamp and were connected to the chip using PVC tubing. The tubing was tied to the syringes and chip using a cable tie and epoxy glue respectively, allowing the oils and samples to flow through to the chip.

Calcium alginate gel micro-beads containing Jurkat cells were produced on-chip once the acidified oil came in contact with the sample containing nano-precipitated calcium carbonate. To encapsulate the cells effectively, connections were placed above the chip to allow the natural flow of fluids (oils and samples) with gravity. The syringes containing the fluids were adjusted as close as possible to the microfluidic chip, in order to minimise the distance travelled by the samples in the tubing. Thus the tip of the syringe containing the samples (alginate/ cell solution) was 22 cm above the chip and the tips of the syringes containing the oils were 44 cm above the chip. By-pass connectors were used to control the release of the samples and oils. When the samples were ready to be injected, the carrier by-pass oil connector was closed and the sample connector was opened, allowing the sample and oils to be injected into the chip and producing alginate gel micro-beads containing cells. These microbeads were then collected in a 24 well plate.

3.2.1.4 Connections and tubing

The chips were connected to the syringes using polytetrafluoroethylene **(**PTFE) Tubing (0.012"ID x 0.030"OD). The connectors (bootlace ferrules) were attached to the chips

manually and bonded together using epoxy glue and they were left to cure overnight. The syringes were attached by connecting the PTFE tubing to a small piece of PVC tubing and then to a luer lock adapter. The small tubing was further secured with some epoxy and cable ties to prevent any leakages once high pressures of samples and oils passed through the tubes to the chip.

3.2.1.5 Camera

The microfluidic setup described in this chapter was coupled to a Lumenera monochrome camera (Lumenera Co. Ottawa, Canada) to detect the formation of the alginate gel micro-beads and to take images simultaneously. The digital video resolution was adjusted to 800×600 pixels as it captured sharper images of the micro-beads in the microchannels of the microfluidic chips. The Lu-cam software used for taking images and video snaps was provided with the Lumenera camera, and the camera was controlled by a program, which was written in house by Dr. Bernard Treves Brown using National Instruments LabVIEW software.

3.2.2 Methodology

3.2.2.1 Acidified oil preparation

Acidified oil was used to gelify the alginate gel micro-beads. The acidified oil was made up initially by mixing 1 mL of 99.8% glacial acetic acid with 50 mL of vegetable oil (Sainsbury, UK) in a universal centrifuge tube.

3.2.2.2 Alginate solution preparation

The alginate solution (1.1% w/w) was then made up by adding 0.55 g of sodium alginate to 47.5 mL of sterile PBS and 2.5 mL gelatine (2% w/v) as described in Chapter 2. This was followed by the addition of 0.2 g nano-precipitated calcium carbonate (NPCC) to 15 mL of alginate solution 1.1% (w/v). The alginate solution containing NPCC solution was then

subjected to sonication overnight at room temperature, in order to allow the solution to become as homogenous as possible.

3.2.2.3 The process of encapsulating cells in calcium alginate gel microbeads

Attempts to generate monodisperse and spherical alginate gel microbeads containing Jurkat cells were carried out using the microfluidic setup shown in Figure 3.1. The sample (sodium alginate/ nano- precipitated calcium carbonate and cells), oil containing glacial acetic acid (acidified oil) and vegetable oil (carrier oil) were then introduced into the relevant syringes (sample in the 1ml syringe and oils in the two 10 mL syringes). These syringes were held in upright positions as shown in Figure 3.1, to allow the fluids (oils and samples) to travel through the microchannels of the microfluidic chip by gravity. The syringes were fixed at suitable heights in comparison to the microfluidic chip and were opened to allow the fluids to flow through the connected tubes and into the microchannels of the chip. The height of the syringe containing the sample (cells and sodium alginate solution) was positioned 22 cm above the microfluidic chip, and the syringes containing the samples were placed 44 cm above the chip, since these were found to be the most suitable heights for the successful production of spherical calcium alginate gel microbeads containing cells.

Prior to loading the sample into the relevant syringe, Jurkat cells were subcultured as described in chapter 2, section 2.3.1 and the cell pellet (with a density of 6.3×10^5) was resuspended in 1 mL of 1.1% alginate solution containing nano-precipitated calcium carbonate. Calcium alginate gel microbeads were produced using vegetable oil and acidified vegetable oil as two distinct organic phases and the sample (1.1% (w/w) sodium alginate containing NPCC and Jurkat cells in sterile PBS) as the aqueous phase. The acidified oil inlet was loaded into the first inlet of the organic phase, the vegetable oil (carrier oil) was loaded into the second inlet of the continuous phase, and the aqueous

sample was loaded into the third inlet Figure 3.2. The acidified oil inlet was closed initially in order to minimise blockages in the microchannels of the chip, and remained closed until the production of sodium alginate droplets became as consistent as possible. Moreover, the other two syringes containing the sample and carrier oil were adjusted to produce microbeads at a steady rate. Once a regular frequency of alginate microdroplets was observed, the acidified oil inlet was then opened, which caused a reduction in pH and in turn liberated the calcium ions, which enabled the instant gelation of calcium alginate microbeads containing cells on-chip.

Snapshots from videos taken showing the production and solidification of alginate micro-beads were taken using the Lumenera camera. In order to improve imaging, a white sheet of paper was attached 2 cm away from the bottom of the microfluidic chip. Snapshots showing calcium alginate gel microbeads containing Jurkat cells, which were produced using this microfluidic system, is shown in the following section Figures 3.4 and 3.5.

3.3 Results and discussion

Calcium alginate gel microbeads containing Jurkat cells (Figure 3.4 and 3.5) were successfully produced using the microfluidic setup and internal gelation method described in this chapter. The production of alginate gel microbeads was monitored and digital images were taken using a Lumenera monochrome camera that was attached to the microfluidic setup. The alginate gel microbeads were polydisperse with a size distribution ranging from (70- 400 μm) and had different shapes. The polydispersity of the beads produced using this cell encapsulation method was possibly due to droplets merging (coalescence) (293,294). The occurrence of microdroplet fusion/merging is not necessarily a result of two microdroplets colliding. A study carried out by Bremond and colleagues revealed that the coalescence of microdroplets is a result of the closely spaced separation between the microdroplets in the separation process (293). Another study showed that for coalescence to occur, the continuous phase needs to dry out bringing the droplets in close proximity for a critical amount of time. Fusions of the microdroplets take place as result of variations in the surface tension of the microdroplet surfaces, which disturbs the interface between both the two phases (oil and water). Many approaches have been investigated to overcome undesired coalescence such as the addition of surfactants, which results in the reduction of the surface tension between the oil and aqueous phases (294,295).

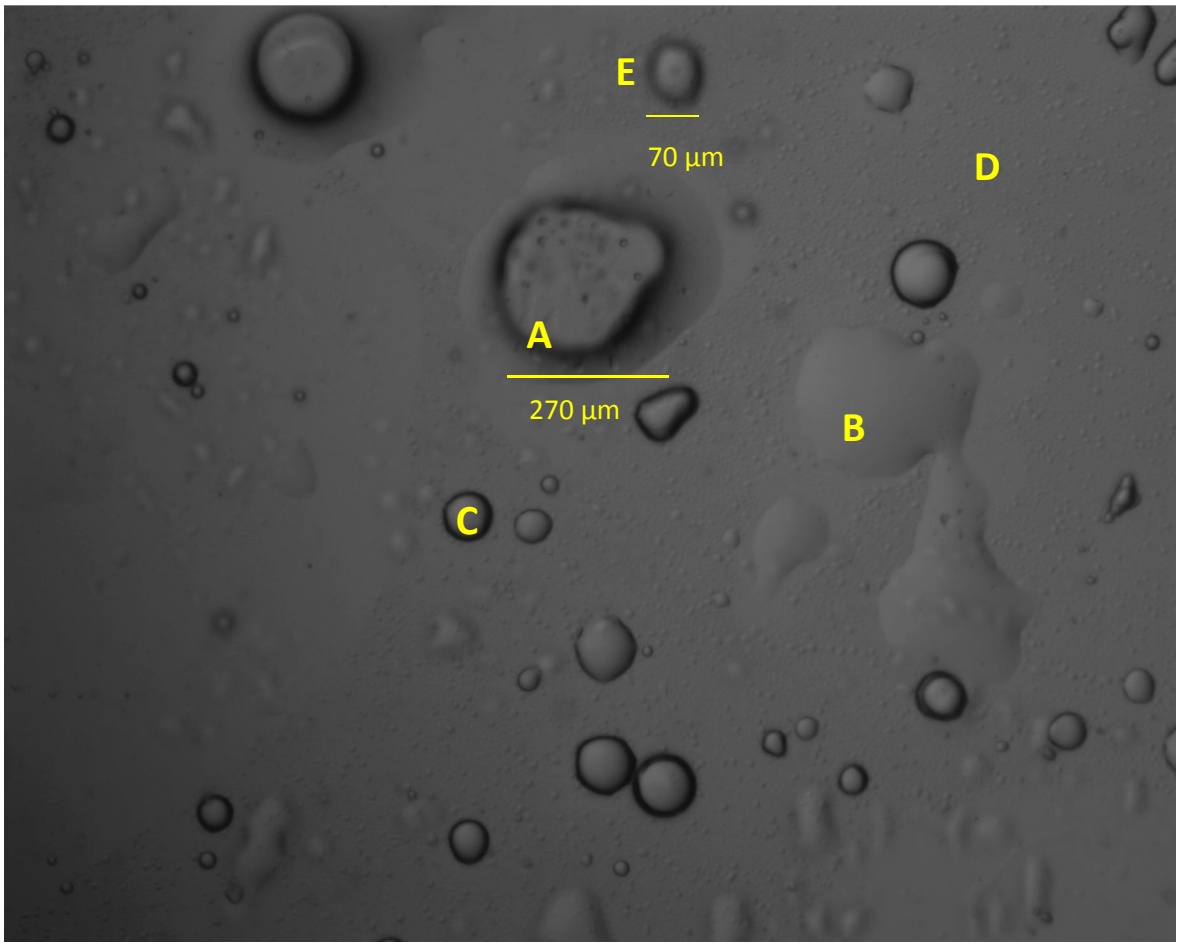

Figure 3.4: Image of encapsulated cells in an alginate gel microbead using gravity. A: a non-spherical microbead containing cells, B: oil, C: a bubble, D: cells and E: a small non- spherical microbead containing cells.

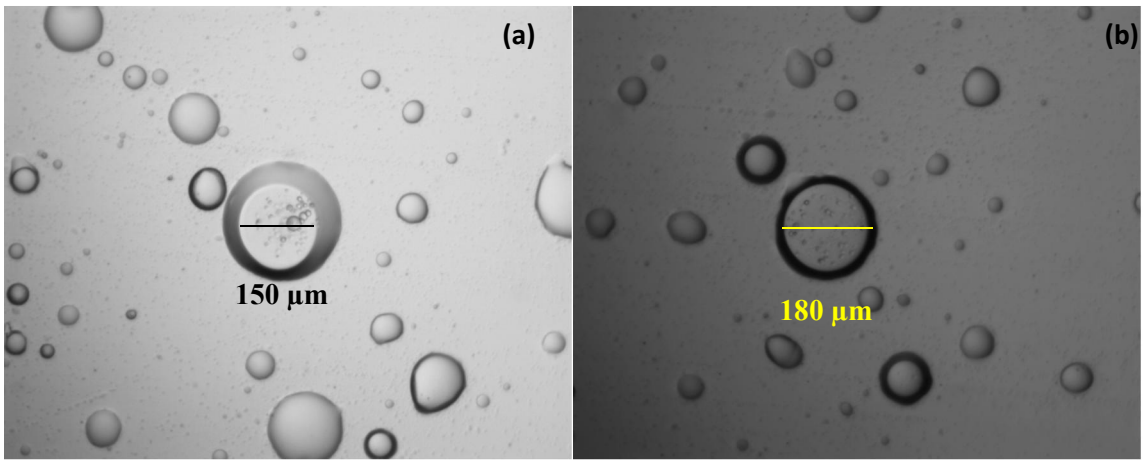

Figure 3.5: (a) and (b) show images of encapsulated Jurkat cells in various sized calcium alginate gel microbeads.

A number of challenges emerged that required addressing despite the successful encapsulation of Jurkat cells in calcium alginate gel microbeads using the microfluidic setup described in this chapter. For instance the PTFE tubing and microchannels clogged up quite easily since gelation occurred on chip with limited the use of high pressures passing though the microfluidic channels. Applying high pressures though the channels caused the disassembly of the polyester laminate sealant, which in turn also impacted the size of the alginate gel microbeads (292). Importantly, the number of times that the polyester laminate sealant could be replaced was also limited, because replacing the process of re-laminating the microfluidic chip damaged the microchannels. Furthermore it has been reported in the literature that the use of adhesives to seal the microfluidic chip has inherent drawbacks, such as: clogging up the microchannels (296), cross contamination, microchannel deformation (297). Moreover, the flow rates of the fluids flowing through the microfluidic setup were not measured, as it was difficult to obtain these measurements. Furthermore polydisperse and non-spherical alginate microbeads were produced as seen in Figures 3.5 and 3.6.

3.4 Conclusion

The microfluidic setup described in this chapter was driven by gravity forces, allowing samples and oils to flow through the microfluidic chip, producing alginate gel micro-beads containing Jurkat cells. These microbeads appeared to be polydisperse and varied in shape. Based on these observations, a number of areas that needed improving were identified, and are summarised as follows:

- Use of syringe pumps instead of gravity to drive the fluids through the microfluidic setup, which in turn has a direct impact on controlling the pressures applied and the sizes of the microbeads.
- Optimisation of the microfluidic chip design allowing for a comparison between external and internal solidification to occur and compare the direct impact on cell viability upon encapsulation.
- Exploring another material that can be used to fabricate a more robust chip.

These improvements are needed since one of the aims of this project was to construct a reliable microfluidic setup that can be used to encapsulate live cells. The microfluidic setup described in this chapter was useful for conducting initial studies; however, the improvements listed were vital for further investigations carried out on cell encapsulation.

The next Chapter (Chapter 4) details the optimised microfluidic setup and alginate solution used to encapsulate live cells in uniform sized and shaped alginate gel-microbeads. In addition, Chapter 4 includes investigations that were carried out to determine the most suitable chip to encapsulate live cells that survived for at least 24 hours.

4 Chapter FOUR Optimisation of Microfluidic Setup

4.1 Introduction

The main aim of the work carried out in this Thesis was to study cell viability in a three dimensional culture medium (alginate gel microbeads), which were produced using a novel microfluidic setup. This setup was attached to two syringe pumps, enabling the fluids to be driven through three different microfluidic chip designs (described in section 4.2.2) in order to produce uniform shape and monodisperse alginate beads containing Jurkat cells and to minimise the exposure of cells to glacial acetic acid. Cross-linking alginate to produce microbeads can be achieved by internal (on chip) or external gelation (off chip by dripping sodium alginate droplets into acidified oil in a beaker) methods depending on the design of the chip (7,8). Two of the chips described in this chapter consisted of three inlets (oil, acidified oil and sample) to allow for internal gelation to occur and one chip consisted of only two inlets (oil and sample) so that external gelation occurs. The reason behind the use of different chip designs and materials described in this chapter was to identify the optimum setup for producing alginate gel microbeads containing cells.

The main findings in this Chapter revealed that internal solidification of alginate gel microbeads was favoured over external solidification of these microbeads for several reasons including: the formation of uniform size and homogenous alginate microbeads containing live cells (185), the sizes and shapes of microbeads containing cells were reproducible and easy to control as they depended on the pressures applied when using the syringe pumps. In addition single cell encapsulation was achieved as desired, since single cell encapsulation has positive potentials in biological applications (such as DNA sequencing (18) and cell signalling studies (16)) and medical applications (such as diabetes

(17,19) and hepatic diseases (17,20)). These findings were supported by live imaging conducted using sophisticated microscopy technology.

4.2 Materials, instrumentation and methodologies

The materials and reagents used to culture and encapsulate Jurkat cells described in this chapter are similar to those used in the two previous chapters (Chapter 2 and 3), with the exception of some materials and reagents, which are listed in Table 4.1.

Table 2.1: The materials used for cell encapsulation in calcium alginate gel microbeads.

Reagents and materials	**Purity, concentration or model**	**Product code**	**Supplier**
Calcein-AM solution	4 mM in DMSO solution	C1359	Sigma-Aldrich, Dorset, UK.
Fusion 400 Touch infusion syringe pump	NA	NA	KR Analytical Ltd, Sandbach, UK.
Harvard '33' twin syringe pump	NA	NA	Harvard apparatus, Pennsylvania, US .
Iwaki dish	NA	P35G-1.5-14-C	MatTek Corporation, Ashland, US.
Propidium iodide (PI)	1.0 mg/ml in water	P4864	Sigma-Aldrich, Dorset, UK.
Polycarbonate sheets			Bay Plastics Ltd

4.2.1 Optimization of the microfluidic setup

The microfluidic setup described in the previous Chapter (Chapter Three) was optimised to solve the problems encountered when encapsulating cells in calcium alginate gel microbeads. The main difference in this setup was that fluids (carrier oil, acidified oil and samples containing cells) were driven through the microfluidic chips by syringe pumps instead of gravity forces. Moreover, the microfluidic chip fabricated for encapsulating cells in alginate microbeads was also modified to produce the desired microbeads with sizes ranging from 100- 150 μm. The optimisation of this microfluidic setup (Figure 4.1) included alterations to the following components:

- The microfluidic chip.
- Fluids (carrier oil, acidified oil and samples containing cells) were injected into the microfluidic chip by syringe pumps rather than gravity forces.
- The alginate solution was sequentially modified to enhance cell survival.

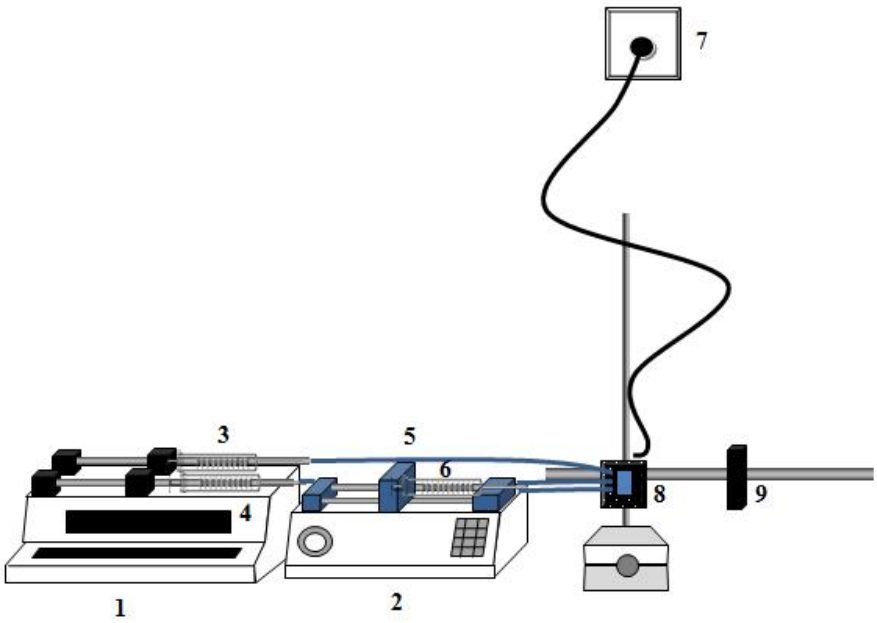

Figure 4.1: Schematic of the microfluidic setup used for encapsulating Jurkat cells in alginate gel microbeads using syringe pumps. 1: Harvard '33' twin syringe pump, 2: Fusion 400 Touch infusion syringe pump, 3: acidified

oil, 4: vegetable oil 5: microfluidic tubing, 6: sample containing alginate solution and Jurkat cells, 7: light source, 8: microfluidic chip and 9: camera.

4.2.2 Microfluidic devices and fabrication

Three microfluidic chips, PMMA MC1, PMMA MC2 and PC MC3 were fabricated to determine the most suitable design and material needed to obtain encapsulated live cells in calcium alginate gel microbeads. The materials used to make the microfluidic devices (chips) described in this chapter were either polymethyl (PMMA) or polycarbonate (PC). PTFE tubing was used to connect the syringes (containing the fluids) from one end and to the microfluidic chip on the other end.

Furthermore, the self-adhesive laminate foil mentioned previously in Chapter Three was used to seal the first two microfluidic chips. On the other hand, the PC MC3 chip was sealed together using screws. The chips were cleaned with deionized water thoroughly prior to sealing, and were then left to dry in an incubator for 30 minutes at 40^{o}C to allow the water to evaporate. The seals of the first two chips were then applied by hand gently to prevent bubbles from forming between the chips and the seals. Once the chips were connected to the systems, water was injected into the systems instead of the alginate/cell samples and oils to ensure that the microfluidic chips worked effectively and that there were no leakages in the chips/ systems. Figure 4.2 is a diagrammatic comparison between the three microfluidic chips used in the experimental work carried out in this chapter.

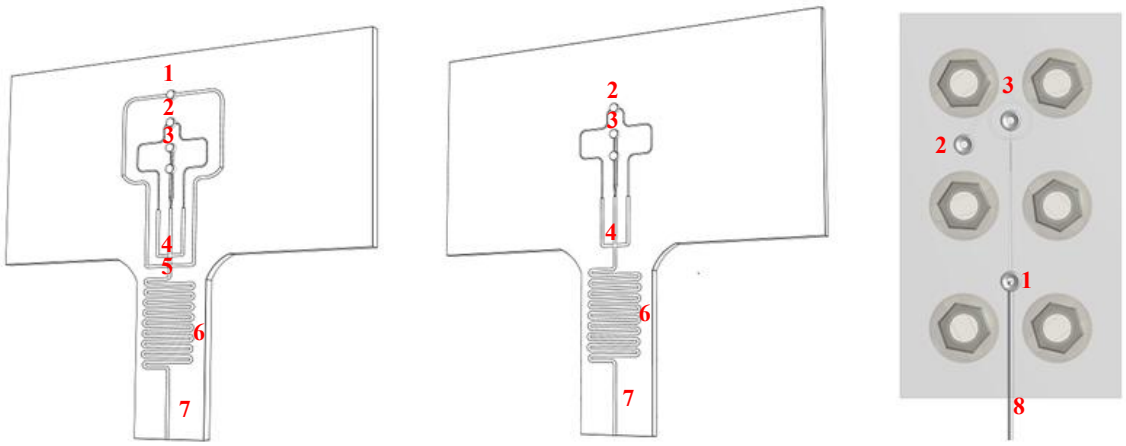

Figure 4.2: Schematic diagrams of the microfluidic chips used to encapsulate Jurkat cells in calcium alginate gel microbeads, where (a) is PMMA MC1, (b) is PMMA MC2 and (c) is PC MC3. The features within the chip were numbered as follows: 1: acidified oil inlet, 2: carrier oil inlet, 3: sample inlet, 4: microbead production area, 5: acidified oil feed, 6: mixing area, 7: outlet and 8: a tube for gelification.

4.2.2.1 PMMA MC1

PMMA MC1 was the first microfluidic chip fabricated to produce alginate gel microbeads containing Jurkat cells. As seen in the schematic diagram (Figure 4.3), sodium alginate microdroplets containing nano-precipitated calcium carbonate were formed at the first pinched flow focusing junction. For cell encapsulation, Jurkat cells are added to the sodium alginate solution prior to being introduced to the microfluidic chip. Another pinched focusing junction was placed down-stream of the first pinched flow focusing junction to introduce the acidified oil into the microfluidic chip, allowing a stream of acidified oil to merge with the main stream (containing the calcium alginate microdroplets). This caused a reduction in pH and in turn calcium ions are released, which then reacts with the sodium alginate microdroplets, causing the formation of calcium alginate gel microbeads containing Jurkat cells down-stream. Nevertheless, as discussed in section 4.3, further improvements were required to form the desired calcium alginate gel microbeads and to prevent the microfluidic channels from clogging due to build up in alginate and cell derbies. This led to the fabrication of a second microfluidic chip (PMMA MC2), as described in the following section.

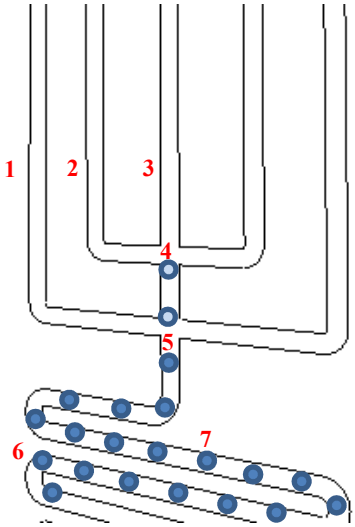

Figure 4.3: A schematic diagram of PMMA MC1 used for the production of alginate gel microbeads containing cells. 1: carrier oil (vegetable oil), 2: acidified oil, 3: sample (sodium alginate solution containing nano-precipitated calcium carbonate and Jurkat cells), 4: 1st pinched flow focusing junction, 5 is the 2nd pinched focusing junction, 6: mixing area and 7: calcium alginate microdroplet undergoing gelation.

4.2.2.2 PMMA MC2

The design of PMMA MC1 was modified to allow for external gelation of the calcium alginate gel microbeads. This modification (PMMA MC2) as shown in Figure 4.2 entailed the removal of the acidified oil microchannel and the removal of the second pinch flow focusing junctions. The non-gelified microdroplets were then dropped into a sterile well containing 1 ml of acidified oil to allow for external gelation to take place. A schematic diagram showing the design of PMMA MC2 is shown in Figure 4.4(a), and a magnified section of the pinched flow junction is shown in Figure 4.4(b).

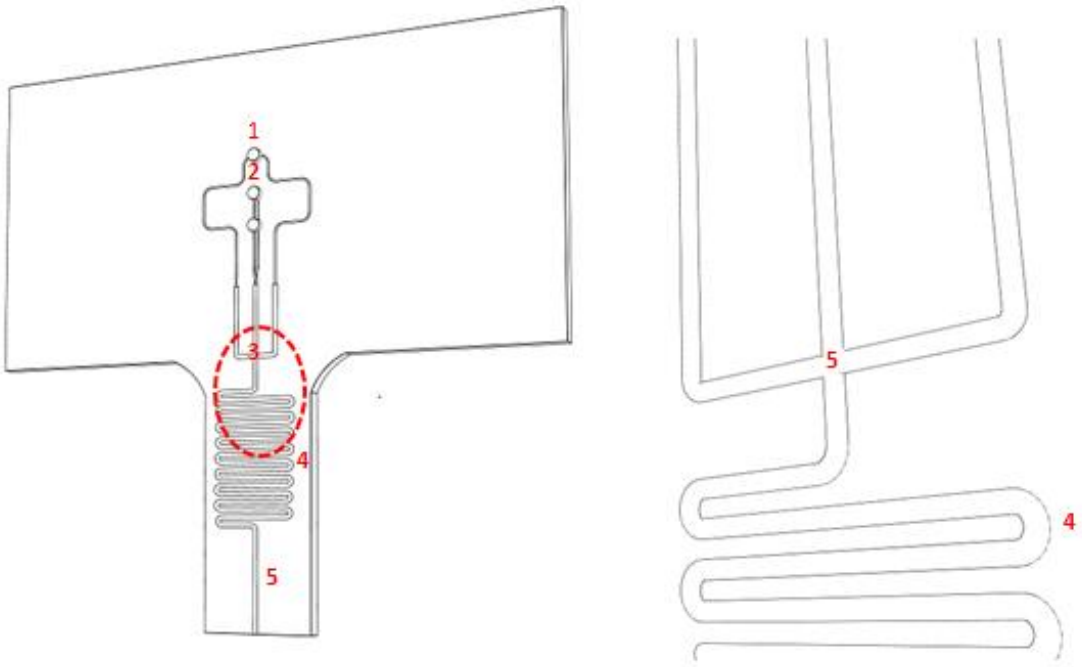

Figure 4.4: A schematic diagram of PMMA MC2, a major component of the optimised microfluidic setup. PMMA MC2 was fabricated to encapsulate Jurkat cells in calcium alginate gel microbeads using an external gelation method. The crucial features within the chip were numbered as follows: 1: carrier oil inlet, 2: sample, 3: microdroplet production area, 4: mixing area and 5: outlet. (b) Magnified section of PMMA showing the pinch flow junction.

As seen in the schematic diagram (Figure 4.5), sodium alginate microdroplets containing nano-precipitated calcium carbonate were formed externally in an acidified oil bath. For cell encapsulation, Jurkat cells were added to the sodium alginate solution prior to being introduced to the microfluidic chip. The pinched focusing junction was designed to produce the sodium alginate microdroplets containing Jurkat cells, which then merge into the main oil stream. The resultant sodium alginate microdroplets were then dropped into an acidified oil bath, which caused a reduction in pH and in turn calcium ions are released, which then reacts with the sodium alginate microdroplets, causing the formation of calcium alginate gel microbeads containing Jurkat cells.

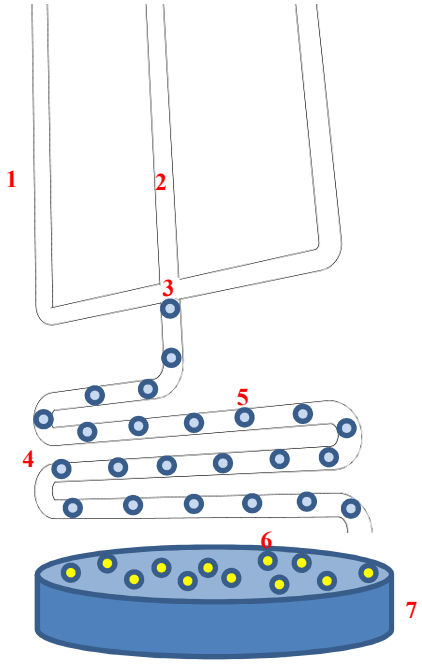

Figure 4.5: A schematic diagram of PMMA MC2 used for the production of alginate gel microbeads containing cells. 1: carrier oil (vegetable oil), 2: sample (sodium alginate solution containing Jurkat cells), 3: pinched flow focusing junction, 4: mixing area, 5: sodium alginate microdroplets, 6: calcium alginate microdroplet undergoing gelation and 7: an acidified oil bath.

The reason behind modifying the chip design of PMMA MC1 was in an attempt to minimise the exposure time of the alginate gel microbeads to the acidified oil, in addition to reducing the chances of clogging up the microchannels with clumps of calcium alginate gels and cell debris. This approach led to the successful encapsulation of some Jurkat cells in monodisperse and spherical calcium alginate gel microbeads and other Jurkat cells in merged (coalesced) calcium alginate gel microbeads. However, as shown in 4.3, the encapsulated Jurkat cells died and therefore, there was a need to optimise the design of microfluidic chip.

4.2.2.3 PC MC3

Jurkat cells were successfully encapsulated in calcium alginate gel microbeads using PMMA MC1 and PMMA MC2, however, there still remained flaws with the microfluidic chip design. The sealant peeled off quite often and easily due to two main reasons: the greasiness of the oils pumped through the chip and the relatively high pressures that were applied to inject the sample and oils through the microfluidic setup. Another challenge

associated with PMMA MC2 was that occasionally, as anticipated, calcium alginate gels accumulated in the channels causing the channels to clog up. The best way to remove the unwanted alginate was to remove the sealant from the chip and replace it with a new one. This solution was not ideal because it is laborious, time consuming, requires materials, funds and produces unnecessary waste. For these reasons the chip was modified to ensure robustness of the chip and reproducibility in terms of the size and shapes of alginate gel microbeads. Therefore, a third microfluidic chip (PC MC3) was fabricated.

The novelty of PC MC3 was the way it was designed for the purpose of encapsulating cells in calcium alginate microbeads using an internal gelation method. PC MC3 (Figure 4.6-4.9) was made up from two blocks of 75×75×6 mm polycarbonate sheets held together with screws and ferrules. The modification in the design of this microfluidic chip meant that relatively high flow rates could be applied through the microfluidic chip without causing any damage to the microchannels, and the time fluids spend in the microchannels was reduced, which resulted in the production of even smaller alginate gel microbeads (with diameters as small as 70 μm).

The bolted construction of PC MC3 consisted of two T-junctions. The first T-junction was machined from the carrier oil inlet (B) to the microfluidic channel (A-C), whereas the second T-junction was machined at the acidified oil inlet (C) at a right angle to the plane of the chip. Figures 4.7 and 4.8 are schematic representations of how the PC MC3 was bolted together.

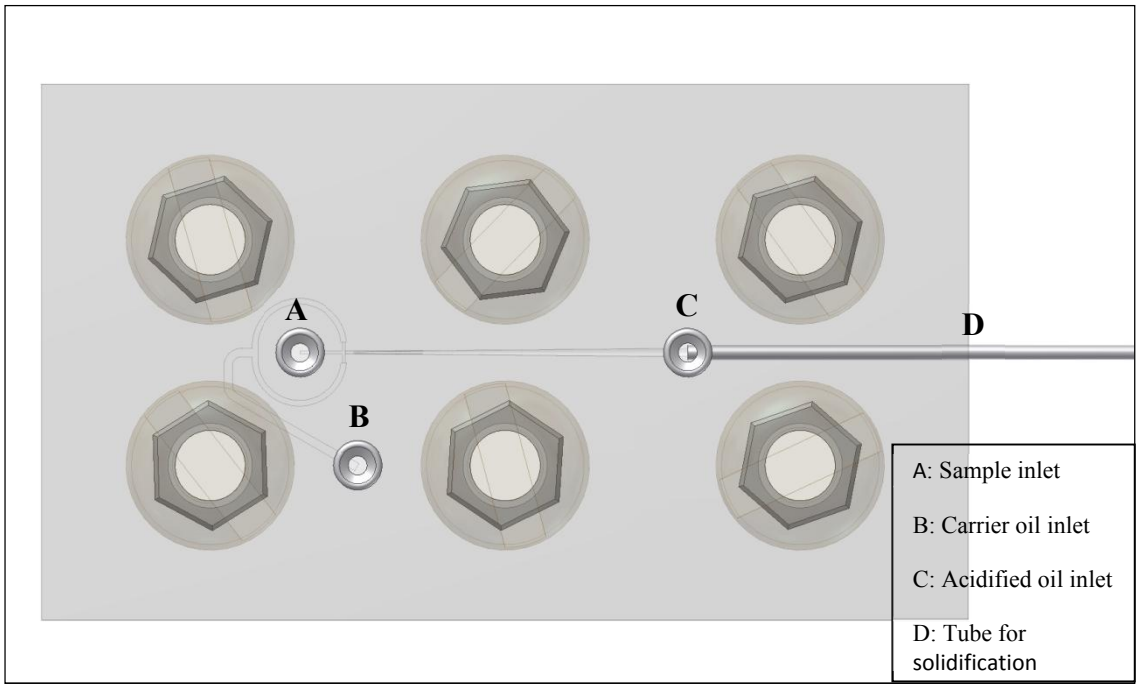

Figure 4.6: Schematic design of the microchannels in PC MC3, which was used to encapsulate cells in alginate gel microbeads.

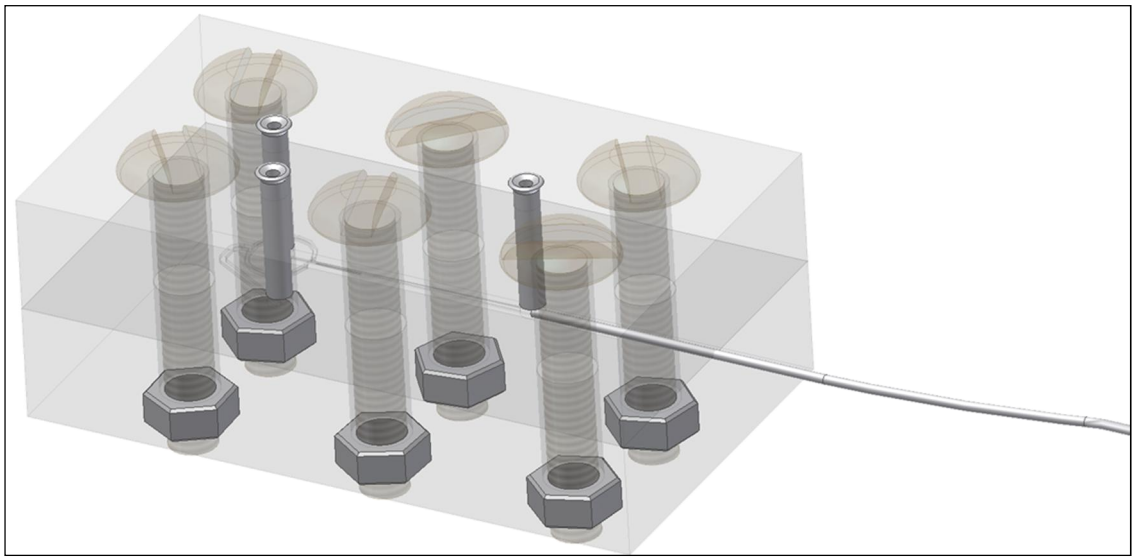

Figure 4.7: Schematic of the third chip (PC MC3) used to encapsulate Jurkat cells in alginate gel microbeads.

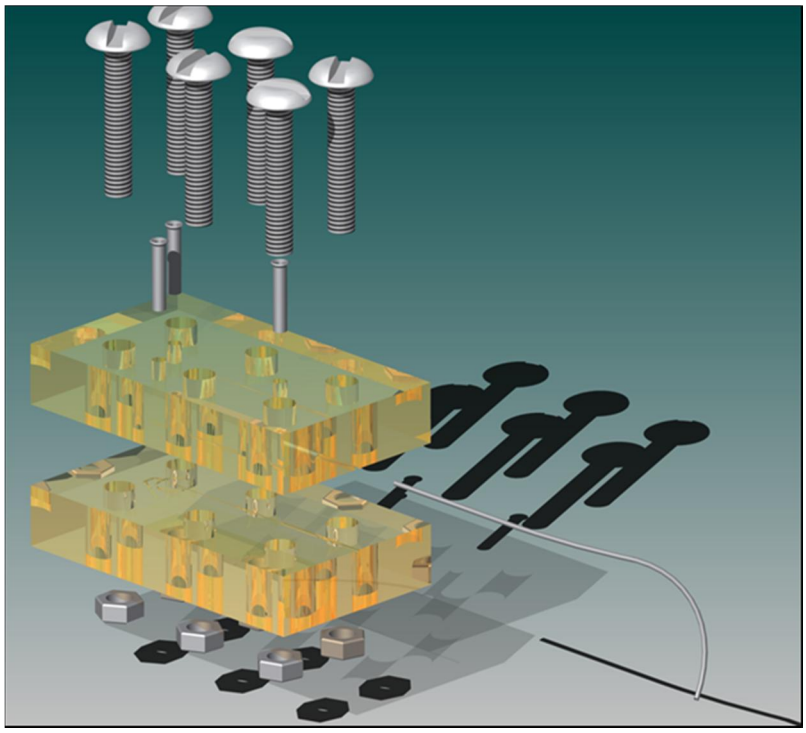

Figure 4.8: Schematic design showing how PC MC3 was screwed together.

As shown in Figure 4.9, sodium alginate microdroplets containing nano-precipitated calcium carbonate were formed at the first T-junction of PC MC3. For cell encapsulation, Jurkat cells were added to the sodium alginate solution prior to being introduced to the microfluidic chip. Another T-junction was placed downstream of the first inlet to introduce the acidified oil into the microfluidic chip, which allowed a stream of acidified oil to merge with the main stream (containing the calcium alginate microdroplets). This caused a reduction in pH and in turn calcium ions were released, which then reacted with the sodium alginate microdroplets, causing the formation of calcium alginate gel microbeads down-stream.

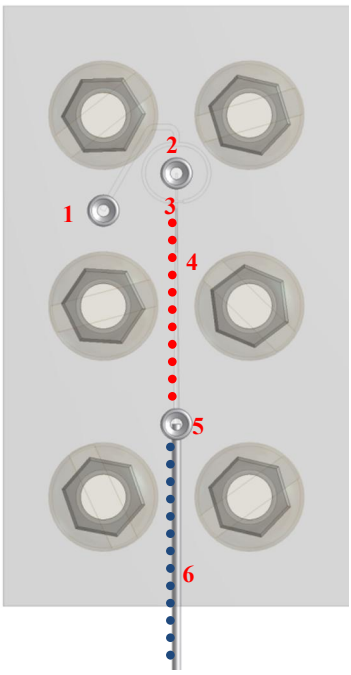

Figure 4.9: A schematic diagram of PC MC3 used for the production of alginate gel microbeads containing cells. 1: carrier oil (vegetable oil), 2: sample (sodium alginate solution containing nano-precipitated calcium carbonate and Jurkat cells), 3: T-junction, 4: sodium alginate microdroplets, 5: T-junction for introduction of acidified oil and 6: calcium alginate microdroplet undergoing gelation.

4.2.3 Fluid injection

The optimised microfluidic setup described in this chapter, and shown in **Error! Reference source not found.**, involved injecting fluids (oil, acidified oil and samples) through the microfluidic chip using syringe pumps rather than gravity forces. A 1 ml disposable luer-lok syringe was connected to a 10A Fusion 400 Touch infusion syringe to inject the sample into the chip, and two 10 ml disposable luer-lok syringes were connected to a Harvard '33' twin syringe used to inject the carrier oil and acidified oil into the chip.

4.2.4 Connections, tubing and camera

The microfluidic chips (PMMA MC1, PMMA MC2 or PC MC3) were tested on different occasions to determine the most suitable microfluidic chip, for encapsulating Jurkat cells in alginate gel microbeads. The microfluidic chips were connected to the syringes containing fluids using PTFE Tubing as described in the previous Chapter (Chapter Three). The same Lumenera monochrome camera (LU165M) attached the setup described in the previous

chapter was also attached to the optimised setup described in the work carried out in this chapter. The camera was used to obtain snapshots and to monitor the formation of calcium alginate gel microbeads in the microchannels of the chips.

4.2.5 Modification of the alginate solution

The 1.1% alginate solution described in chapter three was modified to enhance reproducibility and reduce excess amounts of $CaCO_3$, which in turn reduced the risk of clogging up the micro-channels in further investigations. This modification involved reducing the amount of $CaCO_3$ powder in the sodium alginate solution from 13.3 mg/ ml to 7.5 mg/ ml.

4.2.6 Cell Imaging

The samples (calcium alginate gel microbeads containing Jurkat cells) were transported over a mile of open landscape under ambient conditions. The samples were transported across this relatively long distance, since the microfluidic setup and the fluorescence microscope used to image the cells were located in two different building at the University of Manchester. This journey took approximately 20 minutes. It was predicted that the Jurkat cells would still remain viable, since many biological studies (298,299) are carried out over the same period of time and even longer, without effecting cell viability.

The encapsulated Jurkat cells in calcium alginate gel microbeads were stained 24 hours after encapsulation with propidium iodide (PI) and calcein acetoxymethyl ester (calcein-AM) to determine cell viability. Calcein-AM is permeable through cellular membranes and is highly lipophilic i.e. it tends to combine or dissolve in lipids or fats (300,301). Calcein-AM was used in this Chapter to stain viable encapsulated cells green. Although Calcein-AM is not a fluorescent molecule; intense green signals observed in cells, with excitation and emission wavelengths of 490 nm and 515 nm respectively, is a result of the conversion of Calcein-AM into calcein, which is caused by intracellular enzymes called esterases.

Calcein is retained in intact cells and escapes from cells with damaged membranes; meaning that only the viable cells in the calcium alginate microbeads emit a green fluorescent signal (300).

PI, on the other hand, was used to stain nuclei of dead cells (302,303), as this dye cannot penetrate membranes of viable cells. PI enters the dead cells and reaches the nuclei *via* disrupted regions within the cellular membranes, and intercalates with the DNA within the cells causing the emission of red fluorescence at maximum excitation and emission wavelengths of 535 nm and 617 nm respectively (303). Moreover, since both dyes can be excited at the same wavelength (490 nm), viable and dead cells can be monitored simultaneously using a fluorescence microscope (303).

The encapsulated Jurkat cells were stained by aliquoting 500 µl of sample (alginate gel microbeads containing cells and media) into an Iwaki dish, followed by the addition of 20 µl of calcein-AM and 0.5 µl of PI. This dish was covered immediately with aluminium foil after adding the dyes to the sample, in order to prevent possible photoreactions.

4.2.7 Microscope setup

The Iwaki dish containing the encapsulated Jurkat cells was placed on a stage in the incubation chamber of the microscope. This chamber was maintained at 37°C, 95% humidity and 5% CO_2 to allow the encapsulated cells to survive during analysis. The lens of the microscope was set to 20 × objective and images of the alginate gel beads containing cells were taken with a photon counting CCD camera (Orca II; Hamamatsu Photonics, Welwyn Garden City, UK).

4.3 Results and discussion

4.3.1 Discussion of the effect of fluid flow rates on the size of alginate gel microbead produced using PC MC3

The fundamental principle behind the use of T-junctions and flow focusing geometries is to produce microdroplets by taking advantage of the instability of the flow rates that is caused by interfacial and shear forces. The interfacial force occurs as a result of two phases flowing through the microchannels (continuous and dispersed phases) (304). The flow rates of the fluids driven through the microfluidic setup were controlled using syringe pumps as described in section 4.2.3. A number of different flow rates were tested using PC MC3, in order to determine the flow rates needed to produce alginate microbeads with desired diameters ranging between 150-200 µm. This range was specifically chosen to allow the exchange of nutrients and oxygen (305-307), in addition to reducing the number of encapsulated Jurkat cells, and potentially enabling the encapsulation of single cells. The ability to encapsulate single cells or small groups of cells is beneficial in cases where clinical samples are hard to obtain or when single cell studies are performed (17,19,20,308).

Table 4.2: Flow rates tested to determine the optimum flow rates of the continuous and dispersed phases to produce alginate gel microbeads with diameters ranging from 150- 200 mm.

Continuous phase Flow rate µl/min	Sample flow rate µl/min	Mean average size of alginate gel microbeads µm
2	8	230
2	16	170
2	32	200
6	8	250
6	16	248
6	32	130

Numerous approaches to produce alginate gel microbeads have been reported (207,216,247,309). The size distribution of these microbeads is quite wide, since there are a variety of flow rates and substances used in the formation and gelation processes of

alginate gel microbeads. Table 4.3 lists a number of reported flow rates used to produce alginate gel microbeads of different sizes.

Table 4.3: Flow rates of the continuous and dispersed phases that have been reported in literature to produce alginate gel microbeads with diameters ranging from 150- 200 mm.

Continuous phase flow rate µl/min	Dispersed aqueous phase flow rate µl/min	Size of microbeads µm	References
3 240	4.8 11.2	30 230	(207)
2.7 2.7 3.3	15 8.3 5	98.6 150.7 195.7	(247)
5 5	0.7 1.7	100 140	Supplementary material for (247)
38.3	0.5	190	(309)
1.67 8.33	0.83	50 10	(216)
0.58 2.9	0.07 0.07	91 62	(310)

From Table 4.2, it was observed that the flow rates (both continuous and dispersed phases) have an effect on the size of the alginate gel microbeads. When the flow rate of the continuous phase was kept constant (in both cases at 2 µl/min and 6 µl/min) and the sample flow rate was varied from 8 to 32 µl/min a general decrease in the size of the microbeads was observed. Maintaining a constant continuous phase flow rate of 2 µl/min and increasing the dispersed phase flow rate from 8 to 16 µl/min led to a decrease in the size of the calcium alginate gel microbead from 230 µm to 170 µm. However further increase in the dispersed phase flow rate caused an increase in the size of the calcium alginate gel microbeads (increased from 170 to 200 µm). This could possibly be due to backflow of the sample and aggregation of cells. When the continuous flow rate was kept

at 6 µl/min and the sample flow rates varied from 8 to 32 µl/min, a slight decrease in the size of the microbeads was observed (from 250 to 238 µm), suggesting that the effect of sample flow rate is limited when operating at higher continuous flow rate. Thus based on the result obtained in Table 4.2 an optimum continuous flow rate of 2 µl/min and sample flow rate of 16 µl/min were employed throughout the experiments.

It was aslo noticed that an increase in the flow rate of the continuous phase above this threshold resulted in leakages. Similar findings were also reported by Lin et al. (304). Different flow rates were tested and are listed in Table 4.3, these flow rate were used as a numerous approaches reported in the literatures suggested that to obtain microbeads of a desired size (150-200) the continuous phase flow rate should be between 2-5 µl/min (248), and a sample flow rate ranging between 5-15 µl/min.

4.3.2 Discussion of calcium alginate gel microbead formation using PC MC3

Once the PC MC3 was fabricated, the carrier oil, aqueous solution (containing alginate, nano precipitated calcium carbonate and Jurkat cells) were introduced into the microfluidic chip using the internal gelation method described in section 4.2.2. An image showing the production of calcium alginate microbeads containing Jurkat cells in PC MC3 is shown in Figure 4.10.

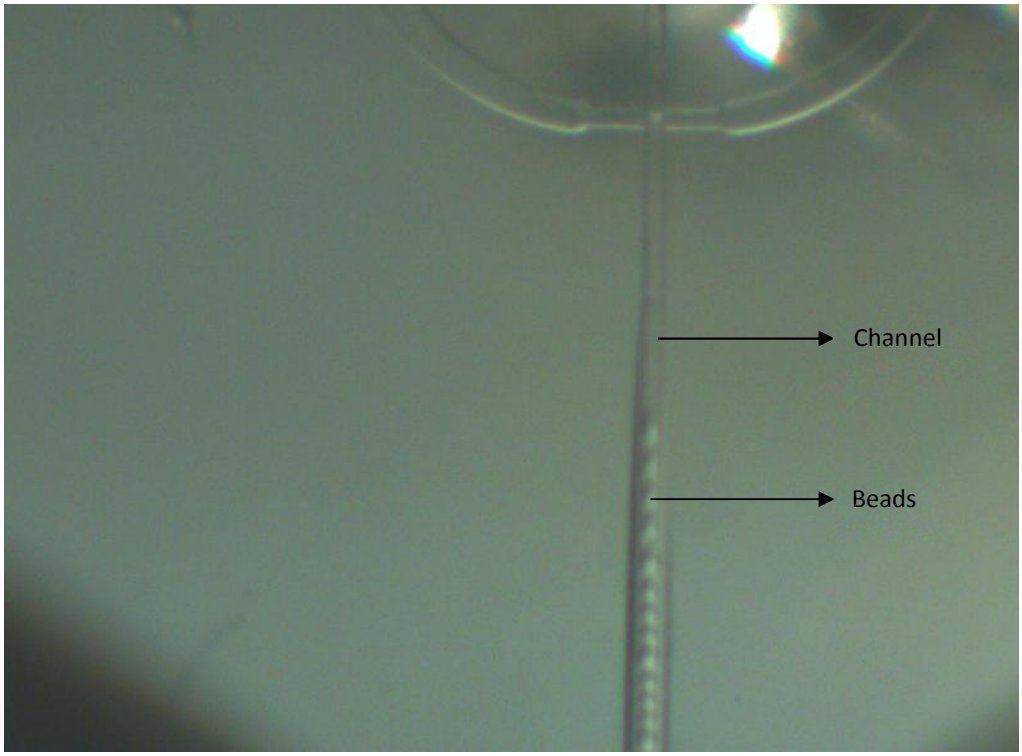

4.10: The formation of calcium alginate gel microbeads in PC MC3.

This internal gelation approach enabled the successful encapsulation of single/ small groups of Jurkat cells in alginate gel microbeads as seen in Figures 4.11 and 4.12. The resultant calcium alginate gel microbeads appeared to be uniform in size and shape as seen in Figure 4.12, which was probably due to a number of reasons, including: the ability to control the flows of the fluids using syringe pumps, and the fact that the syringes were not placed in upright positions, hence the cells and calcium alginates gel microbeads did not

sink down so fast. A bright field microscope was used to visualise and obtain an image of four encapsulated Jurkat cells in an alginate gel microbead, which is shown in Figure 4.11.

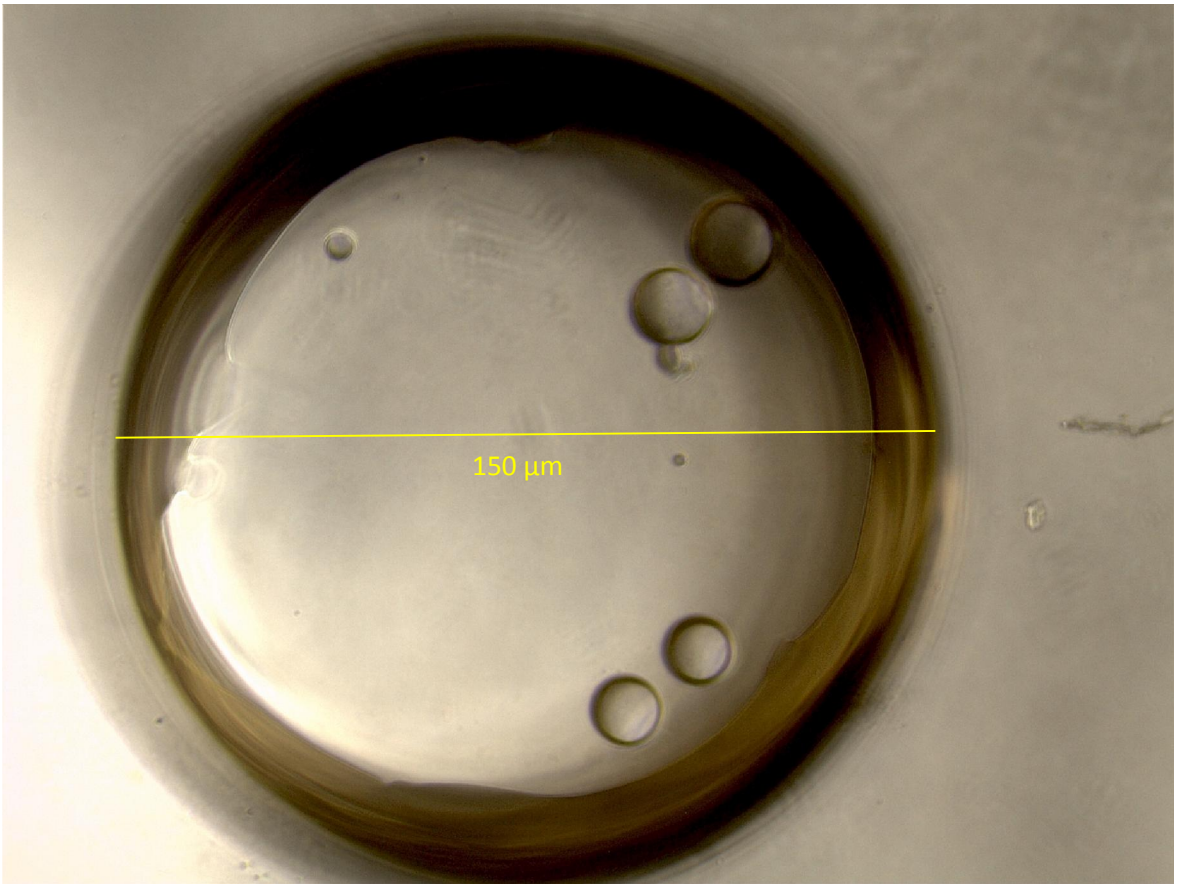

Figure 4.11: A bright field microscope image of four encapsulated Jurkat cells in a spherical alginate gel microbead produced using syringe pumps as a means of fluid injection though the PC MC3 chip. The diameter of this alginate gel microbead is 150 µl.

This approach saw the successful encapsulation of Jurkat cells in uniform sized and shaped alginate gel microbead as seen in Figure 4.14.

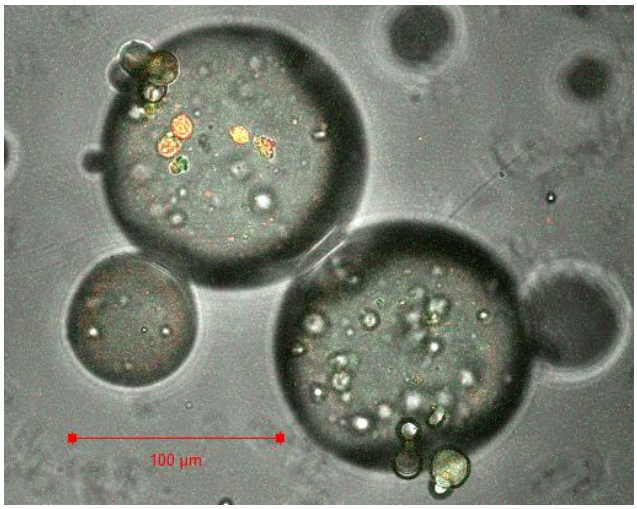

Figure 4.12: Confocal microscopy image of calcium alginate gel microbeads containing jurkat cells. These microbeads are spherical and mono-dispersed produced by using the optimised microfluidic setup and chip.

4.3.3 Results and discussion of cell viability

4.3.3.1 Calcium alginate gel microbeads produced externally using PMMA MC2

In this approach, the carrier oil and aqueous solution (containing alginate, nano precipitated calcium carbonate and Jurkat cells) were introduced into the PMMA MC2 at the first and second inlets respectively via syringe pumps. The flow rates were then adjusted as described in section 4.2.3. The resultant sodium alginate microdroplets containing cells were then dropped into a sterilised 24 well plate containing 1ml of acidified oil for about 1 minute to allow the external gelation process to occur.

The encapsulated Jurkat cells were then stained with calcein-AM and PI dyes 24 hours after encapsulation. The encapsulated Jurkat cells were then visualised under a fluorescence microscope in order to determine cell viability. The fluorescence microscopy images obtained Figures 4.13 and 4.14; showed that red fluorescent signals were emitted from these cells, meaning that the cells died. This observation was most likely due to the fact that the cells were exposed to a larger volume of the acidified oil containing a relatively high concentration of glacial acetic acid (GAA). Once GAA dissociates within a cell it causes cell death via various mechanisms: the build-up of anions can contribute to an increase in pressure (311), which causes the cells to burst. In addition there is a possibility that other cellular anions are expelled, which causes a reduction in intracellular pH, inhibits cell function and/ or causes a feedback inhibition of many vital metabolic pathways (311). Therefore, it was decided that the best way to gelify the alginate gel microbeads was to adapt an internal gelification approach.

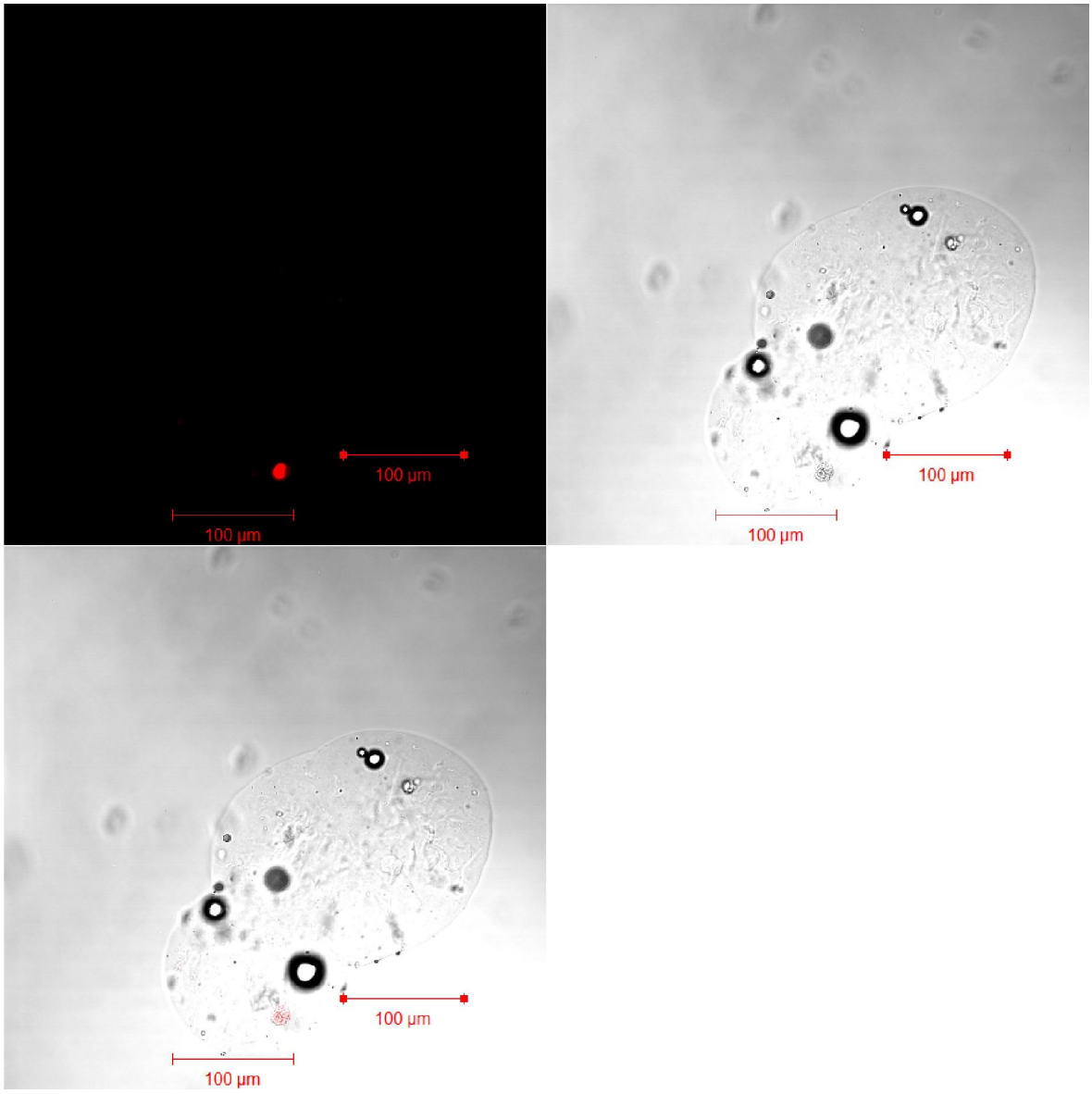

4.13: Microscope images (×20 magnification) of an encapsulated single dead cell in a calcium alginate gel microbead. The upper left image is a fluorescent image, the upper right is a phase contrast image and the lower left is a combination of both the fluorescence and phase contrast images. The encapsulated cell was stained with calcein-AM and PI dyes and imaged 24 hours after encapsulation. This dead cell was encapsulated in a calcium alginate gel microbead using PMMA MC2.

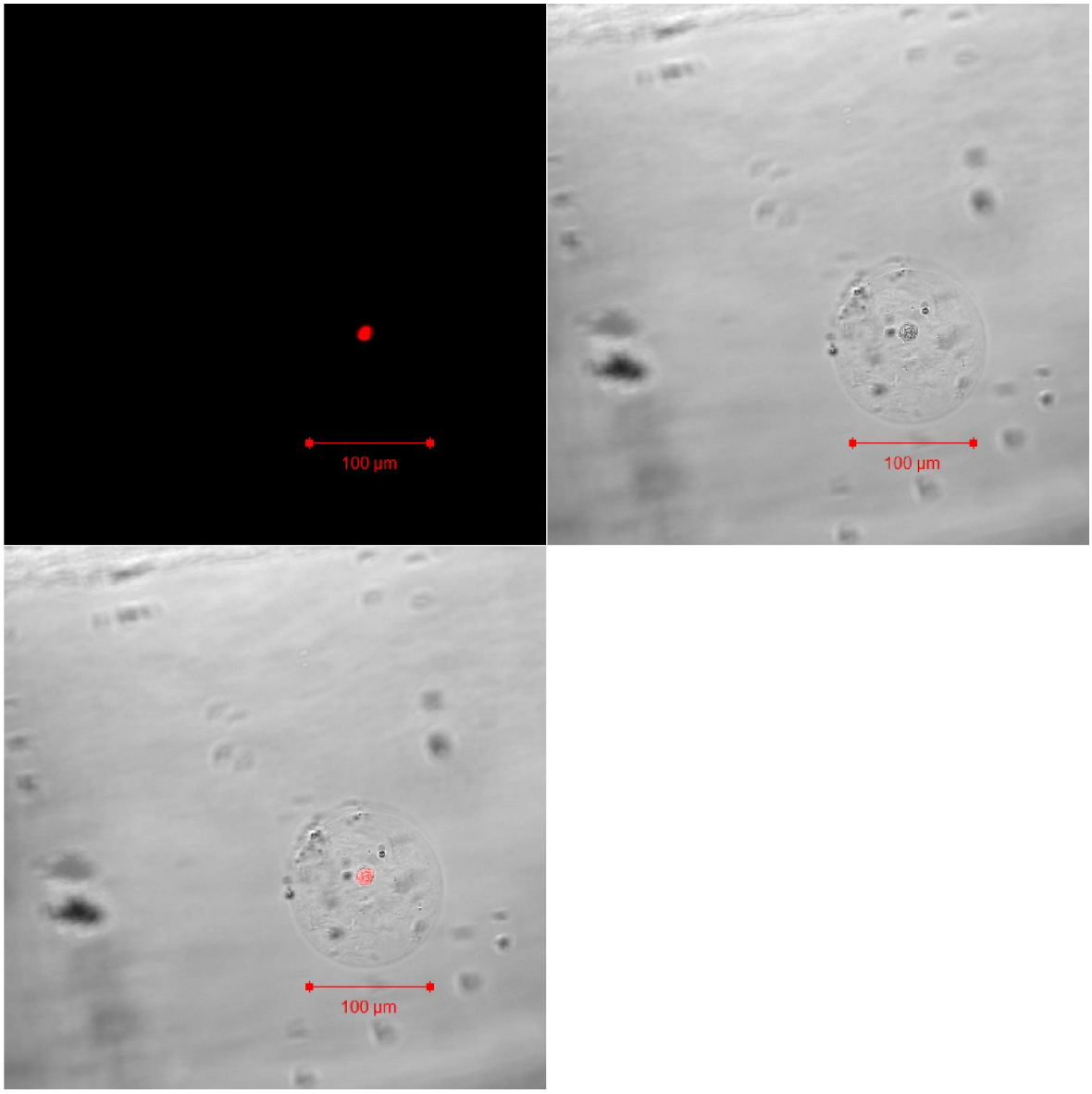

Figure 4.14: Another microscope images (×20 magnification) of an encapsulated single dead cell in a calcium alginate gel microbead. The upper left image is a fluorescence image, the upper right is a phase contrast image and the lower left if a combination of both the fluorescence and phase contrast images. The encapsulated cell was stained with calcein-AM and PI dyes and imaged 24 hours after encapsulation. This dead cell was encapsulated in a calcium alginate gel microbead using PMMA MC2.

4.3.3.2 Calcium alginate gel microbeads produced internally using PMMA MC1

Another attempt to encapsulate live Jurkat cells successfully in alginate gel microbeads was vital to overcome the above mentioned challenges. However, prior to encapsulating the Jurkat cells in the calcium alginate gel microbeads, it was essential to investigate the minimum concentration of GAA needed for the gelation process of the microbeads. The states of the calcium alginate gels were determined visually and by touching the gel with a micropipette tip. The results obtained were summarised in Table 4.4 and showed that 100 µl of glacial acetic acid in 50 ml of vegetable oil was enough to gelify the calcium alginate gel, whereas reducing the amount to 50 µl caused partial gelation to occur.

The term partially gelled was used when the alginate gel was deformed as a result of touching the gel with a micropipette tip. On the other, hand the term gelled was used when the alginate gel restored its state after being provoked with a micropipette tip. Subsequently, the amount of glacial acetic acid was reduced to 100 µl

Table 4.4: Summary of the results obtained to determine the minimum amount of glacial acetic acid needed for alginate gel solidification.

Amount of glacial acetic acid in 50 ml of vegetable oil	State of alginate gel
250 µl	Gel
100 µl	Gel
50 µl	Partially gelled
20 µl	Partially gelled

Once the minimum concentration of GAA was determined, the alginate solution (1.1% w/w) was then made up as described previously in chapter two with the addition of 0.1125 g of nano-precipitated calcium carbonate. The carrier oil, acidified oil and aqueous solution (containing alginate, nano precipitated calcium carbonate and Jurkat cells) were then introduced into PMAA MC1 at the first, second and third inlets respectively using syringe pumps as described in section 4.2.3. Thus the gelation process of the calcium alginate gel

microbeads occurred on chip. This approach enabled the successful encapsulation of single Jurkat cells in monodisperse and uniform sized calcium gel alginate microbeads.

The encapsulated Jurkat cells were stained as described in the previous section with both calcein-AM and PI dyes 24 hours after encapsulation. The cells were then observed under a fluorescence microscope and images of the calcium gel microbeads containing cells were obtained and are shown in Figures 4.15 and 4.16. The encapsulated Jurkat cells appeared to be permeable, i.e. they exhibited both live and dead charactartics. As mentioned previously in the methodology section of this chapter, PI stains the nucleus of a dead cell red by attaching to the cell nucleus, for this to happen there cell membrane must be have been damaged. Whereas, calcein-AM is converted into what is known as calcein by an enzyme called esterases is only retained in a live cell. This means that the encapsulated cells have most likely experienced stress during the encapsulation and gelation process of the calcium alginate gel microbeads, causing slight damage (perhaps a hole) to the cell membranes, which allowed the PI dye to enter and stain the cell nucleus. At the same time, calcein was retained in the cell since the cell membrane was not damaged enough and may have started to recover. Another possible explanation was that the cells could have been subjected to excess pressure (90). There still remains a possibility that the Jurkat cells could have recovered from the initial shock/ stress a couple of days after the encapsulation process took place. Unfortunately, due to both the availability of the fluorescence microscope and time constraints, the encapsulated cells could not be monitored further. Similar observations have also been reported (312). A paper published by Hiraoka, Y and Kimbara, K reported three different categories of cells, which included: viable, dead and permeabilised cells. The cells were categorised based on their take up of live/dead cell dyes, for example: calcein positive cells represented viable cells, PI positive cells represented dead cells and calcein and PI positive cells represented the permeabilised cells.

The cells that were shown to be positive for both live and dead stains were referred to as permeable, because PI for example only enters a cell through damaged membranes, whereas calcein on the other hand is retained in viable cells.

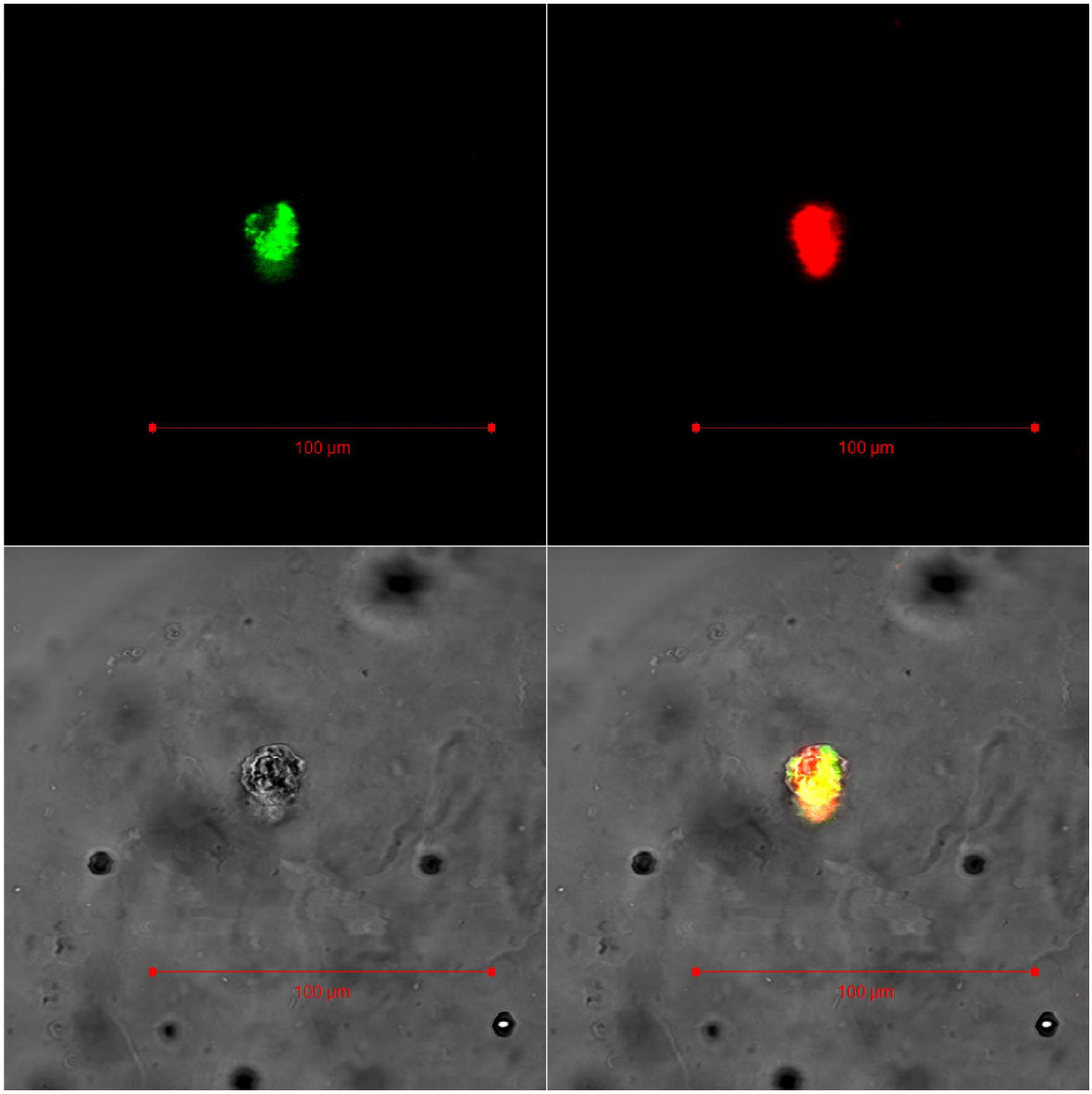

Figure 4.15: Fluorescence microscope image ×20 magnification of an encapsulated cell in an alginate gel microbead after 24 hours of encapsulation. The cell emitted green and red signals meaning that the cell was permeabilised. This cell was encapsulated was encapsulated in a calcium alginate gel microbead using PMMA MC1.

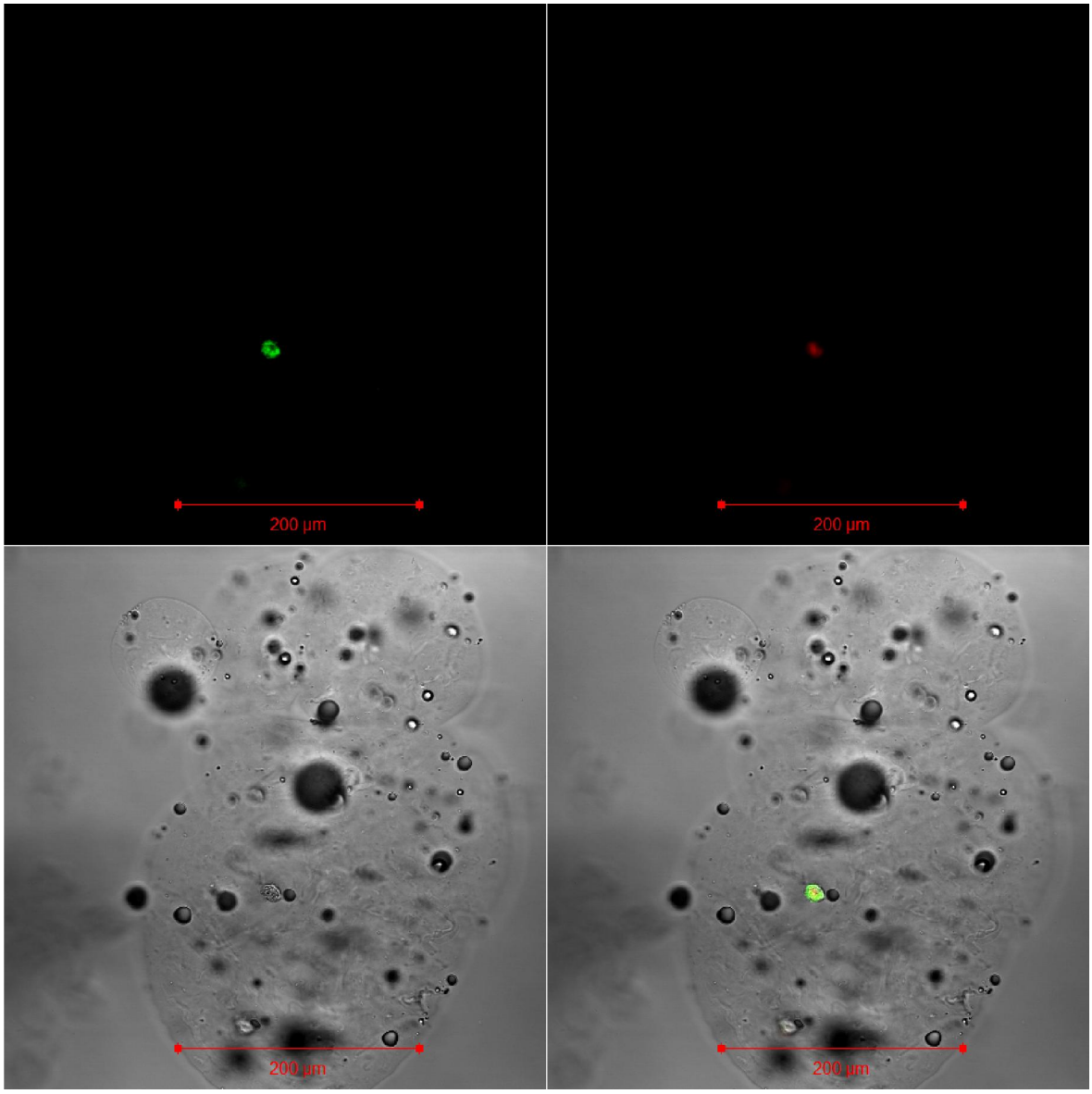

Figure 4.16: Another fluorescence microscope image ×20 magnification of an encapsulated cell in an alginate gel microbead after 24 hours of encapsulation. The cell emitted green and red signals meaning that the cell was permeabilised. This cell was encapsulated was encapsulated in a calcium alginate gel microbead using PMMA MC1.

4.3.4 Calcium alginate gel microbeads produced internally using PC MC3

Another approach to produce alginate gel microbeads containing cells was needed to overcome the challenges caused due to the way that the PMMA MC2 chip was fabricated. This approach therefore, involved modifying the fabrication procedure so that polycarbonate blocks were used instead of PMMA. The encapsulated Jurkat cells were subsequently stained as described in the two previous sections with PI and calcein-Am 24 hours after the cells were encapsulated. The Jurkat cells were then visualised under a fluorescence microscope and images of the calcium alginate gel microbeads containing Jurkat cells were obtained (Figures 17 and 18). The encapsulated Jurkat cell using this approach appeared to be Permeable.

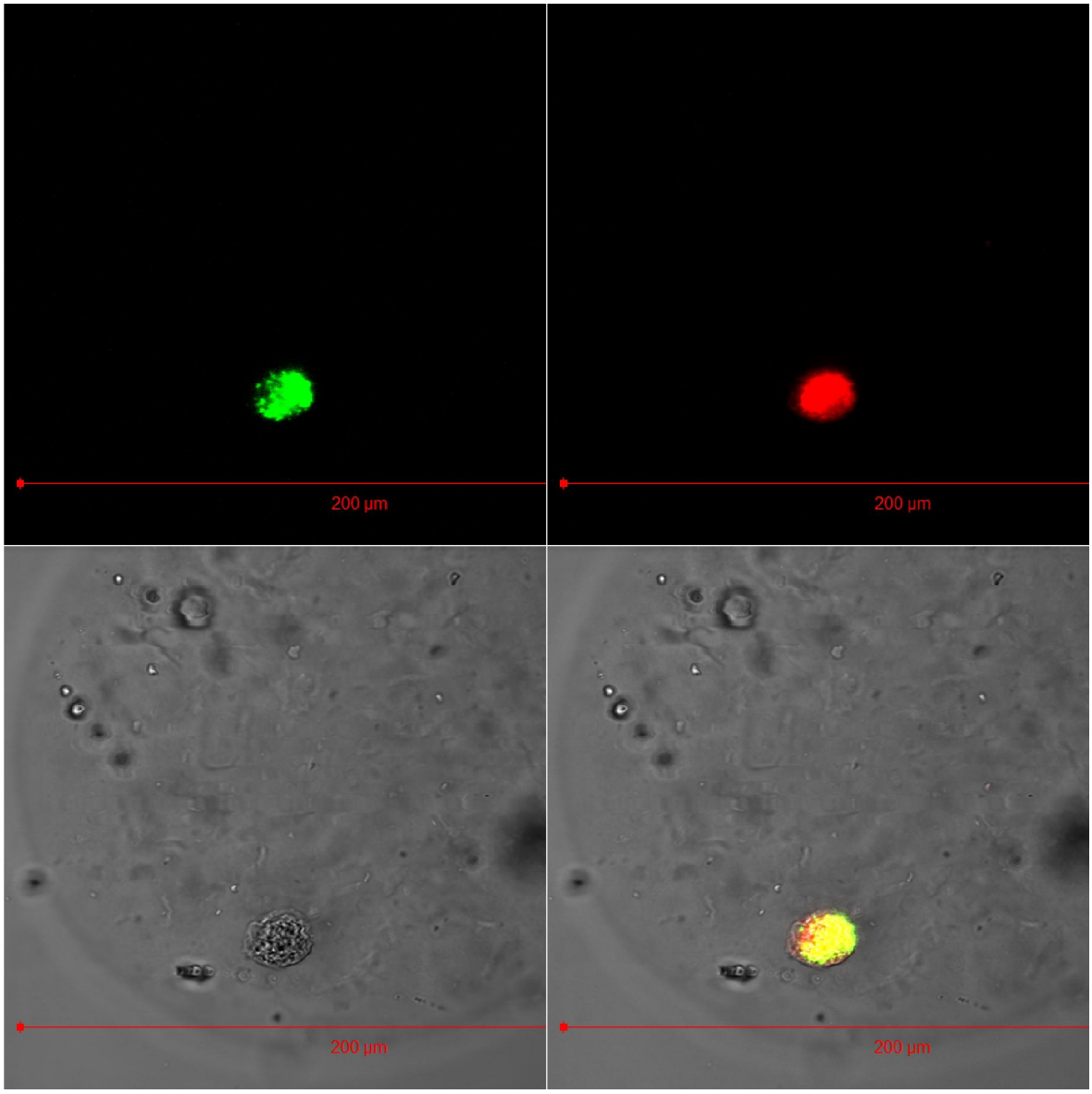

Figure 4.17: Fluorescence microscope image × 20 magnification of an encapsulated cell in an alginate gel microbead after 24 hour of encapsulation. The cell emitted green and red signals meaning that the cellular activity of the cell reduced and began to undergo apoptosis. This cell was encapsulated using the optimised approach to produce alginate gel microbeads.

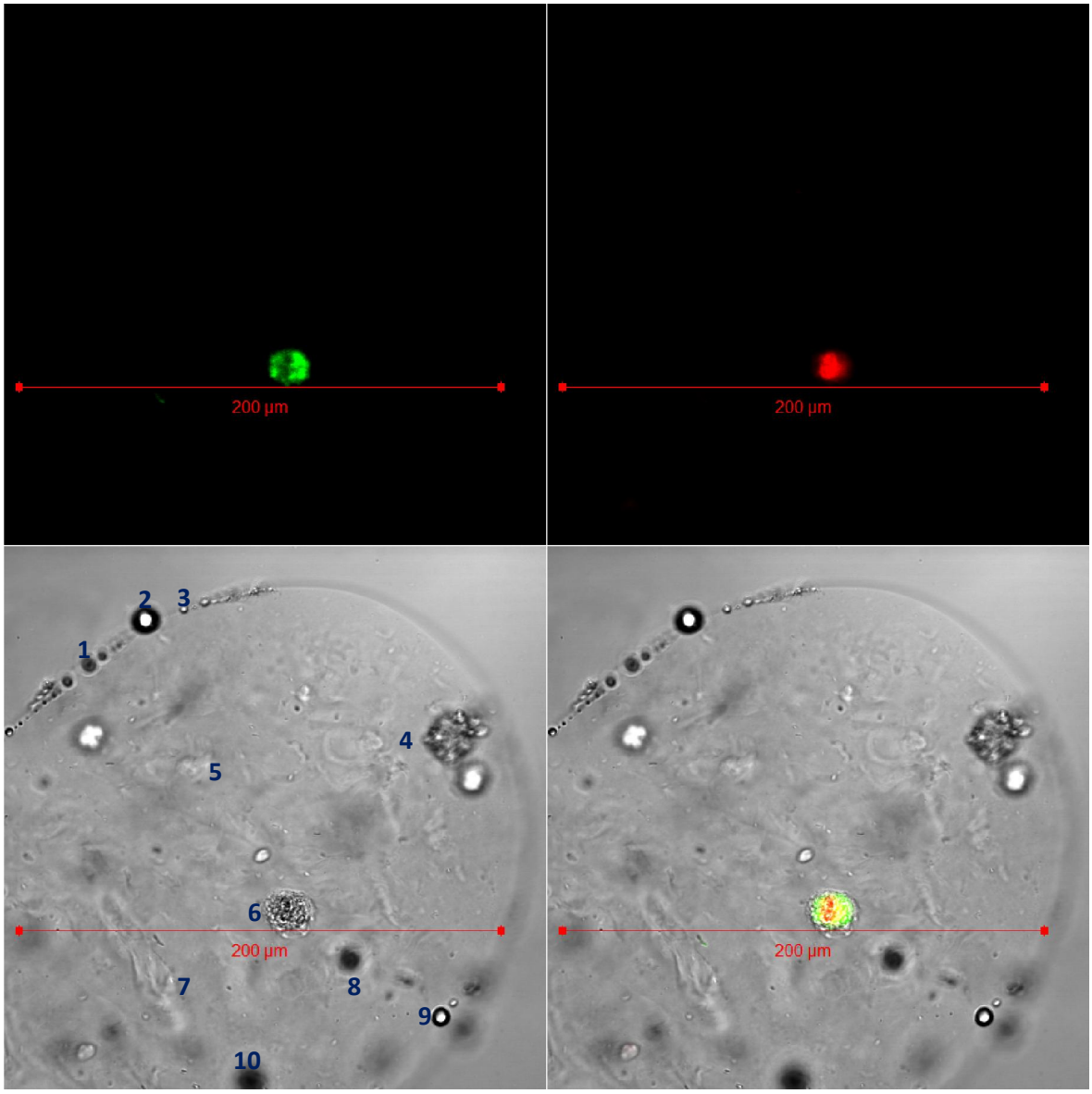

Figure 4.18: Another fluorescence microscope image ×20 magnification of an encapsulated cell in an alginate gel microbead after 24 hours of encapsulation. The cell emitted green and red signals meaning that the cellular activity of the cell reduced and began to undergo apoptosis. This cell was encapsulated using the optimised approach to produce alginate gel microbeads. The different substances within the alginate gel microbeads have been numbered, as follows 1, 3, 8 and 10: air bubbles out of plane of focus, 2 and 9: air bubble, 4: BSA, 5 and7: inconsistencies in the alginate gel, and 6: Jurkat cell (calcein positive and PI positive).

Figure 4.18 has been annotated to describe the other particles that are present in the calcium alginate microbeads. The same particles were also observed in the other fluorescence images presented in this chapter. A number of air bubbles appear to be outside of the plane focus at various points within the calcium alginate gel microbeads. These air bubbles appear as the dark shadows and have been referred to as particle

numbers 2 and 9. Other air bubbles were visualised in line with the focal plane and appeared as white particles. These air bubbles have been numbered 1, 3, 8 and 10. It was unlikely that the aggregate observed in Figure 4.18 (particle number 4) was cell remnant or lost DNA, but rather it was most likely to be BSA from the FCS or a cell ghost (also from FCS), since FCS is never 100% pure and is known to always have various particles floating in it. Such aggregates are always found in cell culture medium and are observed at the same focal plane as the Jurkat cells, but are not calcein or PI positive. If this aggregate was indeed a cell it would have been stained, and it would have been easier to stain than the stained Jurkat cell, since it is as located at the edge of the calcium alginate gel microbeads. These observations provide clear evidence that there is one cell encapsulated in the calcium alginate gel microbeads shown in Figures 4.13- 4.18. If there were more than one encapsulated Jurkat cell in the calcium gel alginate microbeads, every intact Jurkat cell would have been stained green and every complete cell with DNA would have been stained red. Therefore, the calcium alginate gel microbeads in Figures 4.13- 4.18 contained only one cell.

The fluorescence images of the encapsulated Jurkat cells shown in Figures 4.15- 4.18 as mentioned previously, were calcein and PI positive, such cells are referred to as permeable. The viability of these cells can only be determined by looking at the same cells under the fluorescence microscope after 24 hours and 48 hours. The Jurkat cells should have divided if they were viable, or at least the viability status of the Jurkat cells would have been determined by the colour they fluoresce. In addition, the alginate gel microbead might have hindered the Jurkat cell from falling apart, preventing the cell contents from spilling out. Moreover, cells cannot lose their DNA, which means that the DNA (including fragmented DNA stained with PI) cannot diffuse out of the nucleus. Therefore the red stain should be observed for cells containing DNA even if they have crumbled up. Furthermore, despite

not fitting into one field of view, the images of the calcium alginate gel microbeads containing single cells were checked to ensure single Jurkat cells were encapsulated.

Referring back to the growth curve (Figure 2.12) in chapter 2, there was a 24 hour delay in the growth of Jurkat cells after undergoing encapsulation in large calcium alginate gel beads. Thus, the results presented in this chapter and chapter 2 could indicate that many of the encapsulated Jurkat cells either stopped growing for a while, some might have started to grow again and that others might have not.

Another factor that could have resulted in the permeability of the encapsulated Jurkat cells to both stains was that unfortunately they had to be transported for at least 20 minutes under ambient conditions and different weather conditions.

4.4 Conclusion

The main aim of this Chapter was to encapsulate live cells in alginate gel microbeads using a novel microfluidic setup and a purposely fabricated microfluidic chip. The fluids were injected into three specifically designed microfluidic chips using syringe pumps to find the most suitable chip for cell encapsulation. The amount of nano precipitated calcium carbonate and glacial acetic acid used to solidify the alginate gel microbeads was also modified to ensure that the process of solidifying the microbeads had little or no effect on cell survival. The alginate gel microbeads containing cells described in this Chapter were solidified by internal or external gelation methods depending on the chip that was used to encapsulate the cells.

Findings from the work carried out in this chapter revealed that the best approach combined the use of internal gelation methods using a microfluidic chip that was made from polycarbonate sheets. This approach was favoured due to many factors, including: the ability to control the size and shape of the alginate microbeads containing permeable Jurkat cells after 24 hours of encapsulation.

Controlling the size of the microbeads is important as it controlled the number of encapsulated cells and allowed for single cell encapsulation, which is vital for future single cell experiments and cell signalling studies (15). The microbeads produced in this chapter were roughly around 150 μm, which allowed for oxygen and nutrients to enter and escape from the microbeads as and when needed.

The following Chapter (Chapter 5) concludes the thesis and summarises recommendations for future work.

5 Chapter Five Conclusion

5.1 Introduction

This Chapter is divided into four main sections, which also includes this section (section 5.1). Section 1.2 summarises the progress that has been made towards meeting the aims and objectives that were detailed in Chapter 1. Section 5.3 summaries the conclusions derived from each Chapter in this thesis, and section 1.4 provides a summary of suggestions for recommendations and future work.

5.2 Review of aims and objectives

The aims of this research project were the novel design and optimization of a microfluidic setup for single cell encapsulation. These aims were mainly met as a novel microfluidic setup and chip were successfully developed and employed for encapsulating single cells in calcium alginate gel microbeads. However, the encapsulated cells appeared to be permeabilised 24 hours after encapsulation, since the cells were stained with both calcein and PI.

The main objectives of this thesis were to:

- Determine the effect of formulations used for the production and degradation of the alginate gel beads on cell viability.
- Monitor the viability of encapsulated cells in calcium alginate gel beads.
- Construct a novel microfluidic setup, including a simple novel and reusable microfluidic chip to encapsulate single cells in calcium alginate gel microbeads.
- Determine the cell viability of encapsulated cells using the optimal microfluidic setup.

These objectives were mainly met, although further work was required to show that the encapsulated Jurkat cells in calcium alginate gel microbeads, would have potentially still been alive (i.e. no PI stained nuclease) 24 hours and more after the encapsulation process. However, due to time constraints this was not possible.

Cytotoxicity experiments were carried out to determine the effect of formulations used to encapsulate cells and degrade alginate gel beads on cell growth and viability. In these experiments, cells were stained with trypan blue and visualised under a light microscope, allowing for viable and dead cells to be distinguished and counted. Findings from these test showed that prolonged exposure (30 minutes and more) to calcium chloride effected Jurkat cell growth and viability. This finding is not problematic as calcium chloride was only needed in the solidification process of the beads for a period of 10 minutes. Furthermore, the sodium citrate buffer used to dissolve the calcium alginate beads had no significant effect on cell growth or viability.

Following on from the cytotoxicity tests, Jurkat cells were encapsulated in large calcium alginate gel beads (2 mm in diameter), which were produced manually by dropping calcium alginate/ cell solution from a syringe that was attached to a 25 Gauge needle into 1 ml of calcium chloride solution. This resulted in the successful formation of calcium alginate gel beads containing cells. This was followed by a study that was carried out over a period of seven days to monitor cell growth in large calcium alginate gel beads. Findings from this study showed that the growth of encapsulated cells in calcium alginate beads was delayed despite following the same growth trend as non-encapsulated cells. This suggests that alginate is a suitable material for cell encapsulation studies, and was therefore used in the subsequent studies described in this Thesis.

Furthermore, the optimised microfluidic setup described in Chapter Four was used to encapsulate Jurkat cells in calcium alginate gel microbeads. The optimisation process involved designing, fabricating and testing three microfluidic chips in order to determine the most suitable chip design for encapsulating cells in calcium alginate gel microbeads. The favoured chip was made from polycarbonate sheets, and allowed for internal solidification of the alginate gel microbeads to take place.

The microbeads produced were polydisperse and spherical with a diameter of approximately 150-200 μm in size as desired. Moreover, most of the microbeads contained single cells or small groups of cells, which potentially can aid the understanding of certain cellular activities.

The encapsulated cells in calcium alginate gel microbeads were then stained with PI to visualise dead cells red and calcein-AM to visualise viable cells green. Findings from these experiments showed that the cells emitted both green and red signals, indicating that the cells had characteristics of both live and dead cells. These observations could have been due to many factors, such as:

- The cells could have experienced an initial shock during the encapsulation process.
- The high pressures applied could have damaged the cells slightly by making holes in the cell membranes making them permeable to PI yet at the same time retaining the calcein.
- Yeast contamination was observed when the encapsulated cells were visualised under the fluorescence microscope.
- The encapsulated cells were transported across a mile of open landscape 24 hours after encapsulation for fluorescence microscopy imaging.

5.3 Summary of main conclusions

In Chapter 1, a literature survey on cell encapsulation using different materials and the use of microfluidics for encapsulating cells were carried out. The main areas that required improving to encapsulate cells were identified and listed as follows:

The results obtained in Chapter Two showed that alginate is a suitable material for cell encapsulation. In this Chapter a series of cytotoxicity tests were carried out to determine the effect of formulation used to solidify and degrade alginate gel beads on the viability and growth rate of encapsulated cells. In addition a study was carried out to monitor cell growth and viability of encapsulated cells over a period of seven days. Recommendations that were suggested in this Chapter involved using microfluidics to encapsulate cells in alginate gel beads. The results obtained in this Chapter formed the basis of investigations detailed in the two subsequent Chapters (Chapter Three and Four).

The recommendations set in Chapter Two were implemented in Chapter Three, which aimed at constructing a microfluidic setup and chip to encapsulate cells in alginate gel microbeads. The fluids (oil, acidified oil and alginate/cell samples) were driven through the microfluidic setup by gravity. This led to the successful encapsulation of cells in alginate gel microbeads. The alginate gel microbeads produced in this Chapter were solidified internally (on chip), as the chip consisted of an inlet to inject the acidified oil through it. The main findings in this Chapter showed that the described microfluidic setup and chip can be used for the successful encapsulation of cells. However, there were some improvements and recommendations that needed implementing in order to produce alginate gel microbeads of uniform size and shape, while also allowing single cell encapsulation to occur. A further recommendation was to fabricate a more robust chip, which can withstand relatively high pressures.

Based on the results obtained in Chapter three, the microfluidic setup described in Chapter Four was modified. The fluids were injected through this microfluidic setup by syringe pumps instead of gravity. Moreover, three different chips were evaluated to produce alginate gel microbeads containing viable cells, to determine the most suitable material used to fabricate the chip in addition to comparing internal (on chip) and external gelation (off chip) methods on cell viability. The results showed that the microfluidic setup described in this Chapter enabled the successful encapsulation of permeable cells in alginate gel microbeads. Moreover, internal solidification was preferred over external solidification of the alginate gel microbeads as the cells died almost immediately when the beads were solidified externally. Furthermore, polycarbonate sheets were favoured over PMMA for fabricating the microfluidic chip, since the chip fabricated with this material was robust and allowed significantly high pressures to flow through it, enabling single cell encapsulation in 150-200 μm size alginate gel microbeads. However there still remained a drawback to this microfluidic setup as the cells showed both live and dead cell characteristics 24 hours after encapsulation.

5.4 Recommendations and future work

Work carried out in this thesis reports the successful encapsulation of permeable cells in alginate gel microbeads using a novel microfluidic setup and chip. A comparison between two different the microfluidic setups and three chips described in this thesis revealed that, the microfluidic setup driven by syringe pumps and the polycarbonate sheet microfluidic chip enabled the production of uniform size and shape alginate gel microbeads containing permeable cells. However, there still remained some essential improvements.

Table 4.5: Comparison of the developed microfluidic setup, chip and formulations with the characteristics of an ideal alginate gel microbeads.

Ideal characteristics of the microfluidic setup, chip and formulations.	**Developed characteristics**
Encapsulated cells should survive for at least 24 hours.	Encapsulated cells showed characteristics of both live and dead cells.
Uniform size alginate gel microbeads.	The size of alginate gel microbeads were roughly between 150-200 μm.
The alginate gel beads were to be spherical in shape.	The alginate gel beads were spherical.
Encapsulate single cells per bead.	Single cell encapsulation was achieved.
Reproducible	The alginate gel beads were reproducible as the pressure of fluids applied were easily controlled by the syringe pumps.
Easy to use and handle.	The microfluidic setup was easy to use and maintain.
A rigid microfluidic chip.	The microfluidic chip that successfully encapsulated cells in alginate gel microbeads was rigid as applying relatively high pressures did not cause any damage to the chip.
Cost effective	The main costs are associated with the fabrication of the microfluidic setup and chip. In general these are an initial investment, which once made eventually reduces the overall production costs of producing microfluidics.
Inertness of the material used to fabricate the microfluidic chip.	The polycarbonate sheet used to fabricate the optimised microfluidic chip was inert to the cells and did not cause cell death.
The material used to fabricate the microfluidic chip should be optically	The polycarbonate sheet used to fabricate the optimised microfluidic chip was transparent and

translucent, in order to check the progress of cell encapsulation and cell viability if desired.	allowed the visualisation of the progress of cell encapsulation.
The formulations (for example calcium chloride and sodium citrate) and materials (alginate) used to produce and dissolve microbeads should be mild to cells.	Cytotoxicity tests showed that the formulations and materials used to encapsulate cells were mild enough for cells to remain viable.

The comparison, Table 4.5 shows that the microfluidic setup, chip and formulations used to produce alginate gel microbeads containing permeable Jurkat cells satisfied most of the identified characteristics needed to produce the ideal microbead that would be used for cell encapsulation. However, the work conducted in this thesis has some limitations due time constraints, availability of equipment and lack of funding. The areas that have been recommended for future experimental work:

- Monitor cell encapsulation over a period of 24 hours.
- Encapsulate a range of different cells.
- Use of different materials to encapsulate cells and compare them.
- Reduce the size of the setup so that it can fit in a biohazard cabinet.

5.4.1 Monitor cell encapsulation for at least 24 hours.

Snapshots from live imaging of encapsulated cells in alginate gel microbeads were obtained using a fluorescence microscope. Ideally these snapshots should have been taken from live imagining as soon as possible after encapsulation for at least 24 hours, so that cells can be monitored. Unfortunately, due to time constraints and practicalities this was not carried out and instead video snapshots were taken 24 hours after the cells were encapsulated in alginate gel microbeads. This drawback meant that there was no prior knowledge of knowing if the cells were already PI positive immediately after entering the

microfluidic chip, or if the high pressure passing through the microfluidic chips killed the cells sometime after encapsulation.

5.4.2 Encapsulate a range of different cell lines.

The research studies carried out in this thesis involved encapsulating Jurkat cell lines. This cell line was chosen for two main reasons: its availability in the laboratory and because they are easy to maintain in a traditional 2D environment. If possible it would have been ideal to use different cell lines in the work carried out in Chapters Two to Four in order to compare cell survival rates upon encapsulation.

5.4.3 Use different materials to encapsulate cells and compare them.

The work carried out in thesis involved encapsulating cells in alginate gel microbeads. However, as described in Chapter One, there are other materials (natural and synthetic) that could be used to encapsulate cells. It would have been interesting if time and funds Permeabletted to try different encapsulating materials to encapsulate cells using the optimised microfluidic setup and chip. Following on from cell encapsulation, it would have been interesting to investigate cell survival within the different encapsulating material and compare cell survival rates.

5.4.4 Reduce the size of the microfluidic setup.

The size of the optimised microfluidic setup described in thesis is relatively big. The size of this setup could have been reduced by removing the safety box and bringing some of the components slightly closer together. Ideally most of components of the setup, including the pump syringes and microfluidic chip could have been placed in a biohazard cabinet at least while cell encapsulation was taken place to reduce the risk of cross contaminations for long term cell cultures and in vivo. Unfortunately this was not possible due to many factors: the size of the setup, the lack of funds to buy a cabinet and the limited availability of communal biohazard cabinets for sole use over prolonged periods.

References

(1) VL Workman, SB Dunnett, P Kille, DD Palmer: On-chip alginate microencapsulation of functional cells. Macromolecular Rapid Communications 29 (2008) 165-70.

(2) M Guvendiren, JA Burdick: Engineering synthetic hydrogel microenvironments to instruct stem cells. Current opinion in biotechnology 24 (2013) 841-46.

(3) AA Tomei, V Manzoli, CA Fraker, J Giraldo, D Velluto, M Najjar, A Pileggi, RD Molano, C Ricordi, CL Stabler, JA Hubbell: Device design and materials optimization of conformal coating for islets of Langerhans. Proceedings of the National Academy of Sciences of the United States of America 111 (2014) 10514-19.

(4) AP McGuigan, DA Bruzewicz, A Glavan, M Butte, GM Whitesides: Cell Encapsulation in Sub-mm Sized Gel Modules Using Replica Molding. PLoS ONE 3 (2008) e2258.

(5) Z-P Lum, M Krestow, IT Tai, I Vacek, AM Sun: Xenografts of Rat iselts into diabetic mice: An evaluation of new smaller capsules. Transplantation 53 (1992) 1180-83.

(6) WH Tan, S Takeuchi: Monodisperse alginate hydrogel microbeads for cell encapsulation. Advanced Materials 19 (2007) 2696-701.

(7) J Wan: Microfluidic-Based Synthesis of Hydrogel Particles for Cell Microencapsulation and Cell-Based Drug Delivery. Polymers 4 (2012) 1084.

(8) V Trivedi, ES Ereifej, A Doshi, P Sehgal, PJ VandeVord, AS Basu, Microfluidic encapsulation of cells in alginate capsules for high throughput screening, 2009 Annual International Conference of the IEEE Engineering in Medicine and Biology Society, 2009, p. 7037-40.

(9) F Chen, Y Zhan, T Geng, H Lian, P Xu, C Lu: Chemical Transfection of Cells in Picoliter Aqueous Droplets in Fluorocarbon Oil. Analytical Chemistry 83 (2011) 8816-20.

(10) J Clausell-Tormos, D Lieber, J-C Baret, A El-Harrak, OJ Miller, L Frenz, J Blouwolff, KJ Humphry, S KÃ¶ster, H Duan, C Holtze, DA Weitz, AD Griffiths, CA Merten: Droplet-Based Microfluidic Platforms for the Encapsulation and Screening of Mammalian Cells and Multicellular Organisms. Chemistry & Biology 15 (2008) 427-37.

(11) Y Morimoto, W-h Tan, Y Tsuda, S Takeuchi: Monodisperse semi-permeable microcapsules for continuous observation of cells. Lab on a Chip 9 (2009) 2217-23.

(12) S Hong, H-J Hsu, R Kaunas, J Kameoka: Collagen microsphere production on a chip. Lab on a Chip 12 (2012) 3277-80.

(13) VL Workman, Tezera, L. B., Elkington, P.T. and Jayasinghe, S. N.: Controlled generation of microspheres incorporating extracellular matrix fibrils for three-dimensional cell culture. Advanced Functional Materials 24 (2014) 2648-57.

(14) F Pampaloni, EG Reynaud, EHK Stelzer: The third dimension bridges the gap between cell culture and live tissue. Nature Reviews Molecular Cell Biology 8 (2007) 839-45.

(15) P Paszek: From measuring noise toward integrated single-cell biology. Frontiers in Genetics 5 (2014) 408.

(16) P Kaiser, M Werner, V Jérôme, H Hübner, R Buchholz, R Freitag: Cell retention by encapsulation for the cultivation of Jurkat cells in fixed and fluidized bed reactors. Biotechnology and Bioengineering 111 (2014) 2571-79.

(17) H Gurruchaga, L Saenz del Burgo, Js Ciriza, G Orive, RM HernÃ¡ndez, JL Pedraz: Advances in cell encapsulation technology and its application in drug delivery. Expert Opinion on Drug Delivery 0 (2015) 1-17.
(18) P Vinuselvi, S Park, M Kim, JM Park, T Kim, SK Lee: Microfluidic Technologies for Synthetic Biology. International Journal of Molecular Sciences 12 (2011) 3576-93.
(19) RB Elliott, L Escobar, PLJ Tan, M Muzina, S Zwain, C Buchanan: Live encapsulated porcine islets from a type 1 diabetic patient 9.5 yr after xenotransplantation. Xenotransplantation 14 (2007) 157-61.
(20) JP Vacanti, KM Kulig: Liver cell therapy and tissue engineering for transplantation. Seminars in Pediatric Surgery 23 (2014) 150-55.
(21) G Nicodemus, S Bryant: Cell encapsulation in biodegradable hydrogels for tissue engineering applications. Tissue Engineering. Part B, Reviews 14 (2008) 149-65.
(22) KY Lee, DJ Mooney: Hydrogels for Tissue Engineering. Chemical Reviews 101 (2001) 1869-80.
(23) AJE Kuijpers, G. H. M.; Feijen, J.; De Smedt, S. C.; Meyvis, T. K. L.; Demeester, J.; Krijgsveld, J.; Zaat, S. A. J.; Dankert, J: Characterization of the Network Structure of Carbodiimide Crosslinked Gelatin Gels American Chemical Society Journals 32 (1999) 3325-33.
(24) YSH Choi, Sung Ran; Lee, Young Moo; Song, Kang Won; Park, Moon Hyang; Nam, Young Soo Study on gelatin-containing artificial skin: I Preparation and characteristics of novel gelatin-alginate sponge American Chemical Society Journals 20 (1999) 409-17
(25) J Lee, C Kim: Surface tension driven microactuation based on continuous electrowetting. J. Microelectromech. Syst. 9 (2000) 171.
(26) O Smidsrød, G Skja˚k-Br↑k: Alginate as immobilization matrix for cells. Trends in Biotechnology 8 (1990) 71-78.
(27) I Rault, V Frei, D Herbage, N Abdul-Malak, A Huc: Evaluation of different chemical methods for cros-linking collagen gel, films and sponges. Journal of Materials Science: Materials in Medicine 7 (1996) 215-21.
(28) B Chevallay, N Abdul-Malak, D Herbage: Mouse fibroblasts in long-term culture within collagen three-dimensional scaffolds: Influence of crosslinking with diphenylphosphorylazide on matrix reorganization, growth, and biosynthetic and proteolytic activities. Journal of Biomedical Materials Research 49 (2000) 448-59.
(29) PM Kaufmann, S Heimrath, BS Kim, DJ Mooney: Highly porous polymer matrices as a three-dimensional culture system for hepatocytes. Cell Transplantation 6 (1997) 463-68.
(30) AOB Sherry L. Voytik-Harbin, Beverly Z. Waisner, J. Paul Robinson, and Carlton H. Lamar, D.V.M.: Small Intestinal Submucosa: A Tissue-Derived Extracellular Matrix That Promotes Tissue-Specific Growth and Differentiation of Cells in Vitro. 4 (1998) 157- 74.
(31) M Yamamoto, Y Tabata, Y Ikada: Growth Factor Release from Gelatin Hydrogel for Tissue Engineering. Journal of Bioactive and Compatible Polymers 14 (1999) 474-89.
(32) C Perka, R-S Spitzer, K Lindenhayn, M Sittinger, O Schultz: Matrix-mixed culture: New methodology for chondrocyte culture and preparation of cartilage transplants. Journal of Biomedical Materials Research 49 (2000) 305-11.
(33) ZG Ye Q, Benedikt P, Jockenhoevel S, Hoerstrup SP, Sakyama S, Hubbell JA, Turina M.: Fibrin gel as a three dimensional matrix in cardiovascular tissue engineering. European Journal of Cardio-Thoracic Surgery 17 (2000) 587-91.

(34) FK Ikari Y, Yee KO, Schwartz SM.: Alpha(1)-proteinase inhibitor, alpha(1)-antichymotrypsin, or alpha(2)-macroglobulin is required for vascular smooth muscle cell spreading in three-dimensional fibrin gel. The Journal of Biological Chemistry 275 (2000) 12799-805.
(35) M George, TE Abraham: Polyionic hydrocolloids for the intestinal delivery of protein drugs: Alginate and chitosan -- a review. Journal of Controlled Release 114 (2006) 1-14.
(36) PA Klöck G, Ryser C, Gröhn P, Kuttler B, Hahn HJ, Zimmermann U.: Biocompatibility of mannuronic acid-rich alginates. Biomaterials 18 (1997) 707-13.
(37) WR Gombotz, S Wee: Protein release from alginate matrices. Advanced Drug Delivery Reviews 31 (1998) 267-85.
(38) H Uludag, P De Vos, PA Tresco: Technology of mammalian cell encapsulation. Advanced Drug Delivery Reviews 42 (2000) 29-64.
(39) KY Lee, JA Rowley, P Eiselt, EM Moy, KH Bouhadir, DJ Mooney: Controlling Mechanical and Swelling Properties of Alginate Hydrogels Independently by Cross-Linker Type and Cross-Linking Density. Macromolecules 33 (2000) 4291-94.
(40) A Al-Shamkhani, R Duncan: Radioiodination of Alginate via Covalently-Bound Tyrosinamide Allows Monitoring of its Fate In Vivo. Journal of Bioactive and Compatible Polymers 10 (1995) 4-13.
(41) KH Bouhadir, DS Hausman, DJ Mooney: Synthesis of cross-linked poly(aldehyde guluronate) hydrogels. Polymer 40 (1999) 3575-84.
(42) A Haug, B Larsen, O Smidsrød: Studies on the Sequence of Uronic Acid Residues in Alginic Acid. Acta Chemica Scandinavica 21 (1967) 691- 704.
(43) A Haug, B Larsen, O Smidsrød: Qunantitative Determination of the Uronic Acid Composition of Alginates. Acta Chemica Scandinavica 16 (1962) 1908-18.
(44) S Sugawara, T Imai, M Otagiri: The Controlled Release of Prednisolone Using Alginate Gel. Pharmaceutical Research 11 (1994) 272-77.
(45) K Smetana: Cell biology of hydrogels. Biomaterials 14 (1993) 1046-50.
(46) KJ Sultzbaugh, TJ Speaker: A method to attach lectins to the surface of spermine alginate microcapsules based on the avidin biotin interaction. Journal of Microencapsulation 13 (1996) 363-76.
(47) JA Rowley, G Madlambayan, DJ Mooney: Alginate hydrogels as synthetic extracellular matrix materials. Biomaterials 20 (1999) 45-53.
(48) O Smidsrod, and Skjak-Brk, G.: Alginate as immobilization matrix for cells. Trends in Biotechnology 8 (1990) 71-78.
(49) JE Elliott, M Macdonald, J Nie, CN Bowman: Structure and swelling of poly(acrylic acid) hydrogels: effect of pH, ionic strength, and dilution on the crosslinked polymer structure. Polymer 45 (2004) 1503-10.
(50) S Lu, KS Anseth: Photopolymerization of multilaminated poly(HEMA) hydrogels for controlled release. Journal of Controlled Release 57 (1999) 291-300.
(51) A Kidane, JM Szabocsik, K Park: Accelerated study on lysozyme deposition on poly(HEMA) contact lenses. Biomaterials 19 (1998) 2051-55.
(52) MV Sefton, MH May, S Lahooti, JE Babensee: Making microencapsulation work: conformal coating, immobilization gels and in vivo performance. Journal of Controlled Release 65 (2000) 173-86.
(53) TKL Meyvis, SC De Smedt, J Demeester, WE Hennink: Influence of the Degradation Mechanism of Hydrogels on Their Elastic and Swelling Properties during Degradation. Macromolecules 33 (2000) 4717-25.

(54) DW Lim, SH Choi, TG Park: A new class of biodegradable hydrogels stereocomplexed by enantiomeric oligo(lactide) side chains of poly(HEMA-g-OLA)s. Macromolecular Rapid Communications 21 (2000) 464-71.
(55) M Heskins, JE Guillet: Solution Properties of Poly(N-isopropylacrylamide). Journal of Macromolecular Science: Part A - Chemistry 2 (1968) 1441-55.
(56) RA Stile, WR Burghardt, KE Healy: Synthesis and Characterization of Injectable Poly(N-isopropylacrylamide)-Based Hydrogels That Support Tissue Formation in Vitro. Macromolecules 32 (1999) 7370-79.
(57) LE Bromberg, ES Ron: Temperature-responsive gels and thermogelling polymer matrices for protein and peptide delivery. Advanced Drug Delivery Reviews 31 (1998) 197-221.
(58) KM Huh, J Hashi, T Ooya, N Yui: Synthesis and characterization of dextran grafted with poly(N-isopropylacrylamide-co-N,N-dimethyl-acrylamide). Macromolecular Chemistry and Physics 201 (2000) 613-19.
(59) BR Lentz: Special Issue Functional Dynamics of Lipids in Biomembranes Polymer-induced membrane fusion: potential mechanism and relation to cell fusion events. Chemistry and Physics of Lipids 73 (1994) 91-106.
(60) JL West, JA Hubbell: Polymeric Biomaterials with Degradation Sites for Proteases Involved in Cell Migration. Macromolecules 32 (1999) 241-44.
(61) B Jeong, YK Choi, YH Bae, G Zentner, SW Kim: New biodegradable polymers for injectable drug delivery systems. Journal of Controlled Release 62 (1999) 109-14.
(62) WS Dai, TA Barbari: Hydrogel membranes with mesh size asymmetry based on the gradient crosslinking of poly(vinyl alcohol). Journal of Membrane Science 156 (1999) 67-79.
(63) J Bo: Study on PVA hydrogel crosslinked by epichlorohydrin. Journal of Applied Polymer Science 46 (1992) 783-86.
(64) NA Peppas, SR Stauffer: Reinforced uncrosslinked poly (vinyl alcohol) gels produced by cyclic freezing-thawing processes: a short review. Journal of Controlled Release 16 (1991) 305-10.
(65) T Taguchi, A Kishida, M Akashi: Apatite formation on/in hydrogel matrices using an alternate soaking process: II. Effect of swelling ratios of poly(vinyl alcohol) hydrogel matrices on apatite formation. Journal of Biomaterials Science, Polymer Edition 10 (1999) 331-39.
(66) KE Uhrich, SM Cannizzaro, RS Langer, KM Shakesheff: Polymeric Systems for Controlled Drug Release. Chemical Reviews 99 (1999) 3181-98.
(67) AK Andrianov, LG Payne: Protein release from polyphosphazene matrices. Advanced Drug Delivery Reviews 31 (1998) 185-96.
(68) J Cappello, J Crissman, M Dorman, M Mikolajczak, G Textor, M Marquet, F Ferrari: Genetic Engineering of Structural Protein Polymers. Biotechnology Progress 6 (1990) 198-202.
(69) MT Krejchi, EDT Atkins, MJ Fournier, TL Mason, DA Tirrell: Observation of a Silk-Like Crystal Structure in a Genetically Engineered Periodic Polypeptide. Journal of Macromolecular Science, Part A 33 (1996) 1389-98.
(70) Y Temiz, RD Lovchik, GV Kaigala, E Delamarche: Lab-on-a-chip devices: How to close and plug the lab? Microelectronic Engineering 132 (2015) 156-75.
(71) SC Terry, JH Jerman, JB Angell: A gas chromatographic air analyzer fabricated on a silicon wafer. Electron Devices, IEEE Transactions on 26 (1979) 1880-86.
(72) GM Whitesides: The origins and the future of microfluidics. Nature 442 (2006) 368-73.

(73) H Bourbaba, CB achaiba, B Mohamed: Mechanical behavior of polymeric membrane: Comparison between PDMS and PMMA for micro fluidic application. Energy Procedia 36 (2013) 231-37.
(74) H Becker, C Gartner: Polymer microfabrication methods for microfluidic analytical applications. Electrophoresis 21 (2000) 12.
(75) T McCreedy: Fabrication techniques and materials commonly used for the production of microreactors and micro total analytical systems. TrAC Trends in Analytical Chemistry 19 (2000) 396-401.
(76) PDI Fletcher, SJ Haswell, E Pombo-Villar, BH Warrington, P Watts, SYF Wong, X Zhang: Micro reactors: principles and applications in organic synthesis. Tetrahedron 58 (2002) 4735-57.
(77) DWL Tolfree: Microfabrication using synchrotron radiation. Reports on Progress in Physics 61 (1998) 313.
(78) A Manz, N Graber, HM Widmer: Miniaturized total chemical analysis systems: A novel concept for chemical sensing. Sensors and Actuators B: Chemical 1 (1990) 244-48.
(79) DJ Beebe, GA Mensing, GM Walker: Physics and Applications of Microfluidics in Biology. Annual Review of Biomedical Engineering 4 (2002) 261-86.
(80) GM Whitesides: The origins and the future of microfluidics. Nature 442 (2006) 368-73.
(81) SK Sia, GM Whitesides: Microfluidic devices fabricated in poly (dimethylsiloxane) for biological studies. Electrophoresis 24 (2003) 3563-76.
(82) H Bourbaba, CB achaiba, B Mohamed: Mechanical Behavior of Polymeric Membrane: Comparison between PDMS and PMMA for Micro Fluidic Application. Energy Procedia 36 (2013) 231-37.
(83) H Becker, C Gärtner: Polymer microfabrication methods for microfluidic analytical applications. Electrophoresis 21 (2000) 12-26.
(84) BH Weigl, RL Bardell, CR Cabrera: Lab-on-a-chip for drug development. Advanced Drug Delivery Reviews 55 (2003) 349-77.
(85) H Andersson, A van den Berg: Microfluidic devices for cellomics: a review. Sensors and Actuators B: Chemical 92 (2003) 315-25.
(86) PM Valencia, OC Farokhzad, R Karnik, R Langer: Microfluidic technologies for accelerating the clinical translation of nanoparticles. Nat Nano 7 (2012) 623-29.
(87) O Reynolds: An Experimental Investigation of the Circumstances Which Determine Whether the Motion of Water Shall Be Direct or Sinuous, and of the Law of Resistance in Parallel Channels. Philosophical Transactions of the Royal Society of London 174 (1883) 935-82.
(88) B Zhao, JS Moore, DJ Beebe: Surface-directed liquid flow inside microchannels. Science 291 (2001) 1023-26.
(89) MWJ Prins, WJJ Welters, JW Weekamp: Fluid Control in Multichannel Structures by Electrocapillary Pressure. Science 291 (2001) 277-80.
(90) VPM van Empel, AT Bertrand, R van der Nagel, S Kostin, PA Doevendans, HJ Crijns, E de Wit, W Sluiter, SL Ackerman, LJ De Windt: Downregulation of apoptosis-inducing factor in harlequin mutant mice sensitizes the myocardium to oxidative stress-related cell death and pressure overload-induced decompensation. Circulation Research 96 (2005) e92-e101.
(91) PM Thieman William: Introduction to Biotechnology, Pearson Education, Inc, San Francisco 2004.
(92) C TM: Semipermeable Microcapsules. Science 146 (1964) 524-25.

(93) XL Wei Wang, Yubing Xie, Hua'an Zhang, Weiting Yu, Ying Xiong, Weiyang Xie and, X Ma: Microencapsulation using natural polysaccharides for drug delivery and cell
implantation. Materials Chemistry (2006) 3252-67.
(94) FLaA Sun: Microencapsulated islets as bioartificial endocrine pancreas Science 210 (1980) 908-10.
(95) GD Nicodemus, SJ Bryant: Cell Encapsulation in Biodegradable Hydrogels for Tissue Engineering Applications. Tissue Engineering. Part B, Reviews 14 (2008) 149-65.
(96) G Orive, Hernandez, R. M., Gascon, A. R., Calafiore, R., Chang, T. M. S., Vos, P. De., Hortelano, G., Hunkeler, D., Lacik, I., Shapiro, A. M. J. and Pedraz, Jose L.: Cell encapsulation: Promise and progress. Nat Med 9 (2003) 104-07.
(97) C-M Shi, and Cheng, T-M.: Differentiation of dermis-derived multipotent cells into insulin-producing pancreatic cells in vitro. World Journal of Gastroenterology : WJG 10 (2004) 2550-52.
(98) BD Ratner, SJ Bryant: Biomaterials: Where We Have Been and Where We Are Going. Annual Review of Biomedical Engineering 6 (2004) 41-75.
(99) L Gasperini, JF Mano, RL Reis: Natural polymers for the microencapsulation of cells. Journal of The Royal Society Interface 11 (2014).
(100) J-Y Leong, W-H Lam, K-W Ho, W-P Voo, MF-X Lee, H-P Lim, S-L Lim, B-T Tey, D Poncelet, E-S Chan: Advances in fabricating spherical alginate hydrogels with controlled particle designs by ionotropic gelation as encapsulation systems. Particuology 24 (2016) 44-60.
(101) DR Buddy, JB Stephanie: Biomaterials: Where We Have Been and Where We Are Going. Annual Review of Biomedical Engineering 6 (2004) 41-75.
(102) RPL Willem M. Kühtreiber, William Louis Chick: Cell encapsulation technology and therapeutics Boston: Birkhäuser.
(103) J Schrezenmeir, J Kirchgessner, L Gerö, LA Kunz, J Beyer, W Mueller-Klieser: Effect of microencapsulation on oxygen distribution in islets organs. Transplantation 57 (1994) 1308-14.
(104) P de Vos, MM Faas, B Strand, R Calafiore: Alginate-based microcapsules for immunoisolation of pancreatic islets. Biomaterials 27 (2006) 5603-17.
(105) S Sakai, K Kawabata, T Ono, H Ijima, K Kawakami: Development of mammalian cell-enclosing subsieve-size agarose capsules (<100 μm) for cell therapy. Biomaterials 26 (2005) 4786-92.
(106) X Ma, I Vacek, A Sun: Generation of Alginate-Poly-L-Lysine-Alginate (APA) Biomicrocapsules: the Relationship Between the Membrane Strength and the Reaction Conditions. Artificial Cells, Blood Substitutes, and Biotechnology 22 (1994) 43-69.
(107) P De Vos, B De Haan, J Pater, R Van Schilfgaarde: Association between capsule diameter, adequacy of encapsulation, and survival of microencapsulated rat iselt allografts1. Transplantation 62 (1996) 893-99.
(108) S Sakai, C Mu, K Kawabata, I Hashimoto, K Kawakami: Biocompatibility of subsieve-size capsules versus conventional-size microcapsules. Journal of Biomedical Materials Research Part A 78A (2006) 394-98.
(109) R Robitaille, J-F Pariseau, FA Leblond, M Lamoureux, Y Lepage, J-P Hallé: Studies on small (<350 μm) alginate-poly-L-lysine microcapsules. III. Biocompatibility of smaller versus standard microcapsules. Journal of Biomedical Materials Research 44 (1999) 116-20.

(110) DI Zeugolis, RG Paul, G Attenburrow: Post-self-assembly experimentation on extruded collagen fibres for tissue engineering applications. Acta Biomaterialia 4 (2008) 1646-56.
(111) JM Pachence: Collagen-based devices for soft tissue repair. Journal of Biomedical Materials Research 33 (1996) 35-40.
(112) S Ber, G Torun KÃ¶se, V HasÄ±rcÄ±: Bone tissue engineering on patterned collagen films: an in vitro study. Biomaterials 26 (2005) 1977-86.
(113) M van der Rest, R Garrone: Collagen family of proteins. The FASEB Journal 5 (1991) 2814-23.
(114) A El-Fiqi, JH Lee, E-J Lee, H-W Kim: Collagen hydrogels incorporated with surface-aminated mesoporous nanobioactive glass: Improvement of physicochemical stability and mechanical properties is effective for hard tissue engineering. Acta Biomaterialia 9 (2013) 9508-21.
(115) KS Weadock, EJ Miller, EL Keuffel, MG Dunn: Effect of physical crosslinking methods on collagen-fiber durability in proteolytic solutions. Journal of Biomedical Materials Research 32 (1996) 221-26.
(116) S Pulapura, J Kohn: Trends in the Development of Bioresorbable Polymers for Medical Applications. Journal of Biomaterials Applications 6 (1992) 216-50.
(117) AJ Kuijpers, GHM Engbers, J Feijen, SC De Smedt, TKL Meyvis, J Demeester, J Krijgsveld, SAJ Zaat, J Dankert: Characterization of the Network Structure of Carbodiimide Cross-Linked Gelatin Gels. Macromolecules 32 (1999) 3325-33.
(118) AS Hoffman: "Intelligent" polymers in medicine and biotechnology. Macromolecular Symposia 98 (1995) 645-64.
(119) S Sakai, S Ito, H Inagaki, K Hirose, T Matsuyama, M Taya, K Kawakami: Cell-enclosing gelatin-based microcapsule production for tissue engineering using a microfluidic flow-focusing system. Biomicrofluidics 5 (2011) 013402.
(120) CM Hwang, S Sant, M Masaeli, NN Kachouie, B Zamanian, S-H Lee, A Khademhosseini: Fabrication of three-dimensional porous cell-laden hydrogel for tissue engineering. Biofabrication 2 (2010) 035003-03.
(121) D Rana, TSS Kumar, M Ramalingam: Cell-Laden Hydrogels for Tissue Engineering. Journal of Biomaterials and Tissue Engineering 4 (2014) 507-35.
(122) YS Choi, SR Hong, YM Lee, KW Song, MH Park, YS Nam: Study on gelatin-containing artificial skin: I. Preparation and characteristics of novel gelatin-alginate sponge. Biomaterials 20 (1999) 409-17.
(123) AI Van Den Bulcke, B Bogdanov, N De Rooze, EH Schacht, M Cornelissen, H Berghmans: Structural and Rheological Properties of Methacrylamide Modified Gelatin Hydrogels. Biomacromolecules 1 (2000) 31-38.
(124) TC Laurent, JR Fraser: Hyaluronan. The FASEB Journal 6 (1992) 2397-404.
(125) A Shiedlin, R Bigelow, W Christopher, S Arbabi, L Yang, RV Maier, N Wainwright, A Childs, RJ Miller: Evaluation of Hyaluronan from Different Sources:â€‰ Streptococcus zooepidemicus, Rooster Comb, Bovine Vitreous, and Human Umbilical Cord. Biomacromolecules 5 (2004) 2122-27.
(126) G Kogan, L Šoltés, R Stern, P Gemeiner: Hyaluronic acid: a natural biopolymer with a broad range of biomedical and industrial applications. Biotechnology Letters 29 (2007) 17-25.
(127) EA Balazs: Viscosupplementation for treatment of osteoarthritis: from initial discovery to current status and results. Surgical technology international 12 (2004) 278-89.
(128) YS Choi, SR Hong, YM Lee, KW Song, MH Park, YS Nam: Studies on gelatin-containing artificial skin: II. Preparation and characterization of cross-linked

gelatin-hyaluronate sponge. Journal of Biomedical Materials Research 48 (1999) 631-39.
(129) Y Yeo, CB Highley, E Bellas, T Ito, R Marini, R Langer, DS Kohane: In situ cross-linkable hyaluronic acid hydrogels prevent post-operative abdominal adhesions in a rabbit model. Biomaterials 27 (2006) 4698-705.
(130) J Necas, L Bartosikova, P Brauner, J Kolar: Hyaluronic acid (hyaluronan): a review. Veterinarni Medicina 53 (2008) 397–411.
(131) MN Collins, C Birkinshaw: Comparison of the effectiveness of four different crosslinking agents with hyaluronic acid hydrogel films for tissue-culture applications. Journal of Applied Polymer Science 104 (2007) 3183-91.
(132) SK Seidlits, ZZ Khaing, RR Petersen, JD Nickels, JE Vanscoy, JB Shear, CE Schmidt: The effects of hyaluronic acid hydrogels with tunable mechanical properties on neural progenitor cell differentiation. Biomaterials 31 (2010) 3930-40.
(133) SA Bencherif, A Srinivasan, F Horkay, JO Hollinger, K Matyjaszewski, NR Washburn: Influence of the degree of methacrylation on hyaluronic acid hydrogels properties. Biomaterials 29 (2008) 1739-49.
(134) YD Park, N Tirelli, JA Hubbell: Photopolymerized hyaluronic acid-based hydrogels and interpenetrating networks. Biomaterials 24 (2003) 893-900.
(135) IL Kim, RL Mauck, JA Burdick: Hydrogel design for cartilage tissue engineering: A case study with hyaluronic acid. Biomaterials 32 (2011) 8771-82.
(136) C Chung, JA Burdick: Influence of 3D Hyaluronic Acid Microenvironments on Mesenchymal Stem Cell Chondrogenesis. Tissue engineering. Part A 15 (2009) 243-54.
(137) MW Mosesson: Fibrinogen and fibrin structure and functions. Journal of Thrombosis and Haemostasis 3 (2005) 1894-904.
(138) AO Oseni, PE Butler, AM Seifalian, in J. Basu, W.J. Ludlow (Eds.), Organ Regeneration: Methods and Protocols. Humana Press, Totowa, NJ, 2013, p. 145-52.
(139) JW Weisel, Advances in Protein Chemistry. Academic Press, 2005, p. 247-99.
(140) RI Litvinov, OV Gorkun, SF Owen, H Shuman, JW Weisel: Polymerization of fibrin: specificity, strength, and stability of knob-hole interactions studied at the single-molecule level. Blood 106 (2005) 2944-51.
(141) STB Ho, SM Cool, JH Hui, DW Hutmacher: The influence of fibrin based hydrogels on the chondrogenic differentiation of human bone marrow stromal cells. Biomaterials 31 (2010) 38-47.
(142) SL Rowe, S Lee, JP Stegemann: Influence of thrombin concentration on the mechanical and morphological properties of cell-seeded fibrin hydrogels. Acta Biomaterialia 3 (2007) 59-67.
(143) I Catelas, N Sese, BM Wu, JCY Dunn, SAM Helgerson, B Tawil: Human mesenchymal stem cell proliferation and osteogenic differentiation in fibrin gels in vitro. Tissue engineering 12 (2006) 2385-96.
(144) Q Ye, G Zünd, P Benedikt, S Jockenhoevel, SP Hoerstrup, S Sakyama, JA Hubbell, M Turina: Fibrin gel as a three dimensional matrix in cardiovascular tissue engineering. European Journal of Cardio-Thoracic Surgery 17 (2000) 587-91.
(145) KM Lorentz, S Kontos, P Frey, JA Hubbell: Engineered aprotinin for improved stability of fibrin biomaterials. Biomaterials 32 (2011) 430-38.
(146) Y Ikari, K Fujikawa, KO Yee, SM Schwartz: α1-Proteinase Inhibitor, α1-Antichymotrypsin, or α2-Macroglobulin Is Required for Vascular Smooth Muscle Cell Spreading in Three-dimensional Fibrin Gel. Journal of Biological Chemistry 275 (2000) 12799-805.

(147) A Fu, C Spence, A Scherer, F Arnold, S Quake: A microfabricated fluorescence-activated cell sorter. Nat. Biotechnol. 17 (1999) 1109.
(148) R Meena, AK Siddhanta, K Prasad, BK Ramavat, K Eswaran, S Thiruppathi, M Ganesan, VA Mantri, PVS Rao: Preparation, characterization and benchmarking of agarose from Gracilaria dura of Indian waters. Carbohydrate Polymers 69 (2007) 179-88.
(149) PL Indovina, E Tettamanti, MS Micciancio-Giammarinaro, MU Palma: Thermal hysteresis and reversibility of gel–sol transition in agarose–water systemsa. The Journal of Chemical Physics 70 (1979) 2841-47.
(150) N Pernodet, M Maaloum, B Tinland: Pore size of agarose gels by atomic force microscopy. ELECTROPHORESIS 18 (1997) 55-58.
(151) J Narayanan, J-Y Xiong, X-Y Liu, Determination of agarose gel pore size: Absorbance measurements vis a vis other techniques, Journal of Physics: Conference Series. IOP Publishing, 2006, p. 83.
(152) P Aymard, DR Martin, K Plucknett, TJ Foster, AH Clark, IT Norton: Influence of thermal history on the structural and mechanical properties of agarose gels. Biopolymers 59 (2001) 131-44.
(153) S Tang, W Yang, X Mao: Agarose/collagen composite scaffold as an anti-adhesive sheet. Biomedical Materials 2 (2007) S129.
(154) G Karoubi, ML Ormiston, DJ Stewart, DW Courtman: Single-cell hydrogel encapsulation for enhanced survival of human marrow stromal cells. Biomaterials 30 (2009) 5445-55.
(155) A Guaccio, C Borselli, O Oliviero, PA Netti: Oxygen consumption of chondrocytes in agarose and collagen gels: a comparative analysis. Biomaterials 29 (2008) 1484-93.
(156) W-J Chi, Y-K Chang, S-K Hong: Agar degradation by microorganisms and agar-degrading enzymes. Applied Microbiology and Biotechnology 94 (2012) 917-30.
(157) L-M Zhang, C-X Wu, J-Y Huang, X-H Peng, P Chen, S-Q Tang: Synthesis and characterization of a degradable composite agarose/HA hydrogel. Carbohydrate Polymers 88 (2012) 1445-52.
(158) PJ Emans, LW van Rhijn, TJM Welting, A Cremers, N Wijnands, F Spaapen, JW Voncken, VP Shastri: Autologous engineering of cartilage. Proceedings of the National Academy of Sciences 107 (2010) 3418-23.
(159) PD Benya, JD Shaffer: Dedifferentiated chondrocytes reexpress the differentiated collagen phenotype when cultured in agarose gels. Cell 30 (1982) 215-24.
(160) RL Mauck, SL Seyhan, GA Ateshian, CT Hung: Influence of seeding density and dynamic deformational loading on the developing structure/function relationships of chondrocyte-seeded agarose hydrogels. Annals of biomedical engineering 30 (2002) 1046-56.
(161) EB Hunziker: Articular cartilage repair: basic science and clinical progress. A review of the current status and prospects. Osteoarthritis and cartilage 10 (2002) 432-63.
(162) M Rinaudo, G Pavlov, J Desbrieres: Influence of acetic acid concentration on the solubilization of chitosan. Polymer 40 (1999) 7029-32.
(163) MNVR Kumar: A review of chitin and chitosan applications. Reactive and functional polymers 46 (2000) 1-27.
(164) M Hayes, B Carney, J Slater, W BrÃ¼ck: Mining marine shellfish wastes for bioactive molecules: Chitin and chitosan ndash; Part A: extraction methods. Biotechnology journal 3 (2008) 871-77.

(165) X Fei Liu, Y Lin Guan, D Zhi Yang, Z Li, K De Yao: Antibacterial action of chitosan and carboxymethylated chitosan. Journal of Applied Polymer Science 79 (2001) 1324-35.
(166) A Percot, C Viton, A Domard: Optimization of chitin extraction from shrimp shells. Biomacromolecules 4 (2003) 12-18.
(167) GV Martins, EG Merino, JF Mano, NM Alves: Crosslink Effect and Albumin Adsorption onto Chitosan/Alginate Multilayered Systems: An in situ QCMâ€ D Study. Macromolecular bioscience 10 (2010) 1444-55.
(168) GV Martins, JF Mano, NM Alves: Dual responsive nanostructured surfaces for biomedical applications. Langmuir 27 (2011) 8415-23.
(169) NL Costa, P Sher, JF Mano: Liquefied capsules coated with multilayered polyelectrolyte films for cell immobilization. Advanced Engineering Materials 13 (2011) B218-B24.
(170) CR Correia, RL Reis, JF Mano: Multilayered hierarchical capsules providing cell adhesion sites. Biomacromolecules 14 (2013) 743-51.
(171) CR Correia, P Sher, RL Reis, JF Mano: Liquified chitosan–alginate multilayer capsules incorporating poly (L-lactic acid) microparticles as cell carriers. Soft Matter 9 (2013) 2125-30.
(172) K Tomihata, Y Ikada: In vitro and in vivo degradation of films of chitin and its deacetylated derivatives. Biomaterials 18 (1997) 567-75.
(173) T Freier, HS Koh, K Kazazian, MS Shoichet: Controlling cell adhesion and degradation of chitosan films by N-acetylation. Biomaterials 26 (2005) 5872-78.
(174) C Chatelet, O Damour, A Domard: Influence of the degree of acetylation on some biological properties of chitosan films. Biomaterials 22 (2001) 261-68.
(175) A Chenite, M Buschmann, D Wang, C Chaput, N Kandani: Rheological characterisation of thermogelling chitosan/glycerol-phosphate solutions. Carbohydrate Polymers 46 (2001) 39-47.
(176) A Chenite, C Chaput, D Wang, C Combes, MD Buschmann, CD Hoemann, JC Leroux, BL Atkinson, F Binette, A Selmani: Novel injectable neutral solutions of chitosan form biodegradable gels in situ. Biomaterials 21 (2000) 2155-61.
(177) DS Couto, Z Hong, JF Mano: Development of bioactive and biodegradable chitosan-based injectable systems containing bioactive glass nanoparticles. Acta Biomaterialia 5 (2009) 115-23.
(178) JF Mano, GA Silva, HS Azevedo, PB Malafaya, RA Sousa, SS Silva, LF Boesel, JM Oliveira, TC Santos, AP Marques: Natural origin biodegradable systems in tissue engineering and regenerative medicine: present status and some moving trends. Journal of The Royal Society Interface 4 (2007) 999-1030.
(179) R Jayakumar, M Prabaharan, RL Reis, J Mano: Graft copolymerized chitosan-present status and applications. Carbohydrate Polymers 62 (2005) 142-58.
(180) G Klöck, A Pfeffermann, C Ryser, P Gröhna, B Kuttler, H-J Hahn, U Zimmermann: Biocompatibility of mannuronic acid-rich alginates. Biomaterials 18 (1997) 707-13.
(181) H Uludag, P De Vos, PA Tresco: Technology of mammalian cell encapsulation. Advanced Drug Delivery Reviews 42 (2000) 29-64.
(182) P Sánchez, RM Hernández, JL Pedraz, G Orive: Encapsulation of cells in alginate gels. Immobilization of Enzymes and Cells: Third Edition (2013) 313-25.
(183) AnJ Ribeiro, C Silva, D Ferreira, F Veiga: Chitosan-reinforced alginate microspheres obtained through the emulsification/internal gelation technique. European Journal of Pharmaceutical Sciences 25 (2005) 31-40.

(184) D Poncelet, R Lencki, C Beaulieu, JP Halle, RJ Neufeld, A Fournier: Production of alginate beads by emulsification/internal gelation. I. Methodology. Applied Microbiology and Biotechnology 38 (1992) 39-45.
(185) D Quong, RJ Neufeld, G Skjåk-Bræk, D Poncelet: External versus internal source of calcium during the gelation of alginate beads for DNA encapsulation. Biotechnology and Bioengineering 57 (1998) 438-46.
(186) S Mazzitelli, A Tosi, C Balestra, C Nastruzzi, G Luca, F Mancuso, R Calafiore, M Calvitti: Production and characterization of alginate microcapsules produced by a vibrational encapsulation device. Journal of Biomaterials Applications (2008).
(187) GF Christopher, SL Anna: Microfluidic methods for generating continuous droplet streams. Journal of Physics D: Applied Physics 40 (2007) R319.
(188) L Rosenfeld, T Lin, R Derda, SY Tang: Review and analysis of performance metrics of droplet microfluidics systems. Microfluidics and Nanofluidics 16 (2014) 921-39.
(189) JAM Rowley, Gerard; Mooneyb, David J. : Alginate hydrogels as synthetic extracellular matrix materials Biomaterials 20 (1999) 45-53
(190) CS Wang, Russell J.; Kopecek, Jindrich: Hybrid hydrogels assembled from synthetic polymers and coiled-coil protein domains

397 (1999) 417-20
(191) A Ros: Microfluidics in cell analysis Analytical and Bioanalytical Chemistry 390 (2007) 799-800.
(192) S Mazzitelli, M Borgatti, G Breveglieri, R Gambari, C Nastruzzi: Encapsulation of eukaryotic cells in alginate microparticles: cell signaling by TNF-alpha through capsular structure of cystic fibrosis cells. Journal of cell communication and signaling 5 (2011) 157-65.
(193) S Mazzitelli, L Capretto, F Quinci, R Piva, C Nastruzzi: Preparation of cell-encapsulation devices in confined microenvironment. Advanced Drug Delivery Reviews 65 (2013) 1533-55.
(194) P De Vos, B De Haan, R Van Schilfgaarde: Effect of the alginate composition on the biocompatibility of alginate-polylysine microcapsules. Biomaterials 18 (1997) 273-78.
(195) D Di Carlo, N Aghdam, LP Lee: Single-Cell Enzyme Concentrations, Kinetics, and Inhibition Analysis Using High-Density Hydrodynamic Cell Isolation Arrays. Analytical Chemistry 78 (2006) 4925-30.
(196) MJ Rosenbluth, WA Lam, DA Fletcher: Force microscopy of nonadherent cells: A comparison of leukemia cell deformability. Biophysical Journal 90 (2006) 2994-3003.
(197) KK Rozman, J Doull: Dose and time as variables of toxicity. Toxicology 144 (2000) 169-78.
(198) B Jeong, SW Kim, YH Bae: Thermosensitive sol–gel reversible hydrogels. Advanced Drug Delivery Reviews 54 (2002) 37-51.
(199) D Roy, WLA Brooks, BS Sumerlin: New directions in thermoresponsive polymers. Chemical Society Reviews 42 (2013) 7214-43.
(200) L Klouda, AG Mikos: Thermoresponsive hydrogels in biomedical applications. European Journal of Pharmaceutics and Biopharmaceutics 68 (2008) 34-45.
(201) MA Ward, TK Georgiou: Thermoresponsive polymers for biomedical applications. Polymers 3 (2011) 1215-42.
(202) EA Bekturov, LA Bimendina, Speciality Polymers. Springer, 1981, p. 99-147.

(203) ÝA Mørch, D Ivan, BL Strand, G Skjåk-Bræk: Effect of Ca2+, Ba2+, and Sr2+ on alginate microbeads. Biomacromolecules 7 (2006) 1471-80.
(204) CK Kuo, PX Ma: Ionically crosslinked alginate hydrogels as scaffolds for tissue engineering: part 1. Structure, gelation rate and mechanical properties. Biomaterials 22 (2001) 511-21.
(205) E Amici, G Tetradis-Meris, CP de Torres, F Jousse: Alginate gelation in microfluidic channels. Food Hydrocolloids 22 (2008) 97-104.
(206) L Liu, F Wu, X-J Ju, R Xie, W Wang, CH Niu, L-Y Chu: Preparation of monodisperse calcium alginate microcapsules via internal gelation in microfluidic-generated double emulsions. Journal of colloid and interface science 404 (2013) 85-90.
(207) H Zhang, E Tumarkin, R Peerani, Z Nie, RMA Sullan, GC Walker, E Kumacheva: Microfluidic Production of Biopolymer Microcapsules with Controlled Morphology. Journal of the American Chemical Society 128 (2006) 12205-10.
(208) S-Y Cheng, I Constantinidis, A Sambanis: Insulin secretion dynamics of free and alginate-encapsulated insulinoma cells. Cytotechnology 51 (2006) 159-70.
(209) G Skjåk-Bræk, H Grasdalen, O Smidsrød: Inhomogeneous polysaccharide ionic gels. Carbohydrate Polymers 10 (1989) 31-54.
(210) LW Chan, HY Lee, PWS Heng: Mechanisms of external and internal gelation and their impact on the functions of alginate as a coat and delivery system. Carbohydrate Polymers 63 (2006) 176-87.
(211) JM Radovich: Mass transfer effects in fermentations using immobilized whole cells. Enzyme and microbial technology 7 (1985) 2-10.
(212) MC Annesini, G Castelli, F Conti, LC De Virgiliis, L Marrelli, A Miccheli, E Satori: Transport and consumption rate of O2 in alginate gel beads entrapping hepatocytes. Biotechnology Letters 22 (2000) 865-70.
(213) RWJ Lencki, RJ Neufeld, T Spinney, Method of producing microspheres. Google Patents, 1989.
(214) H Song, W Yu, M Gao, X Liu, X Ma: Microencapsulated probiotics using emulsification technique coupled with internal or external gelation process. Carbohydrate Polymers 96 (2013) 181-89.
(215) D Poncelet, BP De Smet, C Beaulieu, ML Huguet, A Fournier, RJ Neufeld: Production of alginate beads by emulsification/internal gelation. II. Physicochemistry. Applied Microbiology and Biotechnology 43 (1995) 644-50.
(216) H Liu, G Li, X Sun, Y He, S Sun, H Ma: Microfluidic generation of uniform quantum dot-encoded microbeads by gelation of alginate. RSC Advances 5 (2015) 62706-12.
(217) MN Singh, KSY Hemant, M Ram, HG Shivakumar: Microencapsulation: a promising technique for controlled drug delivery. Research in pharmaceutical sciences 5 (2011) 65-77.
(218) U Prüsse, L Bilancetti, M Bučko, B Bugarski, J Bukowski, P Gemeiner, D Lewińska, V Manojlovic, B Massart, C Nastruzzi: Comparison of different technologies for alginate beads production. Chemical Papers 62 (2008) 364-74.
(219) E Santos, G Orive, A Calvo, R Catena, P Fernández-Robredo, AG Layana, RM Hernández, JL Pedraz: Optimization of 100 μm alginate-poly-l-lysine-alginate capsules for intravitreous administration. Journal of Controlled Release 158 (2011) 443-50.
(220) H Brandenberger, D Nüssli, V Piëch, F Widmer: Monodisperse particle production: A method to prevent drop coalescence using electrostatic forces. Journal of Electrostatics 45 (1999) 227-38.

(221) E Cukierman, R Pankov, KM Yamada: Cell interactions with three-dimensional matrices. Current Opinion in Cell Biology 14 (2002) 633-40.
(222) RD Levit, N Landázuri, EA Phelps, ME Brown, AJ García, ME Davis, G Joseph, R Long, SA Safley, JD Suever, AN Lyle, CJ Weber, WR Taylor: Cellular encapsulation enhances cardiac repair. Journal of the American Heart Association 2 (2013).
(223) L Zhu, Y Li, Q Zhang, H Wang, M Zhu: Fabrication of monodisperse, large-sized, functional biopolymeric microspheres using a low-cost and facile microfluidic device. Biomedical microdevices 12 (2010) 169-77.
(224) S Sugiura, M Nakajima, N Kumazawa, S Iwamoto, M Seki: Characterization of spontaneous transformation-based droplet formation during microchannel emulsification. The Journal of Physical Chemistry B 106 (2002) 9405-09.
(225) I Cohen, H Li, JL Hougland, M Mrksich, SR Nagel: Using selective withdrawal to coat microparticles. Science 292 (2001) 265-67.
(226) K-S Huang, T-H Lai, Y-C Lin: Manipulating the generation of Ca-alginate microspheres using microfluidic channels as a carrier of gold nanoparticles. Lab on a Chip 6 (2006) 954-57.
(227) DK Hwang, J Oakey, M Toner, JA Arthur, KS Anseth, S Lee, A Zeiger, KJ Van Vliet, PS Doyle: Stop-flow lithography for the production of shape-evolving degradable microgel particles. Journal of the American Chemical Society 131 (2009) 4499-504.
(228) CN Baroud, H Willaime: Multiphase flows in microfluidics. Comptes Rendus Physique 5 (2004) 547-55.
(229) D Dendukuri, K Tsoi, TA Hatton, PS Doyle: Controlled synthesis of nonspherical microparticles using microfluidics. Langmuir 21 (2005) 2113-16.
(230) C-H Yang, K-S Huang, J-Y Chang: Manufacturing monodisperse chitosan microparticles containing ampicillin using a microchannel chip. Biomedical microdevices 9 (2007) 253-59.
(231) S Shin, JS Hong, K-H Lee, S-H Lee: Oil-free generation of small polymeric particles using a coaxial microfluidic channel. Langmuir 25 (2009) 12361-66.
(232) CN Baroud, F Gallaire, R Dangla: Dynamics of microfluidic droplets. Lab on a Chip 10 (2010) 2032-45.
(233) Y Hu, Q Wang, J Wang, J Zhu, H Wang, Y Yang: Shape controllable microgel particles prepared by microfluidic combining external ionic crosslinking. Biomicrofluidics 6 (2012) 026502.
(234) T Nisisako, T Torii, T Higuchi: Novel microreactors for functional polymer beads. Chemical Engineering Journal 101 (2004) 23-29.
(235) M De Menech, P Garstecki, F Jousse, HA Stone: Transition from squeezing to dripping in a microfluidic T-shaped junction. journal of fluid mechanics 595 (2008) 141-61.
(236) T Glawdel, C Elbuken, CL Ren: Droplet formation in microfluidic T-junction generators operating in the transitional regime. I. Experimental observations. Physical Review E 85 (2012) 016322.
(237) A Gupta, SMS Murshed, R Kumar: Droplet formation and stability of flows in a microfluidic T-junction. Applied physics letters 94 (2009) 164107.
(238) N Tarchichi, F Chollet, J-Fo Manceau: New regime of droplet generation in a T-shape microfluidic junction. Microfluidics and Nanofluidics 14 (2013) 45-51.
(239) M Zhang, J Wu, L Wang, K Xiao, W Wen: A simple method for fabricating multi-layer PDMS structures for 3D microfluidic chips. Lab on a Chip 10 (2010) 1199-203.

(240) J Lim, F Maes, Vr Taly, J-C Baret: The microfluidic puzzle: chip-oriented rapid prototyping. Lab on a Chip 14 (2014) 1669-72.
(241) C-H Choi, J-H Jung, YW Rhee, D-P Kim, S-E Shim, C-S Lee: Generation of monodisperse alginate microbeads and in situ encapsulation of cell in microfluidic device. Biomedical microdevices 9 (2007) 855-62.
(242) L Capretto, S Mazzitelli, C Balestra, A Tosi, C Nastruzzi: Effect of the gelation process on the production of alginate microbeads by microfluidic chip technology. Lab on a Chip 8 (2008) 617-21.
(243) L Capretto, S Mazzitelli, G Luca, C Nastruzzi: Preparation and characterization of polysaccharidic microbeads by a microfluidic technique: application to the encapsulation of Sertoli cells. Acta Biomaterialia 6 (2010) 429-35.
(244) E Um, D-S Lee, H-B Pyo, J-K Park: Continuous generation of hydrogel beads and encapsulation of biological materials using a microfluidic droplet-merging channel. Microfluidics and Nanofluidics 5 (2008) 541-49.
(245) M-H Wu, W-C Pan: Development of microfluidic alginate microbead generator tunable by pulsed airflow injection for the microencapsulation of cells. Microfluidics and Nanofluidics 8 (2010) 823-35.
(246) J Hong, SN Jayasinghe: Bio-electrospraying and droplet-based microfluidics: control of cell numbers within living residues. Biomedical Materials 5 (2010) 021001.
(247) C Kim, KS Lee, YE Kim, K-J Lee, SH Lee, TS Kim, JY Kang: Rapid exchange of oil-phase in microencapsulation chip to enhance cell viability. Lab on a Chip 9 (2009) 1294-97.
(248) H Shintaku, T Kuwabara, S Kawano, T Suzuki, I Kanno, H Kotera: Micro cell encapsulation and its hydrogel-beads production using microfluidic device. Microsystem technologies 13 (2007) 951-58.
(249) VL Workman, SB Dunnett, P Kille, DD Palmer: Microfluidic chip-based synthesis of alginate microspheres for encapsulation of immortalized human cells. Biomicrofluidics 1 (2007) 014105.
(250) RK Shah, HC Shum, AC Rowat, D Lee, JJ Agresti, AS Utada, L-Y Chu, J-W Kim, A Fernandez-Nieves, CJ Martinez: Designer emulsions using microfluidics. Materials Today 11 (2008) 18-27.
(251) AS Utada, LY Chu, A Fernandez-Nieves, DR Link, C Holtze, DA Weitz: Dripping, jetting, drops, and wetting: the magic of microfluidics. Mrs Bulletin 32 (2007) 702-08.
(252) CJ Martinez, JW Kim, C Ye, I Ortiz, AC Rowat, M Marquez, D Weitz: A microfluidic approach to encapsulate living cells in uniform alginate hydrogel microparticles. Macromolecular bioscience 12 (2012) 946-51.
(253) S Hjertén, J-l Liao: High-performance liquid chromatography of proteins on compressed, non-porous agarose beads: I. Hydrophobic-interaction chromatography. Journal of Chromatography A 457 (1988) 165-74.
(254) S Lahooti, MV Sefton: Effect of an immobilization matrix and capsule membrane permeability on the viability of encapsulated HEK cells. Biomaterials 21 (2000) 987-95.
(255) D Luo, SR Pullela, M Marquez, Z Cheng: Cell encapsules with tunable transport and mechanical properties. Biomicrofluidics 1 (2007) 034102.
(256) Y-J Eun, AS Utada, MF Copeland, S Takeuchi, DB Weibel: Encapsulating bacteria in agarose microparticles using microfluidics for high-throughput cell analysis and isolation. ACS chemical biology 6 (2010) 260-66.

(257) A Kumachev, J Greener, E Tumarkin, E Eiser, PW Zandstra, E Kumacheva: High-throughput generation of hydrogel microbeads with varying elasticity for cell encapsulation. Biomaterials 32 (2011) 1477-83.
(258) Y Yang, G Zhang, Y Hong, Z Gu, F Fang: Calcium cation triggers and accelerates the gelation of high methoxy pectin. Food Hydrocolloids 32 (2013) 228-34.
(259) U Schneider, Schwenk, H., and Bornkamm, G.: Characterization of EBV-genome negative "null" and "T" cell lines derived from children with acute lymphoblastic leukemia and leukemic transformed non-Hodgkin lymphoma. International Journal of Cancer 19 (1977) 621-26.
(260) J Ge, DK Wood, DM Weingeist, S Prasongtanakij, P Navasumrit, M Ruchirawat, BP Engelward: Standard fluorescent imaging of live cells is highly genotoxic. Cytometry Part A 83A (2013) 552-60.
(261) DLCaT Schroeder: Probing cellular processes by long-term live imaging – historic problems and current solutions. journal of Cell Science 126 (2013) 3805-15.
(262) HPJ Bonarius, CD de Gooijer, J Tramper, G Schmid: Determination of the respiration quotient in mammalian cell culture in bicarbonate buffered media. Biotechnology and Bioengineering 45 (1995) 524-35.
(263) H Eagle: Buffer Combinations for Mammalian Cell Culture. Science 174 (1971) 500-03.
(264) MJ Bissell, DC Radisky, A Rizki, VM Weaver, OW Petersen: The organizing principle: microenvironmental influences in the normal and malignant breast. Differentiation 70 (2002) 537-46.
(265) KY Lee, DJ Mooney: Alginate: properties and biomedical applications. Progress in polymer science 37 (2012) 106-26.
(266) W Strober, Current Protocols in Immunology. John Wiley & Sons, Inc., 2001.
(267) JP Magyar, M Nemir, E Ehler, N Suter, J-C Perriard, HM Eppenberger: Mass Production of Embryoid Bodies in Microbeads. Annals of the New York Academy of Sciences 944 (2001) 135-43.
(268) SB Lee, HW Jeon, YW Lee, YM Lee, KW Song, MH Park, YS Nam, HC Ahn: Bio-artificial skin composed of gelatin and (1→3), (1→6)-β-glucan. Biomaterials 24 (2003) 2503-11.
(269) GM Lee, BK Han, JH Kim, BO Palsson: Effect of calcium chloride treatment on hybridoma cell viability and growth. Biotechnology Letters 14 (1992) 891-96.
(270) KM McGinnis, KKW Wang, ME Gnegy: Alterations of extracellular calcium elicit selective modes of cell death and protease activation in SH-SY5Y human neuroblastoma cells. Journal of neurochemistry 72 (1999) 1853-63.
(271) H Gudapati, J Yan, Y Huang, DB Chrisey: Alginate gelation-induced cell death during laser-assisted cell printing. Biofabrication 6 (2014) 035022.
(272) D Serp, E Cantana, C Heinzen, U Von Stockar, IW Marison: Characterization of an encapsulation device for the production of monodisperse alginate beads for cell immobilization. Biotechnology and Bioengineering 70 (2000) 41-53.
(273) H Zimmermann, SG Shirley, U Zimmermann: Alginate-based encapsulation of cells: past, present, and future. Current diabetes reports 7 (2007) 314-20.
(274) L-H Hung, AP Lee: Microfluidic devices for the synthesis of nanoparticles and biomaterials. Journal of Medical and Biological Engineering 27 (2007) 1.
(275) G Orive, SK Tam, JL Pedraz, J-P Hallé: Biocompatibility of alginate–poly-l-lysine microcapsules for cell therapy. Biomaterials 27 (2006) 3691-700.
(276) SH Ranganath, A Yang, YY Chan, J Huang, WB Krantz, C-H Wang, Implantable hy-drogel beads entrapping PLGA-paclitaxel microspheres: exploring the effects of

near-zero order drug release for intracranial chemotherapy, AIChE Annual meeting, Philadelphia, USA, 2008.
(277) D Huh, JH Bahng, Y Ling, H-H Wei, OD Kripfgans, JB Fowlkes, JB Grotberg, S Takayama: A Gravity-Driven Microfluidic Particle Sorting Device with Hydrodynamic Separation Amplification. Analytical Chemistry 79 (2007) 1369-76.
(278) KF Almqvist, L Wang, J Wang, D Baeten, M Cornelissen, R Verdonk, EM Veys, G Verbruggen: Culture of chondrocytes in alginate surrounded by fibrin gel: characteristics of the cells over a period of eight weeks. Annals of the rheumatic diseases 60 (2001) 781-90.
(279) MS Shoichet, RH Li, ML White, SR Winn: Stability of hydrogels used in cell encapsulation: An in vitro comparison of alginate and agarose. Biotechnology and Bioengineering 50 (1996) 374-81.
(280) O Gåserød, A Sannes, G Skjåk-Bræk: Microcapsules of alginate-chitosan. II. A study of capsule stability and permeability. Biomaterials 20 (1999) 773-83.
(281) EM Garland, JM Parr, DS Williamson, SM Cohen: In vitro cytotoxicity of the sodium, potassium and calcium salts of saccharin, sodium ascorbate, sodium citrate and sodium chloride. Toxicology in vitro 3 (1989) 201-05.
(282) N Scaglia, JW Chisholm, RA Igal: Inhibition of stearoylCoA desaturase-1 inactivates acetyl-CoA carboxylase and impairs proliferation in cancer cells: role of AMPK. PLoS ONE 4 (2009) e6812.
(283) S-F Lan, B Safiejko-Mroczka, B Starly: Long-term cultivation of HepG2 liver cells encapsulated in alginate hydrogels: a study of cell viability, morphology and drug metabolism. Toxicology in vitro 24 (2010) 1314-23.
(284) N Wang, G Adams, L Buttery, FH Falcone, S Stolnik: Alginate encapsulation technology supports embryonic stem cells differentiation into insulin-producing cells. Journal of biotechnology 144 (2009) 304-12.
(285) A Hibara, M Tokeshi, K Uchiyama, H Hisamoto, T Kitamori: Integrated multilayer flow system on a microchip. Analytical sciences 17 (2001) 89-93.
(286) W Jackson, H Tran, M O'Brien, E Rabinovich, G Lopex: Rapid prototyping of active microfluidic components based on magnetically modified elastomeric materials. J. Vac. Sci. Technol. B 19 (2001) 596.
(287) C-W Tsao, DL DeVoe: Bonding of thermoplastic polymer microfluidics. Microfluidics and Nanofluidics 6 (2009) 1-16.
(288) PM van Midwoud, A Janse, MT Merema, GMM Groothuis, E Verpoorte: Comparison of biocompatibility and adsorption properties of different plastics for advanced microfluidic cell and tissue culture models. Analytical Chemistry 84 (2012) 3938-44.
(289) S Sugiura, M Nakajima, M Seki: Preparation of monodispersed polymeric microspheres over 50 μm employing microchannel emulsification. Industrial & Engineering Chemistry Research 41 (2002) 4043-47.
(290) M Lian, CP Collier, MJ Doktycz, ST Retterer: Monodisperse alginate microgel formation in a three-dimensional microfluidic droplet generator. Biomicrofluidics 6 (2012) 044108.
(291) H Onoe, K Inamori, M Takinoue, S Takeuchi: Centrifuge-based cell encapsulation in hydrogel microbeads using sub-microliter sample solution. RSC Advances 4 (2014) 30480-84.
(292) D Poncelet, R Neufeld, B Bugarski, BG Amsden, J Zhu, MFA Goosen: A Parallel plate electrostatic droplet generator: Parameters affecting microbead size. Applied Microbiology and Biotechnology 42 (1994) 251-55.

(293) N Bremond, AR Thiam, J Bibette: Decompressing emulsion droplets favors coalescence. Physical review letters 100 (2008) 024501.
(294) J Bibette, FL Calderon, P Poulin: Emulsions: basic principles. Reports on Progress in Physics 62 (1999) 969.
(295) S-Y Teh, R Lin, L-H Hung, AP Lee: Droplet microfluidics. Lab on a Chip 8 (2008) 198-220.
(296) CW Shields Iv, CD Reyes, GP López: Microfluidic cell sorting: a review of the advances in the separation of cells from debulking to rare cell isolation. Lab on a Chip 15 (2015) 1230-49.
(297) C Lu, LJ Lee, Y-J Juang: Packaging of microfluidic chips via interstitial bonding technique. Electrophoresis 29 (2008) 1407-14.
(298) F Chen, S Qi, L Lu, Y Xu: Effect of storage temperature on the viability of human periodontal ligament fibroblasts. Dental Traumatology 31 (2015) 24-28.
(299) S Reuveny, D Velez, JD Macmillan, L Miller: Factors affecting cell growth and monoclonal antibody production in stirred reactors. Journal of immunological methods 86 (1986) 53-59.
(300) S Neri, E Mariani, A Meneghetti, L Cattini, A Facchini: Calcein-Acetyoxymethyl Cytotoxicity Assay: Standardization of a Method Allowing Additional Analyses on Recovered Effector Cells and Supernatants. Clinical and Diagnostic Laboratory Immunology 8 (2001) 1131-35.
(301) B Maherani, E Arab-Tehrany, A Kheirolomoom, D Geny, M Linder: Calcein release behavior from liposomal bilayer; influence of physicochemical/mechanical/structural properties of lipids. Biochimie 95 (2013) 2018-33.
(302) T Crompton, MC Peitsch, HR MacDonald, Jr Tschopp: Propidium iodide staining correlates with the extent of DNA degradation in isolated nuclei. Biochemical and Biophysical Research Communications 183 (1992) 532-37.
(303) KH Jones, DA Kniss: Propidium iodide as a nuclear counterstain for immunofluorescence studies on cells in culture. Journal of Histochemistry & Cytochemistry 35 (1987) 123-5.
(304) Y-H Lin, C-T Chen, LLH Huang, G-B Lee: Multiple-channel emulsion chips utilizing pneumatic choppers for biotechnology applications. Biomedical microdevices 9 (2007) 833-43.
(305) S Sugiura, T Oda, Y Izumida, Y Aoyagi, M Satake, A Ochiai, N Ohkohchi, M Nakajima: Size control of calcium alginate beads containing living cells using micro-nozzle array. Biomaterials 26 (2005) 3327-31.
(306) D Chicheportiche, G Reach: In vitro kinetics of insulin release by microencapsulated rat islets: effect of the size of the microcapsules. Diabetologia 31 (1988) 54-57.
(307) FA Leblond, G Simard, N Henley, B Rocheleau, PM Huet, JP Halle: Studies on smaller (approximately 315 microM) microcapsules: IV. Feasibility and safety of intrahepatic implantations of small alginate poly-L-lysine microcapsules. Cell Transplantation 8 (1998) 327-37.
(308) S Moon, E Ceyhan, UA Gurkan, U Demirci: Statistical Modeling of Single Target Cell Encapsulation. PLoS ONE 6 e21580.
(309) Y Hu, G Azadi, AM Ardekani: Microfluidic fabrication of shape-tunable alginate microgels: Effect of size and impact velocity. Carbohydrate Polymers 120 (2015) 38-45.
(310) J Lan, J Chen, N Li, X Ji, M Yu, Z He: Microfluidic generation of magnetic-fluorescent Janus microparticles for biomolecular detection. Talanta (2016).

(311) RA Otto, S Beamer, J Jaczynski, KE Matak: The Effect of Using Citric or Acetic Acid on Survival of Listeria monocytogenes during Fish Protein Recovery by Isoelectric Solubilization and Precipitation Process. Journal of Food Science 76 (2011) M579-M83.
(312) Y Hiraoka, K Kimbara: Rapid assessment of the physiological status of the polychlorinated biphenyl degrader Comamonas testosteroni TK102 by flow cytometry. Applied and environmental microbiology 68 (2002) 2031-35.